Organic-inorganic hybrid coatings : based on polyester resins and in situ formed silica

Organic-Inorganic Hybrid Coatings

based on polyester resins and in situ formed silica

PROEFSCHRIFT

ter verkrijging van de graad van doctor aan de
Technische Universiteit Eindhoven, op gezag van
de Rector Magnificus, prof. dr. M. Rem, voor een
commissie aangewezen door het College voor
Promoties in het openbaar te verdedigen
op woensdag 8 december 1999 om 16.00 uur

door

Suzanne Frings

geboren te Wageningen

Contents

Abbreviations and Symbols

A: area

AdA: adipic acid

AFM: atomic force microscopy

ASTM: American standard test methods

AV: acid value

CHDM: 1,4-cyclohexanedimethylol

CP-MAS: cross polarization magic angle spinning

D: polydispersity ratio

DABCO: 1,4-diazobicyclo[2.2.2]octane

DSC: differential scanning calorimetry

ED: esterdiol

EMM: epoxy molar mass

$\mathbf{E}_r$**:** reduced elastic modulus

F: force

fn: number average functionality

FTIR: Fourier transform infrared spectroscopy

GC: gas chromatography

glymo: γ-glycidoxypropyltrimethoxysilane

GPC: gel permeation chromatography

H: hardness

h: displacement

$\mathbf{h}_c$**:** contact displacement or plastic displacement

$\mathbf{h}_{end}$**:** end displacement

$\mathbf{h}_{max}$**:** maximum displacement

HMMM: hexakis(methoxymethyl)melamine

IPA: isophthalic acid

IPN: interpenetrating network

μ**:** coefficient of friction

MEK: methyl-ethyl-ketone or 2-butanone

MeOH: methanol

Mn: number average molecular weight

MPA: 1-methoxy-2-propylacetate

ν**:** Poisson ratio

NCO-silane: isocyanatopropyltriethoxysilane

NPG: neopentylglycol

NMR: nuclear magnetic resonance spectroscopy

OHV: hydroxyl value

PDMS: polydimethylsiloxane

PE: polyester

pT0.5: prehydrolyzed TEOS, with 0.5 mole water per mole TEOS

pT1: prehydrolyzed TEOS, with 1 mole water per mole TEOS

pT2: prehydrolyzed TEOS, with 2 mole water per mole TEOS

pTSA: para-toluenesulfonic acid

s: interfacial shear strength

S: stiffness

SA: succinic anhydride

SAXS: small angle X-ray scattering

SEM: scanning electron microscopy

Si-PE: silane-modified polyester

T: temperature

t: time

TEM: transmission electron microscopy

TEOS: tetraethoxysilane

Tg: glass transition temperature

TGA: thermal gravimetric analysis

THF: tetrahydrofuran

Tm: melting temperature

TMOS: tetramethoxysilane

TMP: trimethylolpropane

wt.%: weight percentage

Chapter 1

Introduction

Coatings are materials that are applied as a thin continuous layer on a surface [1]. In this thesis the final cured layer is designated as coating, while the material that is to be applied is referred to as coating system. There are inorganic and organic coatings. Inorganic coatings, like ceramic coatings and enamels, are mainly applied for protective purposes, while organic coatings have both functional (such as protection) and decorative functions. The organic coatings are generally divided into two main categories: architectural and industrial coatings [2, 3]. The architectural coatings are used to decorate and protect parts of buildings. The main requirements are fast drying, good adhesion to old coatings and good appearance. For exterior purposes also outdoor durability is important. Industrial coatings are applied in factories and can be subdivided into several groups, depending on their end use: automotive, appliance, aircraft, building, paper, can and coil coatings. They all have their own specific requirements.

The coating systems studied in this thesis are meant for coil coating applications. In the coil coating process, which is schematically shown in Figure 1.1, large rolls of steel or aluminum are coated by roller coating application. The process involves metal cleaning (1), metal treatment with chromate or phosphate for a thin layer against corrosion and for good adhesion (2), application of a primer (3), curing of the primer (4), immediately afterwards application of a topcoat (5) and curing of the topcoat (6). Finally the coated metal sheet is rolled up again. While the primer is a purely functional layer (corrosion protection and good adherence), the topcoat should be decorative beside having good mechanical properties and, in many cases, good outdoor durability. The speed of the metal sheets through the coil coating equipment can be up to 60 m/min. The curing steps must therefore be finished within about 30 seconds. The oven temperatures are above 350 °C, while the peak metal temperature,
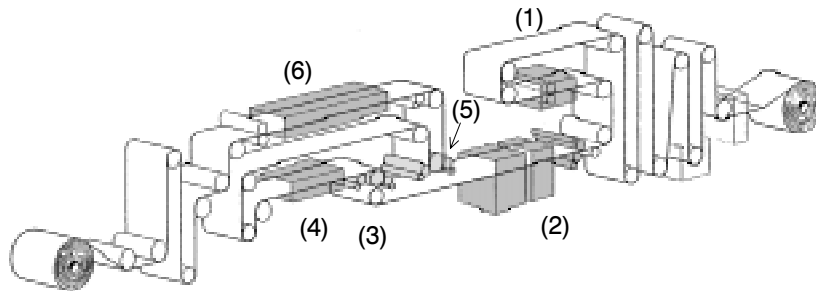
Figure 1.1: *Schematic overview of a coil coating equipment.*

the highest temperature the metal reaches in the oven, is around 250 °C. The coated metal sheets are transported to customers, who will apply them to produce objects, such as garage doors, refrigerators and caravans. Most important requirements for the coatings are high flexibility and excellent exterior durability. Flexibility is necessary because the coated metal must be shaped in various forms, depending on the product. Durability can only be obtained if the coatings are hard and scratch resistant, this way avoiding damage during transport, manufacturing and use.

The composition of an organic coating system consists of a binder, a volatile component, pigments and additives. The binder is the component that forms the continuous film and adheres to the substrate. For coil coating purposes the binder must be sufficiently flexible and is therefore often based on polyester resin. The volatile component is the solvent in the coating system, which is used to adjust the viscosity for good application and which evaporates during curing. The volatile organic compounds (VOC) are the largest concern in the coating industries at the moment, because legislation dictates a reduction for environmental and health reasons. In the coil coating process, though, which is a closed process [4] these VOC's are consumed as fuel for the heating of the curing ovens. Pigments are insoluble solids that are dispersed in the continuous phase (the binder and solvent). They are added to provide the color of the coating, but they also have an influence on other properties. Additives (for example catalysts, stabilizers, flow modifiers) are materials that are included in small quantities to modify application and coating properties.

In this thesis the focus is on the binder system of the coatings and therefore only the binder and the solvent (the continuous phase), without pigments and additives (except the catalyst), has been considered. The use of new organic-inorganic hybrid binder systems has been investigated to combine the properties of organic and inorganic compounds in one new material. Organic-inorganic hybrid materials are defined as materials in which organic and inorganic compounds have intermolecular interactions, such that the properties of both compounds are reflected. Another fea-

ture of hybrid materials is that the compounds have chemical interaction with each other. Hybrid materials are discussed in detail in Section 1.2 and 1.3. To be able to prepare hybrid materials, inorganic compounds must be formed at a temperature that organic compounds can withstand. Traditionally ceramic materials are processed at high temperatures [5]. Glass for example is processed by melting sand mixtures at temperatures above 1000 °C. The development of the so-called sol-gel process [6] enables one to synthesize ceramic materials even at room temperature. The sol-gel process is described in Section 1.1. Using the sol-gel process in combination with formulating organic coatings, organic-inorganic coatings were prepared and characterized, as described in Section 1.4.

1.1   Sol-gel process

The sol-gel process is a method to synthesize ceramic materials by preparation of a sol, gelation of the sol and removal of the solvent [6,7]. The sol, a colloidal suspension of solid materials in a liquid, is prepared from precursors. These precursors are metals or metalloids surrounded by various organic ligands. In this study the metal alkoxide tetraethoxysilane (TEOS) is transformed into silica by the sol-gel process. The molecular structure is shown in Figure 1.2. TEOS is the most thoroughly studied precursor in the sol-gel process: its low reactivity towards hydrolysis makes it possible to follow and control the reactions. Unlike silicates other metal alkoxides (such as titanium alkoxides and zirconium alkoxides) have a higher reactivity due to the lower electronegativity and the ability to exhibit several coordination states of the metal atoms [8]. The size of the ligands influences the reactivity as well. The larger the alkoxide group, the more steric hindrance and the slower the reactions.

$$
\begin{array}{c}
OCH_2CH_3 \\
| \\
CH_3CH_2O\!-\!Si\!-\!OCH_2CH_3 \\
| \\
OCH_2CH_3
\end{array}
$$
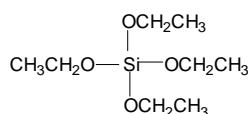
Figure 1.2: *The molecular structure of TEOS.*

In general it is recognized that the polymerization of silicon alkoxides towards silica proceeds in three stages [6,9]: the polymerization of the monomer (the precursor) to form small particles (the sol), the growth of particles and the linking of particles into chains, forming a network (gel). The polymerization of the monomers is described by two processes: the hydrolysis (Figure 1.3) and the condensation (Figure 1.4) reaction. Both reactions are equilibria. They are influenced by the pH of the system [7]. Under acidic conditions (pH < 2.5) hydrolysis takes place by the attack of an hydronium ion (H_3O^+) on the oxygen of one of the alkoxy groups (Figure 1.5). The condensa-

tion, under acidic conditions, proceeds in two steps. First the silanol is protonated, increasing the electrophilic character of the silicon atom, then this protonated silanol combines to another silanol group, liberating H_3O^+, as shown in Figure 1.6. Under basic conditions hydrolysis proceeds by an attack of an OH^- anion forming a silanol group (Figure 1.7). During condensation, under basic conditions, the silanol groups are deprotonated. These deprotonated silanol groups attack on other silicon containing molecules, as shown in Figure 1.8. The above mentioned reaction mechanisms, which are general recognized [7], finally leads to the formation of silica. The rate of hydrolysis and condensation depends upon the pH of the system. Under acidic conditions the hydrolysis is faster than the condensation, while under basic conditions the condensation is faster than the hydrolysis. By applying a two-step process [10] the hydrolysis and condensation reactions have been studied separately [11–13]. In the first step acidic conditions were applied, resulting in mainly hydrolysis. In the second step a base catalyst was added, initiating the condensation. Applying this two-step method the influence of various parameters (concentration, choice of catalyst and solvent temperature) on the sol-gel reactions have been determined.

The formed sol particles are the nuclei for the particle growth. Growth proceeds via the Ostwald ripening mechanism [9]: the smallest particles are more soluble than the larger ones and therefore the smallest particles dissolve and precipitate on the larger ones. Since the solubility depends on the size of the particles this effect finally results in uniformly sized particles. At high pH the solubility of the small particles is higher than at low pH, resulting in larger particles (5-10 nm) under basic conditions than under acidic conditions (2-4 nm). Under basic conditions the particles are negatively charged and repel each other. Therefore they do not collide and are stable as such. Under acidic conditions the charge repulsion is reduced and aggregation occurs, resulting in a branched network.

The sol-gel process is, compared to the traditional methods, a well controllable process in which very pure materials can be synthesized, by using purified precursors. Furthermore, ceramic materials can be synthesized even at room temperature. This provides the opportunity to synthesize silica in the presence of organic compounds, which makes it possible to develop organic-inorganic hybrid materials.

1.2   Hybrid materials

Historically, the development of the sol-gel process initiated the incorporation of organic compounds in inorganic. The first step was the use of complex organic ligands in the sol-gel process that were no longer removed after gelation [14, 15]. Then one or two alkoxide groups of the silanes were replaced by nonhydrolyzable organic lig-

$$\text{Si-OCH}_2\text{CH}_3 \ + \ \text{H}_2\text{O} \ \rightleftharpoons \ \text{Si-OH} \ + \ \text{CH}_3\text{CH}_2\text{OH}$$
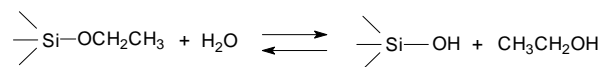
Figure 1.3: *Hydrolysis reaction of TEOS.*

$$\text{Si-OH} \ + \ \text{RO-Si} \ \rightleftharpoons \ \text{Si-O-Si} \ + \ \text{ROH}$$
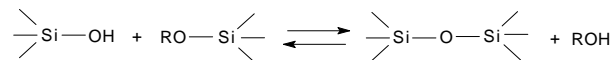
Figure 1.4: *Condensation reaction of TEOS. R is a H or alkyl.*
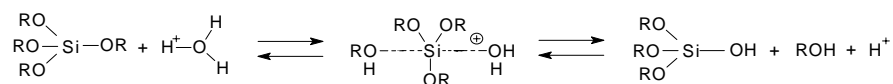
Figure 1.5: *Hydrolysis mechanism of TEOS under acidic conditions.*
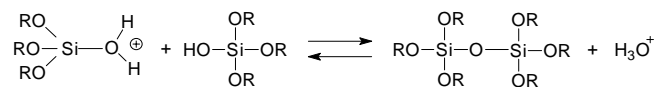
Figure 1.6: *Condensation mechanism of TEOS under acidic conditions.*
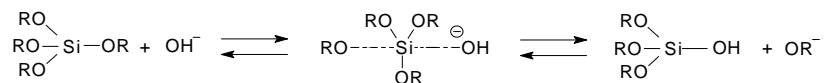
Figure 1.7: *Hydrolysis mechanism of TEOS under basic conditions.*
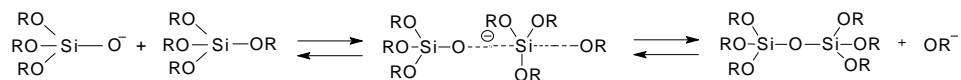
Figure 1.8: *Condensation mechanism of TEOS under basic conditions.*

ands (R') forming $R'_n Si(OR)_{4-n}$ [16]. Such organically modified silane molecules, are called silane coupling agents [17, 18]. By applying these molecules in the sol-gel process organic groups were covalently bonded to the inorganic material. When the organic group (R') is nonfunctional (for example a methyl group) it acts as a network modifier, while a functional organic group (for example a methacryl-propyl or amino-propyl group) can act as a network former [19], or it can form a link with other organic compounds. The group of Schmidt [14, 16, 19–23] combined metal alkoxides, network modifiers and network formers to make flexible and functional glassy materials. De-pendent on the chemical composition they called their hybrid materials 'ormosils' and 'ormocers', organically modified silanes and ceramics, respectively. Another ap-proach to make hybrid materials based on the sol-gel precursors was by substituting the alkyl group of the alkoxy ligands of the metal alkoxides (R) in polymerizable organic monomer (for example a derivative of 2-hydroxyethylacrylate). When these precursors are sol-gel processed the polymerizable monomers are released (as ROH in Figure 1.4, forming for example 2-hydroxyethylacrylate). These monomers do not evaporate as alcohol, but can be polymerized simultaneously or afterwards, forming an organic network within the via sol-gel formed glass [24–27].

The first hybrids reported in literature based on organic polymer chemistry were synthesized by polydimethylsiloxane (PDMS) with TEOS as silica precursor, in which in situ formed silica acts as reinforcement of the elastomer PDMS [28–32]. PDMS, with its siloxane backbone, shows a good compatibility with TEOS. The following step in the formation of hybrid materials was to apply the same strategy to polymers with a carbon backbone [33, 34]. Wilkes and co-workers worked in this area [34–36], they called their hybrid materials 'ceramers', which stands for a composition of ceramics and polymers. They applied a number of oligomers and polymers in combination with various metal alkoxides in the sol-gel process. Hereto, the polymers were modified with silane coupling agents. In this way, a covalent interaction between the organic and inorganic phase was ensured. Also an number of other groups applied this route of making hybrid materials [37–42]. Other hybrid materials gain the interactions between the organic and inorganic phase via hydrogen bonding [43–45] or via the reaction of hydroxyl groups of organic compounds with the alkoxy groups of the sol-gel precursors [46–49]. The interactions between the organic and inorganic phase are discussed in detail in Chapter 4.

The references mentioned in this chapter are meant as examples, to give an overview of developments in this area. Various review papers [36, 50–54] and proceedings [55–58] on hybrid materials have been published. Most reviewers classify the hybrid materials based on the type of interactions between the organic and inorganic phase. The two classes defined by Sanchez [50] are often used: class I for weak or no interaction, class II for covalent interaction. Further subdividing appears arbitrarily and depends on the focus of the writer. We chose to classify the hybrids in the first place based on their continuous phase, showing the hybrid to be more organic based, inorganic based

(a) Inorganic matrix with organic clusters

(b) Organic matrix with inorganic clusters

(c) Interpenetrating network

(d) True hybrid
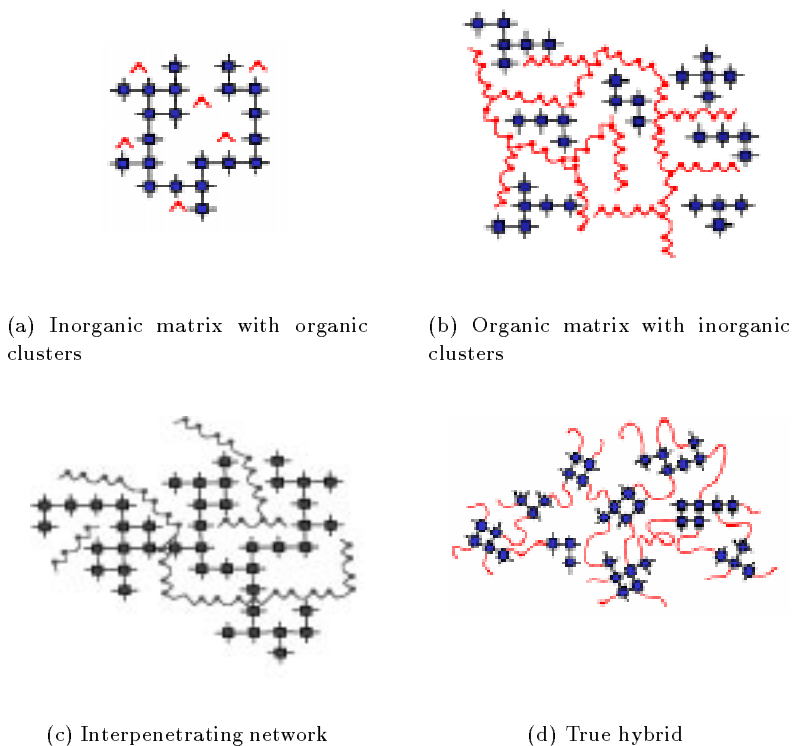
Figure 1.9: *Schematic representation of the four major hybrid classes. The boxes represent the inorganic compound, while the line structures represent the organic compounds.* Reproduced by permission of The Royal Society of Chemistry.-[Journal of Materials Chemistry, 1996, 511-525, Fig. 2, 3, 5 and 10]

or in between. In this way four major classes, which are schematically represented in Figure 1.9, are considered:

- The inorganic matrix with organic clusters (Figure 1.9(a)).

- The organic matrix with inorganic clusters (Figure 1.9(b)).

- The interpenetrating network: when both the organic and the inorganic phase form a network (Figure 1.9(c)).

- The true hybrid: when the organic and inorganic phase together from the network (Figure 1.9(d)).

Within these four classes various interactions between the organic and inorganic phase are possible, such as mentioned above. By applying this classification the above men-

tioned 'ormocers' are typical examples of an inorganic matrix with organic clusters. The so-called 'ceramers' have an organic matrix, in which the inorganic phase is formed in clusters, or as a continuous network. Most hybrid materials in literature are formed under acidic conditions, resulting in the formation of interpenetrating networks. They are further discussed in Chapter 5, while the organic matrix with inorganic clusters is discussed in Chapter 6.

1.3   Hybrid coatings

The range of hybrid materials is enormous and so is the field of potential applications. Here we focus on the possibilities of using hybrid materials for coating purposes. Inorganic coatings are known for their high resistance towards heat and damage, but they are very brittle. Organic coatings, on the other hand, are flexible, adhere good to substrates and can easily be modified or functionalized but do not have a high damage or heat resistance. Hybrid coatings with an inorganic matrix, originating from metal alkoxides and silane coupling agents, have been studied for adhesion purposes on glass [59, 60] and metal [61, 62] substrates. They have been applied in optical applications for the incorporation of organic dyes [63–66] and to obtain special material properties [67, 68]. They were also used to provide special properties, such as anti-soiling and anti-fogging by modifying the surface polarity [69, 70]. Also hybrid coatings based on an organic matrix combined with silane coupling agents have been used to improve adhesion to glass [71, 72], metal [73, 74] and polymer [75] substrates. Silanes have also been incorporated in organic coatings to generate new crosslink mechanisms [76, 77] and to obtain improved coatings properties. Acrylic polymers, for example, have been modified with silanes by incorporation of methacryloxypropyl trimethoxysilane for improved weather resistance [78] and improved scratch resistance [79, 80]. Alkyd coatings were combined with titanium and zirconium alkoxides to prepare hybrid organic-inorganic coatings for corrosion resistance [81, 82] and to study the effect on the overall coatings properties [83, 84]. The alkoxides acted as dryers, increasing the crosslinking, but they also form an inorganic network. Overall, the coatings properties were found to be dependent on the type and amount of sol-gel precursors.

Organic-inorganic hybrid coatings have been extensively studied for improvement of the scratch resistance of polymeric surfaces, both based on inorganic [85–91] and organic [79, 80, 92–97] matrices. In the inorganic based systems the improved scratch resistance is attributed to the hard inorganic backbone [85–87], while the incorporation of organic molecules improves the adhesion with the polymeric substrate and increases the layer thickness. The improved scratch resistance is also obtained from nanoparticles [90, 91] surrounded by silane coupling agents as matrix and stabilizer. Also in the organic based systems both the inorganic backbone [92, 93] and the in-

corporation of nanoparticles [80] are held responsible for improved scratch resistance, while again the organic compound provides the adhesion and flexibility [94].

1.4 Scope of this thesis

The aim of this study is to improve the hardness and scratch resistance of organic based hybrid coatings on steel and aluminum substrates, while the flexibility is maintained. The basis of the organic component is the polyester resin, because of its high flexibility. The inorganic compound is TEOS, as sol-gel precursor for the formation of silica in situ in the organic coating system, because the sol-gel reaction of TEOS is well controllable.

In Chapter 2: *'Materials and Methods of Preparation'*, the choices for both compounds are further explained. The polyester synthesis is described and the inclusion of TEOS in the coatings is studied. Furthermore, a general method of the coating preparation, application and curing is described.

In Chapter 3: *'Characterization of Hybrid Coatings'*, the methods applied for the characterization of the hybrid coatings are discussed. The choices for the used techniques depend largely on the possibilities to characterize materials containing both organic and inorganic characteristics. With respect to coatings the characterization results in extra limitations for several techniques. Furthermore, several parameters of the characterization methods are studied.

Various chemical compositions based on the polyester resin and TEOS have been applied for the preparation of hybrid coatings. A schematic overview is given in Figure 1.10. Depending on the chemical composition various morphologies in the final coatings have been obtained. The influence of the morphology on the properties is studied and discussed in the following chapters.

In Chapter 4: *'Polyester-TEOS Interactions'*, polyester resin is combined with TEOS (Figure 1.10: central box) to study the interactions between the compounds. The formed hybrid coatings are true hybrids.

In Chapter 5: *'Interpenetrating Networks'*, polyester resin is crosslinked with hexakis(methoxymethyl)melamine (HMMM) and combined with TEOS under acidic conditions (Figure 1.10: central box + organic crosslinkers), By the formation of both an organic polyester-HMMM network and an silica network interpenetrating networks are formed. Also the influence of the addition of silane coupling agents was studied (Figure 1.10: + organically modified silane).
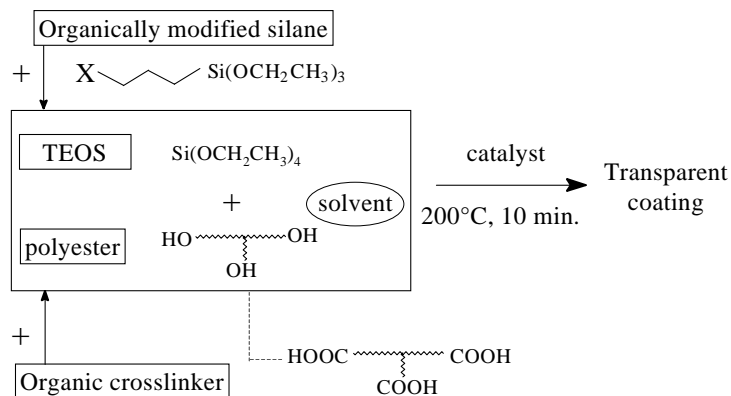
Figure 1.10: *Schematic overview of various systems used in this thesis.*

In Chapter 6: *'Nano-structured Coatings'*, the crosslinking of polyester resin with epoxide in combination with TEOS under basic conditions is described. For the compatibility silane coupling agents were necessary (Figure 1.10: central box + organic crosslinkers + silane coupling agents). Due to the basic conditions, organic matrices with silica nanoparticles are formed.

In Chapter 7: *'Conclusions and Recommendations'*, the final conclusions and recommendations are summarized. In each chapter abbreviations are defined when they first appear. A table of frequently used abbreviations is provided at the beginning of the thesis. The references are numbered throughout the thesis and are given at the end of Chapter 7.

Chapter 2

Materials and Methods of Preparation

2.1 Introduction

The materials and general methods applied in the research on organic-inorganic hybrid coatings are described in this chapter. The choice of materials largely depended upon the potential application purpose of the hybrid coatings: the coil coating application. Most important features hereby were the high curing temperature and the necessity of flexibility, since the pre-coated metal sheets must be shaped afterwards. Polyester resins were chosen as organic basis, because of their ability to be highly flexible. They are often used in coil coating applications because of this property [3,98]. Furthermore polyester properties can be tuned and molecular weight and functionality can be changed by the choice of the monomer composition [2]. The polyester resins were synthesized and characterized, as described in Section 2.2, to have well-defined model compounds as organic basis. For the formation of hybrid coatings the polyesters were combined with the inorganic compounds (as described in Chapter 4), but the polyesters were also crosslinked with organic crosslinkers to be able to form an organic network. For this crosslinking two systems were used. One system consisted of the acid catalyzed crosslinking reactions of hexakis(methoxymethyl)melamine (HMMM) as crosslinker with the hydroxyl-terminated polyesters (described in Chapter 5), and the other system consisted of the base catalyzed crosslinking reaction of epoxides as crosslinker with acid-terminated polyesters (described in Chapter 6). In this way the influence of the pH of the hybrid systems on the morphology and properties of the hybrid coatings could be studied.

As the hardness of the organic-inorganic hybrid coatings has to be obtained from the inorganic phase, tetraethoxysilane (TEOS) was chosen as precursor. TEOS is often used as precursor for the formation of silica by the sol-gel reaction in the synthesis of hybrid materials. Silicon alkoxides have a low reactivity towards hydrolysis compared to other metal alkoxides, because silicon is less electropositive. This makes silicon comparatively less susceptible to nucleophilic attack [6]. Because of its low reactivity, it is possible to control the reactions by temperature and catalyst and adjust them to the rates of the organic crosslinking reactions. It was found that under the curing temperatures used in this research (200 °C), TEOS could evaporate from the coatings. In order to prevent evaporation the use of prehydrolyzation of TEOS was studied, as described in Section 2.3.

Beside the organic resin and the inorganic compound, the coating systems contained a solvent and a catalyst. In the synthesis of hybrid materials often ethanol and tetrahydrofuran were used as the solvent [46,99,100]. But when high curing temperatures are applied, as in this research, these solvents are not suitable, because of their low boiling temperatures and high evaporation rates. In industrial coating applications often a blend of solvents is used to achieve an appropriate balance on fast evaporation and good film formation [3]. In this research a single solvent was chosen to limit the complexity of the model systems. Beside a high boiling temperature to prevent a too fast evaporation during curing other demands for the solvent were compatibility with both the organic and inorganic compounds and the ability of the solvent to contain water, since water is necessary for the sol-gel reaction. MPA (1-methoxy-2-propylacetate) did fulfill these demands and was used in general.

By analog with the use of HCl as catalyst in the sol-gel process [10,11], HCl is often used in the synthesis of hybrid materials. But at the high curing temperatures as used in this research, HCl can evaporate. Furthermore HCl has undesirable corrosive properties. Since para-toluenesulfonic acid (pTSA) is generally used in the polyester-HMMM reaction [98], it was chosen as acidic catalyst. For the base catalyzed reactions of acid-terminated polyester with epoxides, in general amines are used as catalyst [2]. Since triethylamine was found to evaporate easily at the curing temperatures used in this research, 1,4-diazobicyclo[2.2.2]octane (DABCO) was applied instead. Both pTSA and DABCO are solid compounds, which were dissolved in MPA before they were applied in the coating systems. With the above mentioned basic compounds coatings were prepared as generally described in Section 2.4.

2.2   Polyester synthesis

Polyesters with a high flexibility were chosen as organic compound in the hybrid systems. They were synthesized with a low glass transition temperature (Tg) by the choice of monomer composition. The molecular structures of the monomer compounds applied, are shown in Figure 2.1. The polyesters synthesized were hydroxyl-terminated. The first series of polyesters (PE1-PE6), which only varied in molecular weight and functionality, consisted of the diacids isophthalic acid and adipic acid and the diol neopentylglycol (PE1-PE3). For the synthesis of trifunctional polyesters trimethylolpropane was included (PE4-PE6). In the second series (PE9-PE10) an esterdiol and 1,4-cyclohexanedimethanol were also included in order to improve the compatibility with the inorganic phase. The increased number of diols reduced also crystallization. For characterization purposes, the Tg of the polyesters of the second series was increased by increasing the ratio isophthalic acid:adipic acid from 1:1 to 3:1. The polyesters were synthesized bifunctional (PE9) and trifunctional (PE10). The monomer composition of the various polyesters is summarized in Table 2.1. The hydroxyl-terminated polyesters were synthesized according to conventional methods, as described in Section 2.5. They were characterized by endgroup titration, GPC, ^{1}H NMR, ^{13}C NMR and DSC. Their characteristics are summarized in Table 2.2. The NMR data are summarized in Section 2.5. Acid-terminated polyesters (PE6a, PE9(1)a, PE10a) were synthesized from the hydroxyl-terminated polyesters by reaction of stoichiometric amounts of succinic anhydride at 150 °C until the calculated acid and hydroxyl value were obtained. Their characteristics are also summarized in Table 2.2.

Table 2.1: *Molar monomer composition of the hydroxyl-terminated polyester resins.*

Compounds	IPA	AdA	NPG	ED	CHDM	TMP
PE1	22%	22%	57%			
PE2	23%	23%	54%			
PE3	24%	24%	53%			
PE4	22%	22%	44%			11%
PE5	23%	23%	46%			8%
PE6	24%	24%	47%			6%
PE9	35%	12%	39%	12%	2%	
PE10	35%	12%	33%	12%	2%	6%

Table 2.2: *The characteristics of the polyester resins.*

Polyester	fn°	AV [mg KOH/g]	OHV [mg KOH/g]	Mn^{*} [g/mole]	$Mn^{\dagger}$ [g/mole]	$D^{\dagger}$	$Tg^{\ddagger}$ [°C]
Hydroxyl-terminated polyesters							
PE1	2	0.2	107.3	1044	1695	1.6	
PE2	2	0.2	74.0	1504	2156	1.8	
PE3	2	0.1	55.1	2032	2875	2.0	-8
PE4	3	0.2	121.1	1387	2390	3.0	
PE5	3	0.6	101.1	1655	2413	2.8	-10
PE6(1)	3	0.3	79.7	2105	2879	3.0	
PE6	3	0.0	79.6	2114			
PE9(1)	2	0.1	54.7	2047	2258	2.0	13
PE9	2	0.3	46.6	2392			13
PE10	3	0.2	83.8	2004	2282	3.2	13
Acid-terminated polyesters							
PE6a	3	85.3	0	1973			
PE9(1)a	2	48.0	0.3	2323			
PE10a	3	74.5	18.4	1700			

° Calculated from composition. * Calculated by endgroup titration.

† Determined by GPC, based on polystyrene standards. ‡ Determined by DSC.

HOOC—⬡—COOH $HOOCCH_2CH_2CH_2CH_2COOH$

isophtalic acid   adipic acid
(IPA)   (AdA)

CH_3 CH_3 O CH_3
$HOCH_2CCH_2OH$ $HOCH_2C$—C—OCH_2CCH_2OH
CH_3 CH_3 CH_3

neopentylglycol   esterdiol
(NPG)   (ED)

$HOCH_2$
$HOCH_2$—⬡—CH_2OH $HOCH_2CCH_2CH_3$
$HOCH_2$

1,4-cyclohexanedimethylol   trimethylolpropane
(CHDM)   (TMP)
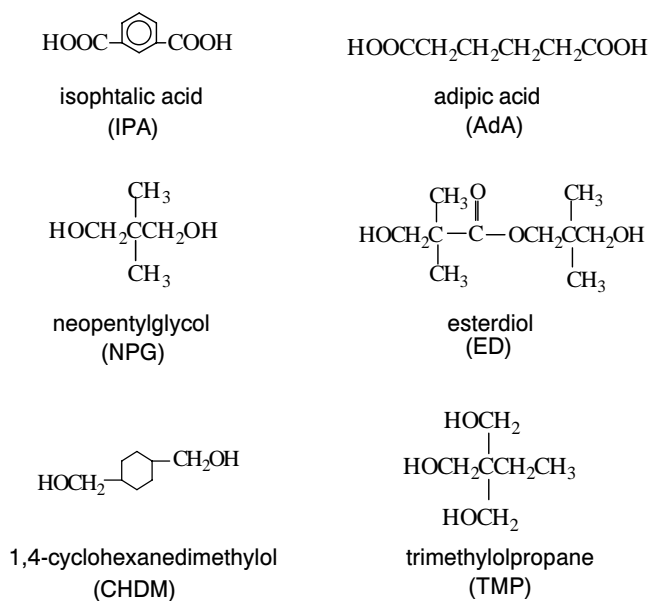
Figure 2.1: *Molecular structures of the monomers used for polyester synthesis.*

2.3   Prehydrolysis of TEOS

TEOS was used as precursor for the inorganic phase. Via the sol-gel process under the influence of water and catalyst, silica will be formed, as described in Section 1.1. The most straightforward way of applying TEOS in hybrid coating systems is to add it directly to the coating mixture. This was successfully done in the polyester-TEOS system (Chapter 4). By putting water in a beaker in the curing oven a moist atmosphere was created, which was found to be sufficient for the hydrolysis of TEOS, since most of the TEOS put in the polyester-TEOS coatings was found back as silica by thermal gravimetric analysis (TGA). The TGA results of a series of PE9(1)-TEOS hybrid coatings applied with 60 and 120 μm, are shown in Table 2.3. The losses for thinner coatings (applied with 60 μm) are higher (15-35%) than for thicker (applied with 120 μm) coatings (5-10%). TEOS has a boiling point of 168 °C and therefore unreacted TEOS may evaporate in an oven of 200 °C. Since the rate of evaporation depends upon the ratio of surface/volume the evaporation from a thinner film will be faster than from a thicker film, resulting in a higher loss for the thinner films [3].

In the organically crosslinked hybrid systems of polyester-HMMM (Chapter 5) and polyester-epoxide (Chapter 6) with TEOS a more severe loss of silica was observed. In Table 2.4 the silica contents of PE3-HMMM and PE9(1)a-epoxide hybrid coatings

Table 2.3: *Silica content of PE9(1)-TEOS hybrids coatings with various amounts of TEOS, applied at 60 and 120 μm, cured 200 °C for 30 min, determined by TGA.*

Calculated wt.% SiO_2	2.9	5.8	10.5	19.0
Measured wt.% SiO_2, 60 μm applied	1.9	4.9	9.0	15.3
Measured wt.% SiO_2, 120 μm applied	2.6	5.3	9.5	17.3

Table 2.4: *Silica content of PE3-HMMM (curing at 140 °C for 1 hour) and PE9(1)a-epoxide (curing at 200 °C for 10 min) hybrids coatings with various amounts of TEOS, determined by TGA and Si elemental analysis.*

	PE3-HMMM		PE9(1)a-epoxide	
Calculated wt.% SiO_2	6.8	10.9	1.9	7.3
Measured wt.% SiO_2 by TGA	0	2.2	0	0
Measured wt.% SiO_2 by Si elemental analysis			0.75	1.4

with various amounts of TEOS are given. As can been seen from this table, almost no silica was kept in these coatings after curing. It is assumed that for both systems no complete hydrolysis and condensation could occur in the short time that the organic crosslinking took place. Therefore unreacted TEOS could evaporate during curing. In contrast with the polyester-TEOS system there is also less possibility for reaction of TEOS with the organic phase, due to the competitive organic crosslinking reactions.

To prevent evaporation of TEOS during curing two methods of prehydrolyzation were studied. This study was done on the polyester-HMMM system (Chapter 5). In method 1 TEOS was allowed to hydrolyze in the presence of polyester, HMMM and pTSA for at least 15 minutes before curing, by addition of one mole distilled water per mole TEOS and continuous stirring. Under these conditions TEOS can form oligomers with hydroxyl groups that can react with the organic part forming Si-O-C bonds and with itself forming Si-O-Si bonds so that evaporation during curing can be prevented. In method 2 TEOS was prehydrolyzed ex situ overnight in ethanol (25 wt.%) with two equivalents of distilled water, at a pH of 2 (pTSA). At this low pH only hydrolysis and hardly any condensation takes place [6]. When the prehydrolyzed TEOS is added to the coating mixture it can react with the organic part and itself directly, in this way evaporation is avoided.

PE5-HMMM hybrid coatings with various amounts of TEOS were prepared using both methods. Also the density of the organic network was varied, by applying a molar ratio

Table 2.5: *Silica content of PE5-HMMM hybrids coatings with various amounts of prehydrolyzed TEOS, determined by the burn-out method.*

calculated wt.% SiO_2	3.1	6.7	11.0
Molar ratio PE5:HMMM 1:0.75	measured wt.% SiO_2		
method 1	0.4	2.0	5.3*
method 2	3.3	7.2	11.5
Molar ratio PE5:HMMM 1:1.5	measured wt.% SiO_2		
method 1	1.6	5.7	5.5
method 2	3.5	7.5	11.0

* Hazy coatings

PE5:HMMM of 1:1.5 and 1:0.75. The silica content in the coatings was measured by the so-called burn-out method (described in Section 2.5). The results are summarized in Table 2.5. Using method 1 a markedly smaller amount of silica was built in than with method 2. The difference between the two methods was more pronounced at low HMMM contents. The coatings made at a polyester:HMMM molar ratio of 1:0.75 and addition of 30 wt.% TEOS (calculated 11.0 wt.% SiO_2) using method 1 were hazy, indicating severe phase separation, but were transparent using method 2, although more silica was present in the latter coatings. The final morphology of the coatings was studied by scanning electron microscopy (SEM). Coatings prepared by method 1 showed clustered particles of very different size, as can be seen in Figure 2.2(a). The largest particles could cause diffraction of light and therefore haziness of the coatings. The coatings prepared by method 2 also showed particle formation, but their appearance is much more uniform an better distributed through the film, as can be seen in Figure 2.2(b). The same effect, only less pronounced was seen for the polyester:HMMM molar ratio 1:1.5, as shown in Figure 2.3. Adding the same amount of TEOS to the composition as for the less dense crosslinked system, no particles could be detected when method 2 was used, but clustered particles were observed when method 1 was used. Probably, due to the increased crosslink density of the organic phase the mobility in the system for the inorganic phase was reduced. This could cause the suppression of inorganic particle formation.

The only advantage of method 1 in the polyester-HMMM system was the observed increase in viscosity, which took place during the prehydrolyzation time, resulting in the possibility to apply thicker coatings. To determine which compound caused the increase in viscosity the relative viscosity in time of a formulation of PE5, HMMM and 30 wt.% TEOS with acid added was measured and compared with that of formulations
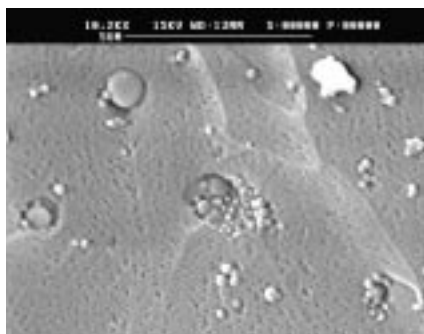
(a) Applied by method 1 resulting in 5.3 wt.% SiO_2.
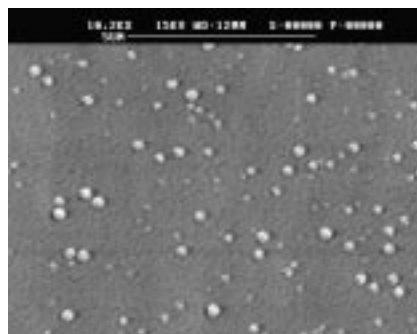
(b) Applied by method 2 resulting in 11.5 wt.% SiO_2.

Figure 2.2: *SEM photographs of crosscuts of hybrid coatings of PE5, HMMM (molar ratio 1:0.75) and 30 % TEOS.*
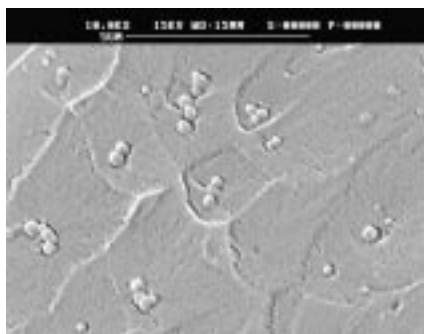
(a) Applied by method 1 resulting in 5.5 wt.% SiO_2.
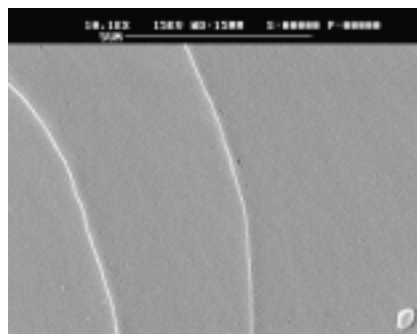
(b) Applied by method 2 resulting in 11.0 wt.% SiO_2.

Figure 2.3: *SEM photographs of crosscuts of hybrid coatings of PE5, HMMM (molar ratio 1:1.5) and 30 % TEOS.*
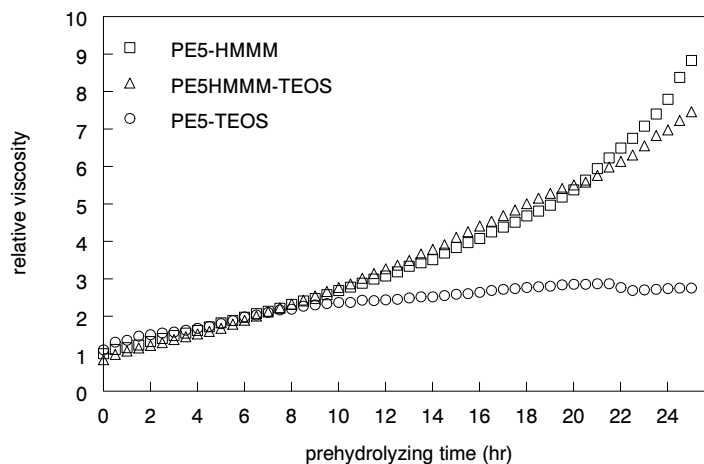
Figure 2.4: *Relative viscosity at room temperature, versus time of mixtures of PE5, HMMM (molar ratio 1:0.75) and 30 wt.% TEOS in MPA. pTSA(1 wt.%) was added at t=0.*

in the absence of TEOS and in the absence of an organic crosslinker. As can be derived from Figure 2.4, the increase in viscosity was caused by the organic crosslinking reaction and not by the prehydrolyzation reaction. Therefore, the increasing viscosity effect can also be achieved, if desirable, when method 2 is used by pre-reacting the polyester and HMMM before addition of the prehydrolyzed TEOS. Method 2 is a better controlled method of prehydrolyzation of TEOS than method 1 and it can be used to prevent evaporation of TEOS during curing completely. Since the hydrolysis of TEOS takes place before application, also in the base catalyzed polyester-epoxide system silica can be formed, by fast condensation of prehydrolyzed TEOS. Method 2 was used in the organically crosslinked systems (Chapter 5 and 6) and will be referred to as pT2: prehydrolyzed TEOS with 2 mole water per mole TEOS.

2.4   General coating preparation

In general, the coatings were prepared by dissolving the organic and inorganic compounds in MPA to obtain a transparent viscous solution. The catalyst was added to the solution. The coating mixtures were applied on glass, chromated aluminum and chromated steel substrates. On acetone cleaned glass plates wet layer thicknesses of 30, 60, 90 or 120 μm were applied with a doctor blade. On aluminum and steel, which were cleaned and heated at 200 °C for at least 15 minutes, to activate the chromate layer, coatings were applied with a wire bar with various pitches. After a flash off time of 5 minutes at room temperature the coatings were cured in an oven. The curing

temperature and time have been varied. Generally used curing conditions were 140 °C for 1 hour (baking conditions) and 200 °C for 10 min. The choice for the curing conditions was based on the goal to have fully cured coatings and reproducible conditions at high temperatures. This was checked by the MEK (methyl-ethyl-ketone) resistance test. The coatings should resist 200 MEK rubs without damage to be qualified well cured. First experiments were performed in a drying oven, while in later experiments an air-circulation oven was used. No difference in the final cure was noticed.

2.5   Experimental details

2.5.1   Materials

The monomers and catalyst for the polyester synthesis were supplied by DSM Resins. The melamine resin hexakis(methoxymethyl)melamine (HMMM) was supplied by Cyanamid (Cymel 303) and Monsanto (Resimene 745). The trifunctional epoxide crosslinker, based on novolac phenolic resin glycidyl ether, was supplied by Shell (Epikote 155. EMM = 182 g/mole, number of epoxy groups per molecule is about 3.6 [98]). Tetraethoxysilane 98% (TEOS, Acros), 1-methoxy-2-propyl acetate (MPA, Merck), ethanol 99.8% (Biosolve), ethyl acetate 99.8% (Biosolve), 2-butanone 99 % (MEK, Aldrich), xylene (Lamers & Pleuger), potassium hydroxide volumetric standards 0.5N and 0.1N in ethanol (KOH, Aldrich), and 1,4-diazabicyclo[2.2.2]octane 98% (DABCO, Merck) were used as received. p-Toluenesulfonic acid monohydrate 99% (pTSA, Acros) was recrystallized from ethyl acetate and dried before use.

2.5.2   Polyester synthesis

Polyesters were synthesized according to conventional methods [2]. Under a nitrogen flow the diacids were melted in a flask of 4 L. The diols and triol were added, together with 1 wt.% n-butylchloro-tin(IV)dihydroxide (Fascat4101). The temperature in the flask was raised and kept at a maximum of 235 °C. To remove the water formed by the reaction a distillation set-up was used. The final amount of water was removed by refluxing with xylene, using a Dean-Stark set-up. The acid value of the polyester reaction product was followed in time and the reaction was stopped at an acid value below 1 mg KOH/g. The remaining xylene and low molecular weight compounds were removed at reduced pressure. The acid-terminated polyesters were synthesized from the hydroxyl-terminated polyester by melting the hydroxyl-terminated polyester together with a stoichiometric amount of succinic anhydride at 150 °C, until the calculated acid number was reached.

2.5.3 Characterization techniques

The acid value, the number of acid groups in the polyester in mg KOH/g, was determined by titration with standardized 0.1 M KOH in ethanol, according to DSM Resins test method TM-2401 (based on ISO 3682).

The hydroxyl value, the number of hydroxyl groups in the polyester in mg KOH/g, was determined by back titration with standardized 0.5 M KOH in ethanol, according to DSM Resins test method TM-2432 (based on C-V 17a, Hüls AG [101]).

NMR spectra were recorded on a Varian Gemini 300, using $CDCl_3$ as solvent with tetramethylsilane as internal standard.

Gel permeation chromatography (GPC) was carried out using a Waters Model 510 pump and a Model 486 UV detector (at 254 nm). The columns used were a PLgel guard-B 10 μm 50*7.5 mm precolumn, followed by 3 PLgel columns in series of 1000 Å (10 μm), 500 Å (5 μm) and 100 Å (5 μm). tetrahydrofuran (Biosolve stabilized with BHT) was used as eluent at a flow rate of 1.0 ml/min.

The glass transition temperature (Tg) was determined by differential scanning calorimetry (DSC, Perkin Elmer DSC7), with a heating rate of 20 °C/min from -40 to 80 °C.

The silica content was determined by thermal gravimetric analysis (TGA, Perkin Elmer TGA7), with a heating rate of 20 or 40 °C/min from 50 to 800 °C. For samples that expanded too much in the small sample holder of the TGA, a so-called gravimetrical 'burn-out' method was developed, in which the organic fraction of the coating is burned out in a ceramic oven. Samples were heated at 200 °C for one hour, then the temperature was set to 400 °C also for one hour, followed by heating up to 1000 °C. Then the oven was switched off, the samples were taken out at a temperature of 500 °C and further cooled down under vacuum, to prevent water condensation on the samples. These ash rests were assumed to be pure silica and weighed. With this method good agreement was found compared to TGA.

With scanning electron microscopy (SEM, Cambridge, Stereoscan 200) cross-sections of the coatings were studied. The samples were etched for 30 minutes with an oxygen plasma (Nanotech Plasmaprep 100) and then sputtered with Pd/Au for 3 minutes (BioRad SEM Coating System).

The viscosity was measured in time using a viscometer (Brookfield Model DV-II, spindle nr. 31).

The MEK resistance of coatings was determined according to ASTM D 4752. When a coating resists 200 MEK rubs it was qualified MEK resistant.

2.5.4   NMR assignments

The assignments of the ^{1}H and ^{13}C NMR spectra of the hydroxyl terminated polyesters (PE1-PE10) are summarized in Table 2.6. The assignments were made by comparing them with polyester assignments in literature [102–105].

Table 2.6: *Assignments of ^{1}H and ^{13}C NMR signals of PE1-PE10.*

ppm	molecular unit	PE1,PE2,PE3	PE4,PE5,PE6	PE9	PE10
^{1}H NMR					
8.67	IPA ring	$\checkmark$	$\checkmark$	$\checkmark$	$\checkmark$
8.22	IPA ring	$\checkmark$	$\checkmark$	$\checkmark$	$\checkmark$
7.56	IPA ring	$\checkmark$	$\checkmark$	$\checkmark$	$\checkmark$
4.5-3.8	CH$_2$	NPG	NPG, TMP	NPG, ED, CHDM	NPG, TMP. ED CHDM
3.3-3.5	CH$_2$OH	NPG	NPG, TMP	NPG, ED, CHDM	NPG, TMP, ED
2.35	AdA CH$_2$	$\checkmark$	$\checkmark$	$\checkmark$	$\checkmark$
1.65	AdA CH$_2$	$\checkmark$	$\checkmark$	$\checkmark$	$\checkmark$
1.5-0.8	CH$_3$	NPG	NPG, TMP	NPG, ED	NPG, TMP, ED
^{13}C NMR					
174	AdA C=O	$\checkmark$	$\checkmark$	$\checkmark$	$\checkmark$
173	AdA C=O	$\checkmark$	$\checkmark$	$\checkmark$	$\checkmark$
166	IPA C=O	$\checkmark$	$\checkmark$	$\checkmark$	$\checkmark$
165	IPA C=O	$\checkmark$	$\checkmark$	$\checkmark$	$\checkmark$
134-129	IPA ring	$\checkmark$	$\checkmark$	$\checkmark$	$\checkmark$
72	CH$_2$		TMP		TMP
70-68	CH$_2$	NPG	NPG	NPG, ED	NPG, ED
43-40	C$_{quart}$		TMP		TMP
36-34.5	C$_{quart}$	NPG	NPG	NPG, ED	NPG, ED
34	AdA CH$_2$	$\checkmark$	$\checkmark$	$\checkmark$	$\checkmark$
27	CH$_2$			CHDM	CHDM
24	AdA CH$_2$	$\checkmark$	$\checkmark$	$\checkmark$	$\checkmark$
22-21.5	CH$_3$	NPG	NPG	NPG, ED	NPG, ED
8-7	CH$_3$		TMP		TMP

Chapter 3

Characterization of Hybrid Coatings

3.1 Introduction

In the characterization of hybrid materials the challenge is to find techniques that can be applied on both organic and inorganic materials. Techniques applied on inorganic materials can often not be used in the same way on organic materials and vice versa, due to differences in properties of the organic and inorganic compounds. In hybrid materials though the properties of both compounds have to be considered simultaneously. Also the characterization of coatings, a thin layer on a thick substrate, can cause difficulties. The influence of the interface and the substrate should always be considered in relation with the properties of the coatings. In this chapter an account is given of the choices and assumptions made for the characterization of the hybrid organic-inorganic coatings. In the characterization of the morphology (Section 3.2) the sample preparation is the most important issue. For the characterization of the mechanical properties (Section 3.3) the interpretation of the results of various techniques is considered to be significant. The conclusions are summarized in Section 3.4. The applied equipment and the experimental details are described in Section 3.5. The preparation of several coating systems used in this chapter are described in the Chapters 4, 5 and 6, as is referred to in the text.

3.2   Morphology

The morphology of hybrid materials is determined by the way the organic and in-organic compounds are mixed. Since this mixing is on a micrometer scale, this can best be studied by scanning electron microscopy (SEM) or transmission electron microscopy (TEM). In general SEM shows features in the micrometer range where TEM visualized a nanometer range, but the sizes of structures visible with both methods depend also on the contrast in the samples. In SEM both surfaces and cross-sections of coatings can be studied. In general, though, the surface of the coating is not representative for the coating as a whole and therefore the study of cross-sections is preferred. Also with TEM cross-sections of the coatings were studied. Important for the preparation of samples for both techniques is not to damage the object to be studied: a thin coating layer supported by a thick substrate, during preparation.

3.2.1   SEM

With SEM a topographical plot of a surface is made. To create representative surfaces of cross-sections of the coatings, the materials must be broken in a brittle way. For coatings applied on metal this cannot be done, since the metal will not fracture but deform plastically. Coatings applied on glass can be used, because when the relatively large glass part is broken, the coating will also break as part of the sample. It is also possible to cool the sample, before breaking, below the glass transition temperature (Tg) of the coating, using liquid nitrogen. During this procedure it may occur that water condenses on the cold sample and penetrates in the coating or at the interface, possibly affecting the microstructure. Both methods were applied and compared on PE10-HMMM (hexakis(methoxymethyl)melamine) hybrid coatings with 11.4 wt.% silica (Chapter 5, Section 5.2). The results are shown in Figure 3.1(a) and 3.1(b). The surface of the sample that was broken after cooling had a rougher surface than the surface of the sample broken without cooling. Since SEM is a topographical method, it is preferable to have a smooth surface in which only the morphological structures cause the height differences. Preferably, the sample is smoothened first and than the morphological structure is revealed by creating contrast between the two phases, for example by etching (as discussed below). Smoothening of the surface of inorganic samples is regularly achieved by polishing. The samples are then embedded in a polymeric matrix, sometimes using high pressure and/or heating. The so-formed embedded samples are polished over several grades of sandpaper and a smooth surface is obtained. The produced pressure and heat, though, can deform the organic matrix, and possible silica particles in the microstructure can be polished away, changing the microstructure. For smoothening surfaces of polymeric materials regularly thin layers of material are cut away with a glass knife. But for the hybrid materials with silica

in the coating this cannot be done, since the silica can be scratched away with the glass knife leaving a damaged surface. Therefore, the rough broken surface is studied as it was and the samples were broken without further cooling.

To obtain the topographical contrast of the morphology of the organic-inorganic samples they are etched. With this technique the 'weakest' compound is removed, while the 'strongest' compound remains at the surface, thus creating a topographical difference. Since organic compounds are more reactive towards oxidation as compared to silica, they can be etched away with an oxygen plasma rather easily. Thus, to obtain contrast between the organic and inorganic phase an oxygen plasma was used to etch the surface of the samples for 30 minutes. Comparing Figure 3.1(b) and 3.1(c) the difference between etching an not etching of broken samples can be seen. The organic phase is etched away, without affecting inorganic particles present in the coating. The inorganic phase is much better visible when etching is used.
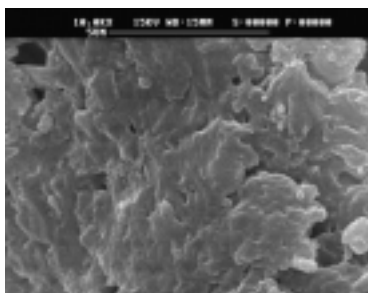
(a) Cold broken, unetched.
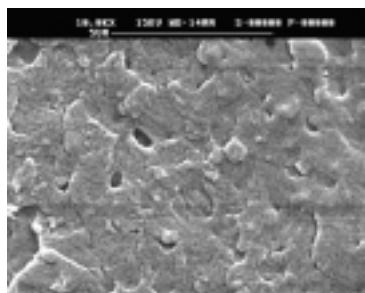
(b) Normal broken, unetched.
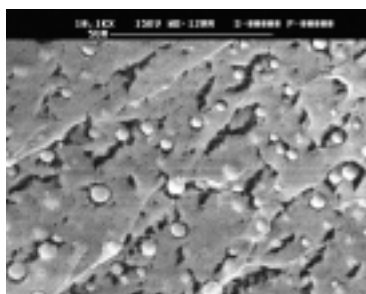
(c) Normal broken, etched for 30 min.

Figure 3.1: *Sample preparation: SEM photographs of PE10-HMMM-11.4 wt.% SiO$_2$ hybrid coatings: brittle fracture and etching.*

To study the samples under SEM, charging by the electron beam must be prevented by making the samples conductive. Therefore a thin layer, of only a few nanometers thick, of Pd/Au was sputtered on the surface and the sides of the glass samples were treated with colloidal carbon. The electron beam can also damage the sample, because of the large amount of energy that is produced. Low voltage will help to prevent this effect, but will also result in loss of resolution.

3.2.2   TEM

With TEM samples are studied in transmission and therefore very thin samples (100 nm) are necessary. To study cross-sections of the coatings on a substrate, layers are cut with a diamond knife. Therefore, it is important that the supported substrate is soft. Plastic substrates are preferable, but these cannot withstand the high curing temperatures used in the coil coating applications. Aluminum as a relatively soft metal can also be cut with a diamond knife. Therefore, the coatings applied on aluminum were used for the TEM studies. The thin layers were floated on a dimethyl sulfoxide/water mixture to be able to pick them up and to put them on TEM grids. The contrast in TEM is obtained from differences in electron densities. Since silicon has a high and carbon a low electron density no further treatment was necessary. One should bear in mind that beside the electron density also the thickness of the sample influences the amount of transmission through the film.

3.3   Mechanical properties

In the research on hybrid organic-inorganic materials for hard and flexible coatings focus was on the increase of the hardness of coatings by the inorganic part. In the practice of coil coating applications the hardness is measured by the pencil hardness test (ASTM D3363). This test only gives practical information relative to known systems. Besides the dependency on adhesion, also the performer and even the brand of pencils used appears to be important [106]. There are several other hardness tests available, which can give more reliable information. Hardness itself is a not well-defined characteristic. [106–109]. Fink-Jensen [107] defined hardness of a substance as 'its ability to resist the temporary or permanent creation of a surface wholly or partly within its original boundaries, when the surface is locally subjected to compressive stresses that vary strongly along the boundary surface'. This is a complex statement to say that hardness is a measure of the resistance to permanent deformation or damage [108]. Even with this definition care should be taken, since the top of a coating is quite often harder than the bulk of the coating. Smoothness of the coating influences the measurements and also the type of substrate, adhesion to the substrate

and heterogeneity within the coating can influence the hardness measurements. For the determination of hardness every coatings branch has developed its own tests, based on its practical applications. These tests can be divided in three general classes: indentation (e.g. Knoop, Buchholtz, Fisherscope), scratch (Pencil, Taber abraser) and pendulum (Persoz, König, Sward) hardness. For details of various methods is referred to the ASTM norms and literature [108–112]. The various classes determine hardness under various conditions, resulting sometimes in different conclusions, depending upon the method used.

The various hardness tests on organic coatings have been compared in literature. The pendulum hardness is described as being comparable with micro-indentation [108, 113]. Especially at very low and very high hardnesses the indentation method differentiates better. The pendulum hardness test has also been compared with the scratch resistance test [114]. It was found that for highly crosslinked coating systems, the scratch or mar (small surface scratches) resistance is determined by the flexibility of the coating. More elastic coatings are better scratch resistant but have a lower König hardness. The same conclusions were made by the group of Jones [115], who compared micro-indentation with micro-scratching. Also Courter [116] found a better mar resistance for systems with a lower indentation hardness and modulus. General relations cannot be made easily. The time scale, which is a very important variable for visco-elastic materials, of for example indentation measurements (minutes) and König hardness measurements (1/50 seconds) is already largely different [108]. It would be better to determine independent materials characteristics like the yield strength and elastic modulus, but the problem herein is that for tensile testing or dynamic mechanical analysis free films of well-defined and uniform thickness and shapes are necessary [110] and these could not be obtained for the systems studied in this research. Instead, various hardness tests (pendulum, indentation and scratching) have been used and studied critically, as described in the following sections.

The flexibility in the hybrid coatings was obtained from the polyester resin. By changing the molecular composition the flexibility can be adapted. It appeared difficult to determine the flexibility quantitatively. In the practice of coil coating applications flexibility is measured by bending the coating and substrate in a T-bend test (ASTM D4145) or Mandrel bend test (ASTM D522), but these methods only give qualitative information and they depend on a number of factors, such as the layer thickness, substrate thickness and adhesion. Other techniques have been investigated to determine flexibility. The bending test is a method applied on inorganic coatings in which the angle of pure bending and the displacement are monitored as function of the applied force until fracturing of the coating occurs [117]. In this way the flexibility is determined in terms of strain at fracture. Unfortunately, this method could not be applied on the flexible hybrid coatings since the strain at fracture was too high to obtain cracking of the film within the limits of the bending of the equipment. It was also not possible to apply tensile testing, a method that measures strain at break directly [110],

since it was not possible to make free films with uniform thickness and shape. No satisfying way was found to determine the flexibility quantitatively. The focus of this research is on the influence of the inorganic component, in situ formed silica in hybrid polyester based coatings, on the hardness. It is expected that the flexibility can be adapted, when necessary, by changing the composition of the polyester.

3.3.1   Pendulum hardness: König hardness

The König hardness measuring device comprises 'two steel balls resting on the horizontal sample surface; connecting bars form the upper side of a vertical frame which encircles the sample. As the centre of gravity of the frame is below the balls the set-up is a pendulum, which, when swinging, gives the balls a reciprocating rolling movement on the coating' [108]. The balls roll over the coating surface with a constant load. The material in front of the balls is compressed and released immediately after passage of the balls. The time necessary for the pendulum amplitude to decrease a defined amount is measured as König hardness. The reciprocal value of this time is a measure of the energy transferred in the material that the balls pass in one second. In fact, friction and deformation are both influencing the time of swinging of the pendel and thus the König hardness. Since both deformation characteristics and friction behavior determine the value of the König hardness, materials with different visco-elastic behavior should not be compared [106]. Furthermore, the König hardness is known to be dependent on the layer thickness. The relation of König hardness versus layer thickness is generally described by a power law function [107]. Such functions can be used to compare results of measured König hardnesses at various layer thicknesses, as explained below.

Experimental results

For various coating systems (preparations are described in Chapter 4, 5 and 6, respectively) the König hardness was measured as function of the final layer thickness of the coating and power law relations of the König hardness versus coating layer thickness were fitted through the results. In Figure 3.2 the results of these measurements on a typical PE9(1)-TEOS (tetraethoxysilane) based system (9 wt.% SiO_2), two days after application and later in time, are shown. The decrease of the König hardness in time is caused by degradation of the network, as will be discussed in Chapter 4. In Figure 3.3 the power law relations of a large number of coatings based on PE6, HMMM and various amounts of pT2 (prehydrolyzed TEOS, see Section 2.3) are plotted. The relations obtained are all very similar. The averaged function for all these measurements is plotted in the figure. For the polyester-epoxide system the
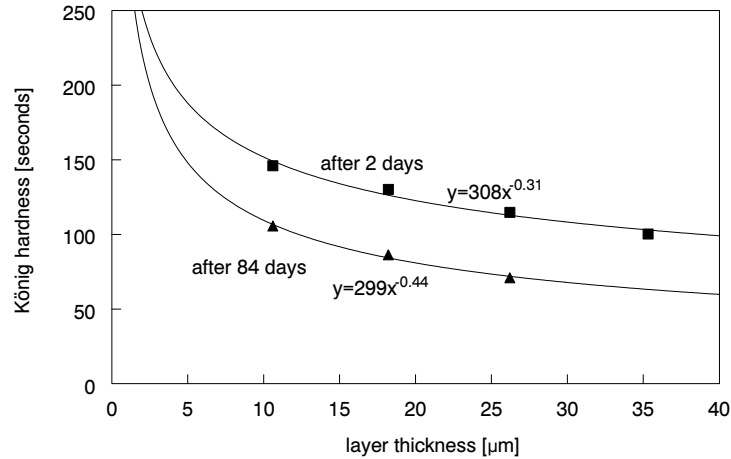
Figure 3.2: *Fitted power law relations of the König hardness as function of the coating thickness for hybrid coatings (containing 9 wt.% SiO_2) based on PE9(1) and TEOS, cured at 140 °C for 30 minutes (Chapter 4), measured after 2 and 84 days.*

power law relations have been determined for silane-modified polyester based system, of which the silane-modification was performed by two different methods: the excess and the stoichiometric method (see Chapter 6). In Figure 3.4 the relations of various systems are shown. When all curves in the Figures 3.2, 3.3 and 3.4 are compared it is clear that the dependency on the layer thickness is small around 20 μm, the usual application thickness of the coatings. Furthermore, the shapes of the various curves are alike, indicating that the coatings show similar visco-elastic behavior and therefore the König hardnesses of the systems can be compared. These power law relations were used in Chapter 4 and 6 to calculated the König hardness for a range of coatings at a certain film thickness knowing the real thickness of the coatings.

3.3.2   Micro-indentation

In indentation tests well-defined geometries of indenters are forced perpendicularly into the coating surface and the area deformed is measured. Indentation measurements are based on the principle that hardness is defined as the ratio of an applied force and the vertical projection of the deformed area [118]. Indentation tests on organic coatings are mainly based on macroscopic deformations [106, 109, 112, 119, 120]. This means that the load of the indenter is high (Newton range) and therefore the indentation is deep. In general it is assumed that when the indentation exceeds 10 % of the film thickness the influence of the substrate starts to count [108]. Furthermore,
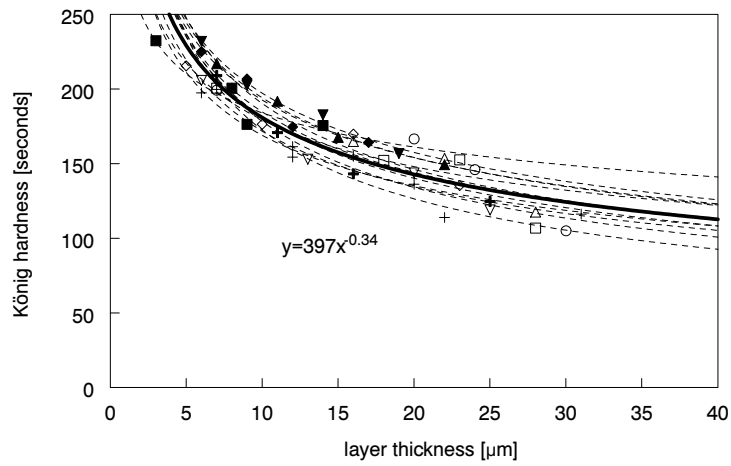
Figure 3.3: *Fitted power law relations of the König hardness as function of the coating thickness for hybrid coatings based PE6, HMMM and various amounts of pT2, cured at 200 ° C for 10 minutes (Chapter 5). The given equation is the average function of all measurements, represented by the thick line.*
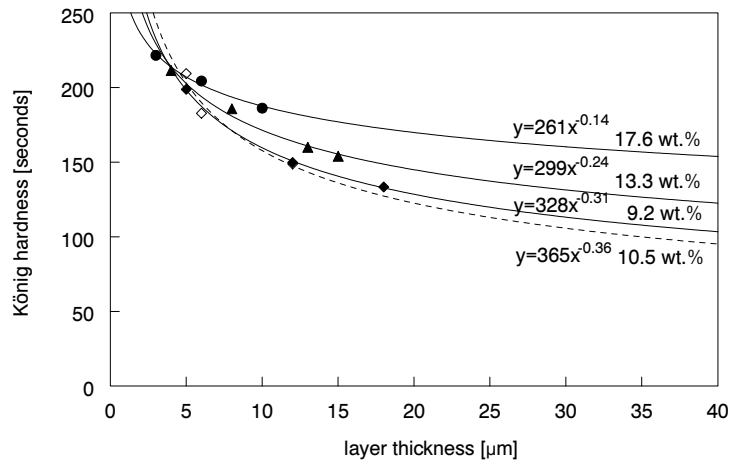
Figure 3.4: *Fitted power law relation of the König hardness as function of the coating thickness for hybrid coatings based on Si-PE6a-epoxide and various amounts of pT2, cured at 200 ° C for 10 minutes. Si-PE6a synthesized by the excess method (open markers and dotted line) and by the stoichiometric method (closed markers and solid lines) (Chapter 6). The weight percentages in the plot are the determined amounts of silica in the coatings.*

the visco-elastic behavior of the coatings complicates the interpretation of the results, since the area (A) changes in time [106, 121]. More fundamental research on (micro)-indentation measurements has been done on metals and ceramic materials, which behave elastic-plastic and for which visco-elastic behavior is less significant than it is for organic materials. In the research on hybrid coatings as described in this thesis the micro-indentation method was used, where relatively low forces are applied (mN range). The influence of the visco-elastic behavior is accounted for as described below.

The basics

In a micro-indentation experiment a well-defined indenter is forced perpendicular into a coating surface while the force is measured as function of the displacement, during loading (increasing force) and unloading (decreasing force). The force (F) and displacement (h) are measured. This results in a curve as schematically plotted in Figure 3.5. The loading curve is conveniently described by a power law relation [122]:

$$F = \alpha h^m \tag{3.1}$$

where α and m are constants. The value of m depends on the geometry of the indenter. Although often the unloading curve is assumed to be linear, this curve can also be described by a power law function [122]. More often, for calculation purposes, the unloading curve is described by a polynomial function [123].

From these curves the hardness and elastic modulus can be calculated. The hardness (H) can be determined as [122]:

$$H = \frac{F_{max}}{A} \tag{3.2}$$

where F_{max} is the maximum force applied and A is the projected area of indentation. The reduced elastic modulus (E_r) can be determined from the stiffness of the material (S) [121, 122, 124]:

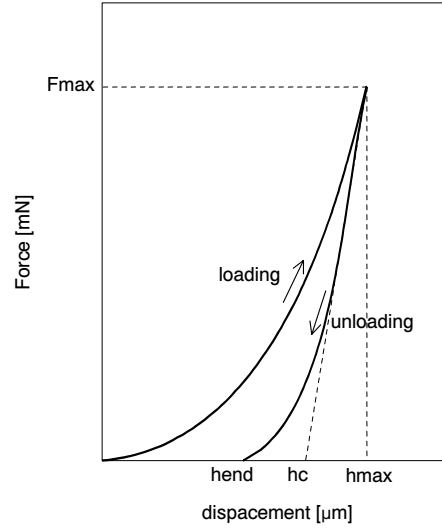$$S = \frac{dF}{dh} = (\frac{2}{\sqrt{\pi}}) E_r \sqrt{A} \tag{3.3}$$

Figure 3.5: *Schematic plot of a force-displacement curve as measured by micro-indentation. F_{max} is the maximum applied force, h_{end} is the final displacement, h_c is the contact displacement and h_{max} is the maximum displacement.*

E_r is a function of the elastic moduli of the material (E) and the indenter (E_i) and their Poisson ratios $(\nu$ and $\nu_i)$ [121, 122, 124]:

$$\frac{1}{E_r} = \frac{(1 - \nu^2)}{E} + \frac{(1 - \nu_i^2)}{E_i} \tag{3.4}$$

These formulations have been developed for materials behaving purely elastic-plastic. For visco-elastic materials time dependency should be taken into account.

Determination of A, H and E

For the calculation of both the hardness and elastic modulus the determination of the area (A) is highly significant, as follows from the equations (3.2) and (3.3). The area (A) of an indentation is not unambiguous. Since the coatings show visco-elastic behavior there is a change of size in time. For the hardness the plastic deformation must be determined and this is best described by the final area, which can be determined by microscopy, after indentation. When the determination took place after a longer period of time than the retardation time this should give valid values. When

the area is too small to find the indentation back on the sample another way must be applied. Using knowledge of the geometry of the indenter, the indentation area can also be calculated. For an ideal Berkovich pyramid (the form of the indenter that has been used in the measurements) the area function can be described as [122, 124]:

$$A(h) = 24.5h^2 \tag{3.5}$$

For the area calculation as used in the determination of the hardness some assumptions must be made. The indentation depth includes both plastic and elastic displacement and hardness is defined as the resistance to plastic deformation. Therefore the elastic part of the indentation must be subtracted from the total indentation [124]. This can be done by assuming that the so-called plastic depth or contact depth (h_c) is the depth of the indenter in contact with the sample under load [122, 124]. This depth can be determined by fitting a straight line to the initial unloading data and extrapolating this line on the depth axis (schematically shown in Figure 3.5). Hereby it is assumed that during initial unloading the area in contact with the indenter remains constant. To calculate the area (A) $h = h_c$ must be applied in equation (3.5). The area for the elastic moduli calculations is the area of elastic contact [122] and is also calculated via the contact displacement (h_c) [122, 124]. The calculations are based on methods derived for inorganic materials and there is not accounted for non-ideal tip shapes, elastic-plastic contact of the tip, machine compliances and time dependency [125].

An influence of the substrate on the values of the hardness and elastic modulus is expected. The hardness of aluminum is in the range of 1 GPa (determined average: 0.94 GPa), while the organic coatings show an hardness of around 0.3 GPa. This means that at deeper indentation depths some effect is expected. For the elastic modulus the influence is expected to be more severe since the elastic modulus of aluminum is around 70 GPa (determined average: 70 GPa), while the elastic modulus of polymeric materials is around 3 GPa. Thus, the difference in elastic modulus is much larger than the difference in hardness and the increase with increasing depth will also be larger. The elastic modulus is thus best determined by extrapolating the calculated value as function of the indentation depth to $h = 0$. But since the top layer of the coating may behave differently from the rest of the coating, care should be taken in extrapolating. The overall statement is that when less than 10% of the film thickness is indented the hardness will not be influenced by the substrate [108]. In this thesis the calculated data for both the hardness and elastic modulus is plotted in the figures and the average values, summarized in the tables, are calculated using the data points below 10 % of indentation.

Experimental results

Before hardness and elastic moduli of various hybrid coatings were calculated and compared, several parameters were studied. An extensive study on the influence of the visco-elastic behavior on the indentation method was not performed, but it was tried to get an indication of the effects. The determination of the area (comparing measured and calculated values), the influence of repetition of the loading-unloading cycles and the influence of the indentation rate were studied on various systems as summarized in Table 3.1. The systems containing HMMM are described in Chapter 5 and the systems containing epoxide are described in Chapter 6. The results of the measurements are described below.

Table 3.1: *The use of various coatings systems (described in Chapter 5 and 6) to study various parameters for the indentation measurements summarized.*

Area determination:	PE10-HMMM
	PE10-HMMM-11.4 wt.% SiO_2
Repetition cycles:	PE10-HMMM
	PE10-HMMM-11.4 wt.% SiO_2
Rate of indentation 0.4 nm/s & 10 nm/s:	PE10-HMMM
Rate of indentation 5 nm/s & 10 nm/s:	PE6-HMMM
	Si-PE6a-epoxide (1.8 wt.% SiO_2)
	Si-PE6a-epoxide-25.1 wt.% SiO_2

Area determination
The areas of the indentations were determined by SEM and compared to the calculated values. An example of an indentation studied by SEM is shown in Figure 3.6. The area was determined by connecting the three top points assuming the indentation to be a perfect triangle. The area calculation was done by applying h_c in equation (3.5). In Figure 3.7 the results are compared and the agreement for both the organic and hybrid systems is satisfying. Consequently, for coatings in which the SEM area could not be determined the relation of equation (3.5), using $h = h_c$, was applied.

Repetition cycles
To be sure that the unloading curve was mostly elastic the loading-unloading cycle was repeated five times [122]. The unloading was performed to 10 % of the maximum indentation force before increasing the force for the next cycle. An example of such a repeated measurement is shown in Figure 3.8. When the behavior is purely elastic the shape of the unloading curve after repetition should not change anymore. To
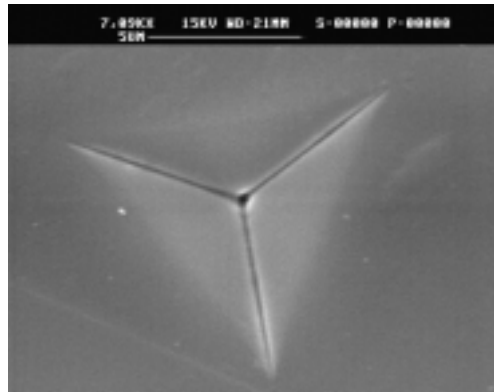
Figure 3.6: *SEM photograph of an indentation of a Berkovich pyramid in a PE10-HMMM coating with a force of 9 mN, repeated 5 times.*
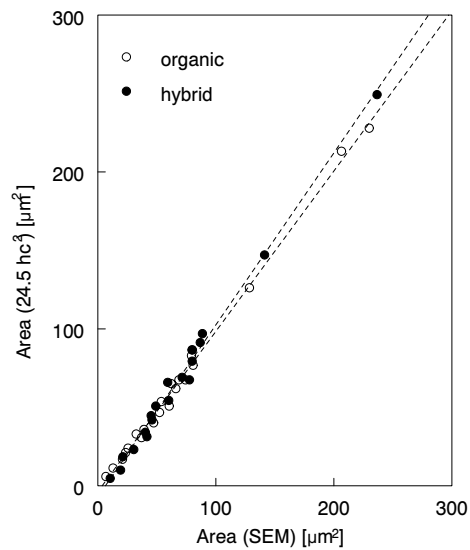

Figure 3.7: *Area determination of the indentations, comparing SEM results with displacement calculations, for an organic (0 wt.% SiO_2) and a hybrid (11.4 wt.% SiO_2) coating based on PE10 and HMMM.*
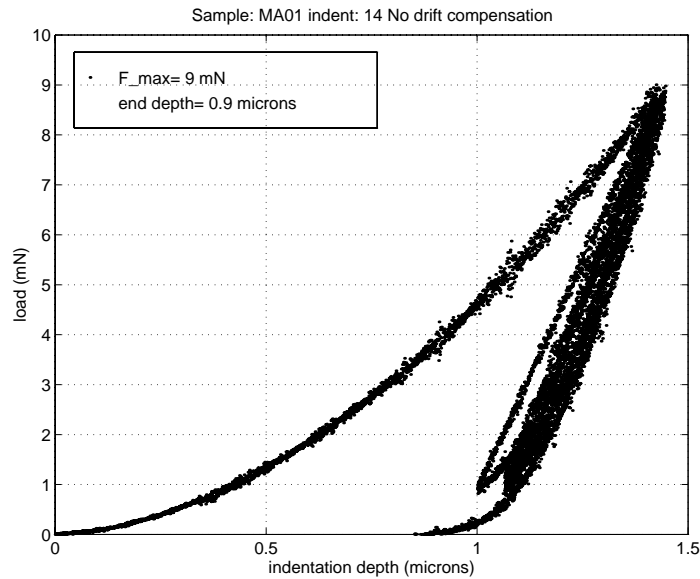
Figure 3.8: *Micro-indentation: force-displacement curve of a PE10-HMMM coating with a maximum force of 9 mN, in which the loading-unloading cycle is repeated five times.*

study the shape of the curve the slope of the various repeat steps of both the organic and the hybrid coatings were determined and the results are plotted in Figure 3.9. The slopes were determined by fitting a polynomial of the second degree through the measuring points and determining the derivative at the maximum force. For the last curves higher polynomial functions were applied, to be able to fit also the last part of the curve. The slope after five indentations differed not much, only the first cycle appears to be slightly smaller. It is concluded from these results that after a repetition of five cycles the unloading curve shows elastic behavior and the elastic modulus can be determined. The last curve was used for the determination of the slopes that were applied for the calculation of E_r.

Although the shape of the curves after repetition did not alter much, the indentation depth after each repetition increased, caused by creep. Creep is the displacement in time at constant force, and could unfortunately not be measured with the current set-up. It is assumed that all coatings show a similar visco-elastic behavior, which was also suggested by the comparable power-law relations of the König hardness as function of the layer thickness. This means that results can be compared but that no absolute values can be obtained.
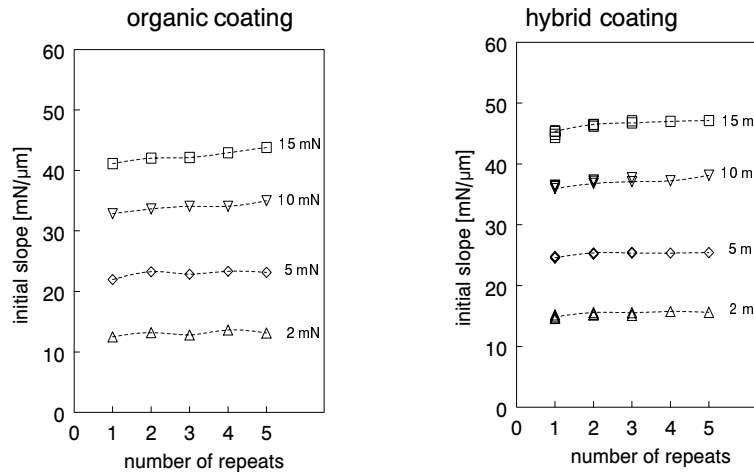
Figure 3.9: *Influence of the number of repeats of the loading-unloading cycles on the slope of the unloading curves for various applied maximum forces. Left: the organic PE10-HMMM coating, right: the hybrid PE10-HMMM coating with 11.4 wt.% SiO₂.*

Rate of indentation

The influence of the rate of indentation was studied on several coatings, as summarized in Table 3.1. The standard rate of 10 nm/s was compared with slower rates by comparing the calculated area (using h_c) and the initial slope, since these two parameters were used for the calculation of the hardness and the elastic modulus. In Figure 3.10 the influence of the rate on the organic PE10-HMMM coating is plotted. No large influence is noticed, even at the very low rate of 0.4 nm/s. But when the organic PE6-HMMM coatings were studied (Figure 3.11), already at 5 nm/s both the area and slope were influenced. The effect of the indentation rates on the slope and area of silane-modified PE6a-epoxide coatings without extra pT2 (1.8 wt.% SiO$_2$ in Figure 3.12) is also a large, but this effect disappeared when extra pT2 was added (25.1 wt.% SiO$_2$ in Figure 3.12). The results described here only give an indication of the influence of visco-elastic behavior on the coatings. When the change of rate influences the properties this means that the retardation times are longer than the measuring time. This makes comparing various results more difficult. The limited influence of the rate of indentation on the PE10-HMMM series and the hybrid silane-modified PE6a-epoxy system shows that these coatings have a less time dependent behavior than the systems which show an effect of the rate of indentation on slope and area determination.

Figure 3.10: *The influence of the rate of indentation on the slope (left) and area (right) as function of the maximum applied force for organic PE10-HMMM coatings.*
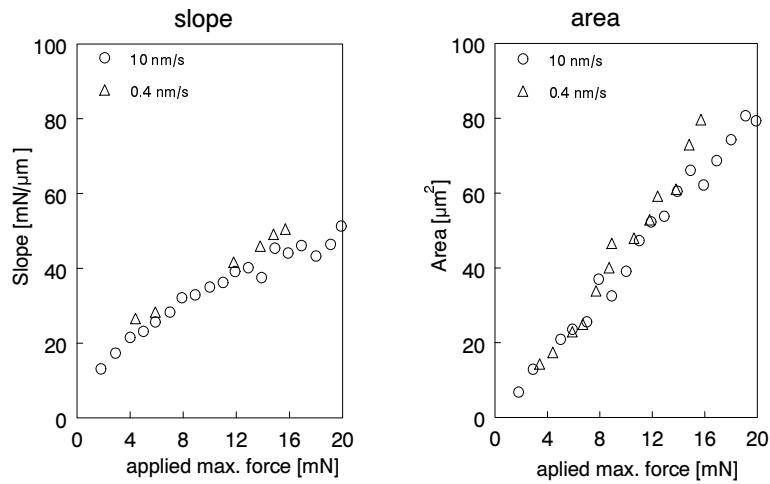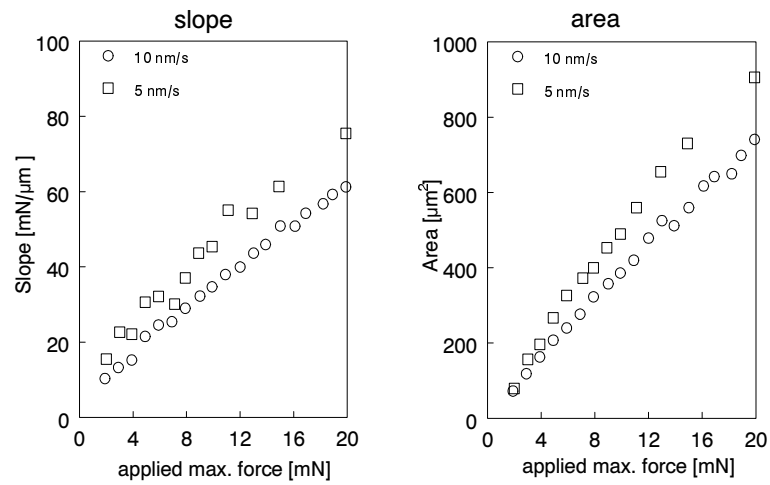

Figure 3.11: *The influence of the rate of indentation on the slope (left) and area (right) as function of the maximum applied force for organic PE6-HMMM coatings.*
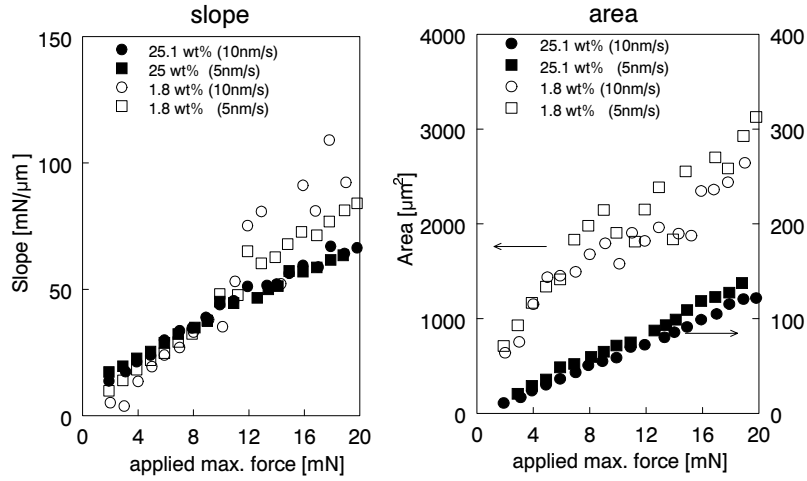
Figure 3.12: *The influence of the rate of indentation on the slope (left) and area (right) as function of the maximum applied force for silane-modified PE6a-epoxide coatings without (1.8 wt.% SiO_2) and with pT2 (25.1 wt.% SiO_2) added. Remark that for the area of the hybrid coatings the scale is 10 times smaller than for the organic coatings.*

3.3.3 Micro-scratching

The scratch resistance of a coating is also a measure of hardness, since it is the resistance of deformation, applied by a forced scratch. The terms scratch resistance, wear resistance and mar resistance are all used for this form of deformation. Mars are surface defects that are large enough to degrade the appearance of a polymer surface, but are small with respect to the coating thickness [126, 127], while in wear removal of materials takes place [128]. Scratch resistance is a more general term for both. Studying well-defined single scratches can give better understanding in the mechanism of wearing and marring [116, 126, 127, 129, 130].

An important feature of scratch resistance is the friction. 'Friction is the tangential resistance to motion which is experienced when one body moves relative to another' [128]. The coefficient of friction, μ, is the frictional force (F_{fric}) divided by the normal force (F_n) on contact:

$$\mu = \frac{F_{fric}}{F_n} \qquad\qquad (3.6)$$

The mechanism of friction is complex because it includes adhesion, roughness of the surface (asperity interaction) and plastic deformation. There are several models to describe the mechanism of friction. The most simple model is the adhesion theory, in which it is assumed that the surface consists of asperities, the interface is made up of asperity contacts and the frictional force is given by [131]:

$$F_{fric} = A_r \cdot s \tag{3.7}$$

in which A_r is the real area of contact and s is the interfacial shear strength. The real contact area is related to the hardness (H) of the material, based on the assumption that the real area must be large enough to support the given load (F_n) [131]:

$$A_r = \frac{F_n}{H} \tag{3.8}$$

This model forms the basis of many other models [128, 131–133]. In an attempt to formulate a general friction equation the separate effects of asperity, debris, ploughing and adhesion were considered [131, 133]. In practical use such equations are simplified by assumptions for the specific situation. For the determination of friction on polymeric materials, for example, the adhesion and ploughing terms are considered to be the most important [134]. The adhesion causes a force necessary to shear during sliding while ploughing (the displacement of materials), is necessary due to interpenetration of asperities [135]. It has also been described in terms of crazes (ploughing) and shear yielding (adhesion) [136, 137].

For the study of scratch resistance on coatings low forces are necessary, to prevent scratching through the total coating into the substrate, since then adhesion to the substrate is measured as well. Various groups have developed equipment for applying low forces. One way followed was to decrease the forces normally used for friction experiments to mN scale [116, 129, 138]. Another way is to adapt an atomic force microscope (AFM) with a harder tip and a cantilever with increased stiffness, increasing the forces applied normally in AFM up to μN [115, 127, 139, 140]. Courter and coworkers [116] compared various methods, both micro-scratchers and micro-indenters, on automotive clear coats. Marring or damaging the surface coating was defined as permanent plastic deformation that could be plastic flow or fracture. They concluded that when fracture is the cause of marring, this can be studied best with the micro-scratcher, while when the dominant failure is plastic deformation the indentation test will give more information. In their study the fracturing appeared to be the most important deformation for marring. This was noticed visually by SEM, but also by increased fluctuation of displacement of the scratcher with increasing force on the scratcher. The same feature for marring, increased fluctuation displacement, was given by Gregorovich and co-workers [129]. Also Jones and coworkers [115, 127, 139, 140] studied

mar resistance using a single stylus scratcher. They quantified the elastic deforma-
tion, plastic deformation and fracture by correlating them to cross-sectional areas
of the deformed regions after scratching. These cross-sections of the scratches were
imaged by AFM. The size of the cross-sectional area of the indenter, the scratch and
also the pile-up at the shoulders of the scratch were determined, assuming them to
be perfect triangles [139]. The recovery of plastic deformation, visco-elastic creep,
was quantified by studying the cross-sections of the scratches in time. The reduction
of the total volume of the shoulders (cross-section area · length of the scratch) was
described as a function of time [140]:

$$V_{tot}(t) = V_0 e^{kt} + V_{plastic} \qquad (3.9)$$

in which the first term describes the volume reduction in time, with V_0 as the initial
volume of the recoverable part and k is the visco-elastic creep rate. The second term
is the permanent plastic deformation. By fitting this relation on the measuring data
points V_0, k and $V_{plastic}$ were determined.

They also defined the practical quantity: the 'micro mar resistance' as the normal
force divided by the cross-sectional area that was between the shoulders and the
scratch. This self-defined quantity is very similar to the hardness of the material as
described in equation (3.2) and (3.8), which is the hardness of the film at the applied
force. The more general applied term is scratch hardness [130,137]. Assuming a round
tip the vertical projected area can be described by πr^2 for pure vertical indentation
and by $\pi r^2/2$ for pure horizontal sliding [137]. Since the vertical speed is many times
smaller than the horizontal speed, purely horizontal slide can be assumed and $A_r = \pi r^2/2$. Briscoe and coworkers [130] ennobled this assumption by a correction factor
distinguishing between rigid plastic and visco-elastic plastic materials. They also
divided the most common deformation regimes into five categories: elastic hysteresis,
ironing, ploughing, regular crack formation and machining. In the first category the
energy dissipation arises from elastic hysteresis loss, without a sign of deformation,
since the scratch fully recovers. In all other categories deformation is noticed and is
getting more severe from ironing to machining. These categories were used to make
scratch maps for polymers, showing that, depending on scratch hardness, scratch
speed, shape of the indenter and temperature, the deformation mechanism alters.

The scratch tester used in this research was designed to bridge the gap between atomic
scale and macroscopic tribology by applying a single well-defined asperity (tip) in
contact with a surface. The forces used were low (mN), so that no influence of the
substrate was expected. The aim of the experiments was to study the well-defined
scratches as a measure of the scratch resistance. For this purpose one scratch speed
(10 μm/s) was chosen and various forces were applied. The scratches were studied
with AFM afterwards.

3.4   Conclusions

By selecting techniques used on organic and inorganic materials, we succeeded in finding useful characterization techniques for hybrid coatings.

For the morphology of the hybrid coatings both SEM and TEM are used. With SEM etched crosscuts of brittle broken coatings on glass substrates can be studied to reveal the silica structure in the coating in the micrometer range. With TEM coatings applied on aluminum substrates can be studied in the nanometer range.

For the flexibility no quantitative methods were found, but from several hardness determination tests information about the mechanical behavior of the hybrid coatings can be obtained. With König hardness quickly an indication of the hardness can be obtained, without too much influence of the layer thickness for coatings of around 20 μm. With micro-indentation measurements hardness can be determined more precisely (in GPa) and also an indicative value of the elastic modulus can be calculated. Furthermore, micro-scratching can give information about the friction behavior of the top of the coatings. With this set of techniques the hybrid coatings are characterized in the following chapters.

3.5   Experimental details

Layer thicknesses of the coatings on glass substrates were determined by a micrometer (Coatchecker VC-2, Evano Instruments). On aluminum substrates they were measured with the eddy current principle (Twincheck, List Magnetik).

Scanning electron microscopy (SEM, Cambridge, Stereoscan 200) was performed on cross-sections of coatings on glass substrates. In case of etching, this was done for 30 minutes with an oxygen plasma (Nanotech Plasmaprep 100). The samples were sputtered with Pd/Au for 3 minutes (BioRad SEM Coating System). For the images of the micro-indentations 1 minute sputtering was applied.

Transmission electron microscopy (TEM, Jeol 2000 FX) was performed on samples with a thickness of 100 nm. The samples were microtomed (Reichert Ultracut E/FC-4D) at -50 °C and subsequently floated on a dimethyl sulfoxide/water mixture.

König hardness was measured with a König pendulum apparatus (Pendelhärteprüfer Model 299/300, Erichsen), according to ASTM D4366, on coatings on glass substrates.

Micro-indentation was performed on a homebuilt nano-indenter, with a Berkovich diamond pyramid indenter.

Micro-scratching was performed on a homebuilt micro-scratcher, using a diamond tip, with a radius of 8 μm. A normal force, perpendicular to the coating surface was applied and scratches were made with a speed of 10 μm/s.

Chapter 4

Polyester-TEOS Interactions

4.1 Introduction

An important feature of hybrid materials is the interaction between the organic and inorganic phase. The final properties of hybrids do not depend only on the properties of the individual organic and inorganic components, but also on their interfacial properties, which are related to the morphology of the hybrid materials [53, 141]. Therefore, hybrid materials are often divided in two classes based on these interactions [50, 54, 142]. Class I materials are physical hybrids that correspond to materials in which the organic and inorganic components exchange weak bonds through van der Waals, hydrogen or ionic interactions. Class II materials are chemical hybrids that correspond to hybrid systems in which the organic and inorganic components are covalently.

The chemical nature of the interactions in hybrid materials has been studied by Landry and co-workers [100] on model systems based on in situ polymerized tetra-ethoxysilane (TEOS) in various polymers. The polymerization of TEOS results in the formation of Si-OH groups and Si-O-Si bonds, as explained in Section 1.1. They concluded that polymers that have no functionality capable of forming covalent bonds with the polymerizing TEOS can form class I hybrids with hydrogen bonding, but only under acidic conditions and when hydrogen bond acceptors are present on the polymer chains. Under these conditions silica chains are highly hydrated and can thus interact with the hydrogen bond acceptors (Figure 4.1: hydrogen bonding). Saegusa [45, 143] determined with FTIR and ^{13}C NMR that class I hybrids were formed by hydrogen-bond interaction between the silanol groups of a silica gel, formed by
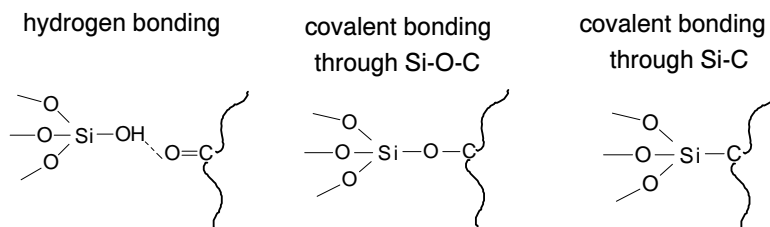
Figure 4.1: *Possibilities of bonding mechanisms between inorganic, siloxane based materials and organic based polymers. The left side of each picture is the inorganic part, while the right side is the polymeric part.*

the sol-gel reaction of TEOS, and the carbonyl groups of various carbonyl-containing polymers. Also Tian and coworkers [144] determined hydrogen bonding with FTIR by a shift of the carbonyl group of poly(ϵ-caprolactone) when in reaction with polymerizing TEOS.

To study the differences between class I and class II hybrid materials Landry and coworkers [145] compared nonfunctional polyacrylates with silane-functionalized polyacrylates, both in combination with polymerizing TEOS. For the silane-modification methacryloxypropyl trimethoxysilane was incorporated in the acrylate backbone. Covalent interactions between the inorganic and organic components are thus formed (Figure 4.1: covalent bonding through Si-C). The morphology and mechanical properties of these class I and class II hybrids were studied. The influence of the silane-functionalization on the morphology was small, compared to the effect of interactions between polymerized TEOS and the organic backbone. Furthermore, for both types of hybrids the same mechanical properties were obtained.

Beside silane-functionalization of organic compounds, class II hybrids can also be achieved via hydroxyl-containing organic compounds. The hydroxyl groups of the organic component can react with silicon alkoxides, thus forming a covalent bond between the organic and inorganic compounds (Figure 4.1: covalent bonding through Si-O-C) This type of bonding is also covalent, but since Si-O-C bonds are sensitive towards hydrolysis, the bonding is less stable than the Si-C bonding. An early example of synthesized hybrid materials was based on hydroxyl-terminated polydimethylsiloxane and TEOS [99, 146]. The reaction between the organic and inorganic phase is based on the formation of Si-O-Si bonds, which is as permanent as an Si-C bonding. When hydroxyl-functional polymers with a carbon backbone reacted with TEOS, Si-O-C bonds can be formed. It appeared difficult to prove the formation of an Si-O-C bonding. It cannot be detected by ^{29}Si NMR as the Si-O-CH$_2$ signal of the interaction cannot be distinguished from the Si-O-CH$_2$ of unhydrolyzed alkoxy groups of TEOS that also will be present in the hybrid system, because the differences in the chemical environment are too small. Alternatively, ^{13}C NMR can be applied for detecting the

Si-O-CH$_2$ bonding. However, few examples have been presented in literature. Novak and co-workers [26] reported on a shift from 59 ppm to 63 ppm in CP-MAS ^{13}C NMR of the resonance of the methylene carbon adjacent to the hydroxyl group of poly(2-hydroxyethyl methacrylate) in reaction with TEOS, thus proving Si-O-CH$_2$ bonding. The assignment of Si-O-CH$_2$ at 63 ppm was confirmed by others [147] in a reaction of polymethylhydrosiloxanes with hexanol. The use of FTIR and Raman spectroscopy shows the same difficulties as NMR: the large similarity of Si-O-C bonds in the hybrid and in TEOS. Besides, another difficulty in proving the formation of the covalent bonding is the small amount of Si-O-C bonds present in the hybrid systems compared to the total number of bonds, causing overlap of signals. To be able to see the small Si-O-C signals in the spectra of hybrid systems, spectra of the individual compounds should be subtracted. With FTIR this has been done for example by Xue and co-workers [148] in their study on the interaction between model polyesters and γ-glycidoxypropyltrimethoxysilane. The difficulty is to find a characteristic signal of the individual compounds to be able to subtract properly.

Proving or disproving reaction between hydroxyl groups of organic compounds and silicon alkoxides has been reported in literature mainly by determining gel contents of the hybrid materials by extraction with organic solvents [33, 43, 149, 150]. When after extraction high amounts of insoluble materials (the gel content) were obtained, Si-O-C bonds between the organic and inorganic compounds were presumed to have been formed. Other ways to prove the formation of Si-O-C bonds reported were by detecting ethanol or methanol by FTIR [48] or GC [49]. These alcohol were claimed to be formed by reaction of TEOS or tetramethoxysilane with hydroxyl groups of the organic compound. However, these alcohols could also have been formed by reaction of the alkoxide groups with any water present in the system. Therefore, this method cannot be used for a full prove of the reaction of an organic hydroxyl group with polymerizing TEOS, unless the system is completely water free.

The hybrid coatings studied and reported in this thesis were all based on a combination of polyester resins and TEOS. The polyesters contain carbonyl groups in the backbone that can form hydrogen-bonds (Figure 4.1: left) with TEOS that has reacted through sol-gel reactions to hydroxyl group containing species (Section 1.1). Furthermore, the polyesters containing hydroxyl endgroups can form Si-O-C bond (Figure 4.1: middle) with TEOS based compounds. By applying silane coupling agents Si-C bonds can be introduced (Figure 4.1: right). In this chapter the interactions between polyesters and TEOS have been studied by combining pure polyester and TEOS under various conditions, using various characterization techniques (Section 4.2). Furthermore, coatings have been prepared and their morphology and properties have been studied, as described in Section 4.3. The stability of the coatings is discussed in Section 4.4 and final conclusions are made in Section 4.5.

4.2   Interactions

To determine which conditions are required to obtain this interaction, various parameters have been varied. Both acid-terminated and hydroxyl-terminated polyesters, both bi- and trifunctional polyesters have applied (PE1-PE9, PE6a) in combination with TEOS. Both acid (para-toluenesulfonic acid (pTSA)) and base (triethylamine, 1,4-diazobicyclo[2.2.2]octane) catalysts have been applied. Also the necessity of the presence of water was studied by applying a moist atmosphere in the curing oven (see Section 2.4) or adding none. By these experiments the conditions to obtain hybrid coatings, and thus interactions, based on only polyester resin and TEOS were determined.

Transparent hybrid coatings of polyester and TEOS were only obtained from hydroxyl-terminated polyesters and TEOS, when the reaction was catalyzed by an acid, in the presence of water. No coatings were obtained from acid-terminated polyesters and TEOS. Neither were coatings formed with a base catalyst. The presence of water appeared to be necessary for the formation of the hybrid coatings. Since the hydroxyl-terminated polyester and TEOS can form a crosslinked coating, there must be an interaction between the two compounds. The necessity of the presence of water indicated that TEOS must be hydrolyzed (see Section 1.1) before interaction with the polyester can take place. This means that the interaction between the inorganic compound and the hydroxyl-terminated polyester proceeds via silanol groups. Under acidic conditions, necessary for this crosslinking, the hydrolysis of TEOS and thus the formation of silanol groups is fast and the condensation, towards Si-O-Si bonds, is slow (see Section 1.1). The interaction of hydrolyzed TEOS with hydroxyl-terminated polyester is possible via hydrogen bridging with the carbonyl groups of the polyester and via reaction of the silanol groups with the hydroxyl endgroups of the polyester. Both types of interactions have been studied.

4.2.1   Hydrogen bonding

The occurrence of H-bridging of silanol groups with carbonyl groups can be detected by a shift of the carbonyl group to lower field in FTIR spectra [45, 100, 144]. When FTIR spectra of hybrid coatings of polyester and TEOS (hydrolyzed by water during curing) were compared with the spectrum of pure polyester no shift of the carbonyl frequency was detected. This could be caused by the fact that the amount of silanol groups in the system was too small compared to the large number of carbonyl groups in the polyester backbone. Therefore, a polyester(PE9(1))-TEOS system with a molar ratio carbonyl:TEOS of 1:1 was studied. This way the possible interaction could take place with all carbonyl groups present. The mixture was applied on KBr and cured in
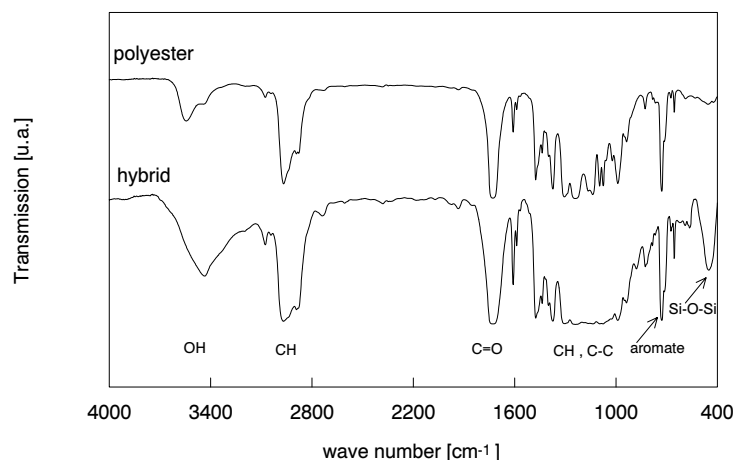
Figure 4.2: *The FTIR spectra of PE9(1)(polyester) and of the PE9(1)-TEOS mixture with a molar ratio carbonyl:TEOS of 1:1 (hybrid), cured in a moist atmosphere at 200 °C for 30 minutes.*

an oven with a moist atmosphere at 200 °C for 30 minutes. No shift of the carbonyl signal, thus no hydrogen bond interaction, was observed as shown in Figure 4.2. The rest of the hybrid spectrum is discussed below in Section 4.2.2.

4.2.2   Covalent bonding through Si-O-C

In order to find evidence for the presence or absence of Si-O-C bondings, CP-MAS ^{13}C NMR has been performed on both the hybrid coating (PE5-TEOS) and the pure polyester (PE5), but all signals in the spectra were too broad to observe the small shift expected from a change of methylene carbon adjacent to the hydroxyl group (C-OH) to the formation of C-O-Si (from 59 to 63 ppm according to literature [26]) The broad overall signals are caused by the fact that the polyester is a random polymer with a large number of slightly different carbon signals and by the low mobility of the molecules in solid state NMR.

Also FTIR and Raman spectroscopy were performed, but both techniques suffered from the strong signals of the polyester that overruled the small signals of possible Si-O-C bands. Figure 4.2 shows an example of the FTIR spectra of pure polyester and a hybrid system with 31 wt.% SiO_2. The assignments of sol-gel compounds are well documented in literature [148, 151–153]. At 460 cm^{-1} the Si-O-Si bonds can be identified, as a result of condensation of hydrolyzed TEOS to a kind of silica
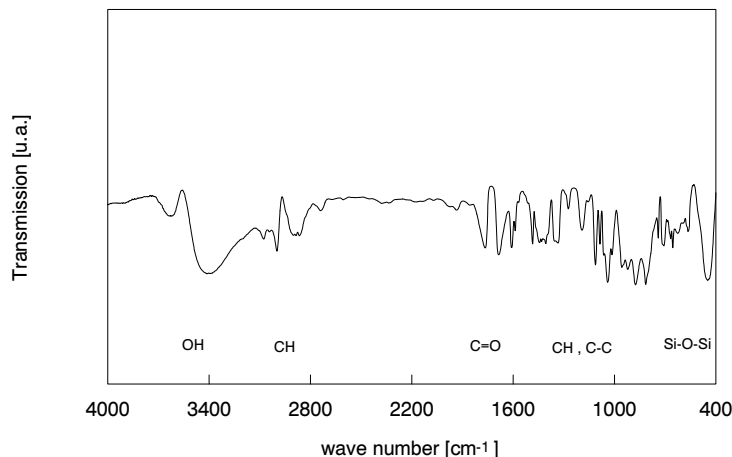
Figure 4.3: *The difference spectrum of the FTIR spectra of the polyester (PE9(1))
and the hybrid (PE9(1)-TEOS mixture), as shown in Figure 4.2, based on the signal
at 729 cm^{-1}.*

network. The increased amount of hydroxyl groups around 3400 cm^{-1} corresponds
to the presence of silanol species. The Si-O-C bonds, expected around 960 cm^{-1} and
1125 cm^{-1}, could not be proven due to the overlap with polyester signals. In this
region of CH and C-C signals (1500 - 1000 cm^{-1}) several extra bands are monitored.
These are attributed to the solvent of the coating system: 1-methoxy-2-propylacetate
(MPA) and possible residual alkoxide groups of TEOS signals, which are still present
in the hybrid system. To get rid of the overlapping signals it was tried to subtract the
polyester spectrum from the hybrid spectrum. For subtracting spectra a characteristic
polyester peak was needed. A characteristic polyester signal is the aromatic band
around 729 cm^{-1}. The polyester spectrum in Figure 4.2 was subtracted from the
hybrid spectrum, after normalizing on the peak at 729 cm^{-1}. The result is plotted
in Figure 4.3. As can be seen no extra information is obtained. With spectroscopic
techniques direct evidence for the formation of Si-O-C bonding could not be obtained.

Since it was not possible to prove the Si-O-C bonding directly, extraction experiments
have been performed to get prove indirectly. A series of coatings made of PE9(1) and
various amounts of TEOS, cured in a moist atmosphere at 200 °C for 30 minutes,
was extracted by refluxing in tetrahydrofuran (THF) overnight. The polyester is well
soluble in THF, thus if no network is formed it will dissolve and will be removed
from the sample. The amount of residual content after extraction is called the gel
content and is a measure of the network formation. The results are plotted in Table
4.1. The gel contents after extraction were larger than the amount of silica present
in the coatings, as determined by thermal gravimetric analysis (TGA). This indicates

Table 4.1: *The results of Soxhlet extraction with THF of PE9(1)-TEOS coatings, with various amounts of silica. The extraction was performed nine months after preparation, unless stated differently.*

wt.% SiO_2 in the coating	2.6	5.3	9.5	17.3	10.5*
wt.% residue after extraction	2.8	10.1	19.6	28.4	38

* Extraction of the sample after 2 days.

that the polyester has indeed reacted with TEOS, since more than only silica was left as residue. The extraction of the series of the hybrid coatings containing 2.6 to 17.3 wt.% SiO_2 was performed nine months after the coating synthesis, while the sample with 10.5 wt.% SiO_2 was extracted two days after synthesis. The fresh coating sample with 10.5 wt.% SiO_2 showed a much higher gel content than the old sample with 9.5 wt.% SiO_2, although the compositions of the two systems were highly comparable. This result can be explained by the effect of degradation of the Si-O-C bonding in time as described in Section 4.4.

4.2.3 Conclusions

No hydrogen bonding was observed and from the extraction experiments it was proven, indirectly, that there is a reaction between the two phases. It can be concluded that interaction between the hydroxyl-terminated polyester and TEOS can only proceed via the hydroxyl endgroups of the polyester and the silanol groups of hydrolyzed TEOS. This is also in agreement with the fact that with acid-terminated polyesters no coatings could be obtained, since the acid-terminated polyesters had the same carbonyl containing backbone as the hydroxyl-terminated polyesters, but different endgroups. It is assumed that the reaction takes place via condensation forming Si-O-C bonds, as presented in Figure 4.4.
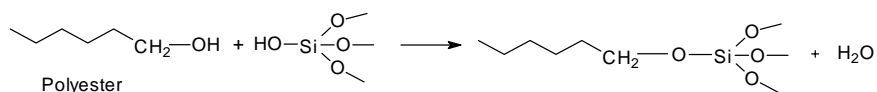

Figure 4.4: *Crosslinking reaction of hydroxyl-terminated polyester with hydrolyzed TEOS. R stands for H, ethyl or SiO-.*

4.3 Hybrid polyester-TEOS coatings

Hybrid coatings based on bifunctional hydroxyl-terminated PE9 or PE9(1) and TEOS under acidic conditions (1 wt.% pTSA) in the presence of water (moist atmosphere) have been prepared as generally described in Section 2.4. The morphology and properties of these coatings have been studied as described below. From the results, together with the information about the interactions between the phases a morphological model is constructed.

4.3.1 Morphology

The morphology of the hybrid polyester-TEOS coatings was studied by scanning electron microscopy (SEM) and transmission electron microscopy (TEM). No microstructures could be observed by both methods. In Figure 4.5(a) and Figure 4.5(b) examples are shown of a SEM and a TEM photograph, respectively. With elemental analysis it was proven that Si was present in the samples.
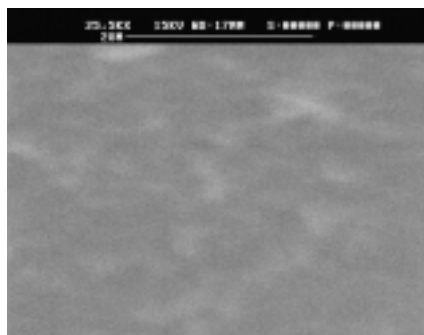
(a) SEM photograph of a PE9-TEOS hybrid coating with 16.9 wt.% silica.
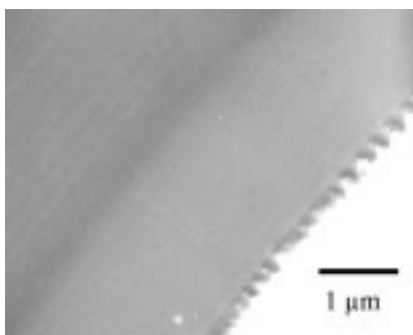
(b) TEM photograph of PE9-TEOS hybrid coating with 8.9 wt.% silica.

Figure 4.5: *SEM and TEM photographs PE9-TEOS hybrid coatings.*

4.3.2 Properties

To study the influence of the amount of silica on the properties of the coatings the König hardness and the glass transition temperature (Tg) were determined as function of the silica content. The latter was determined by TGA. The results are plotted in
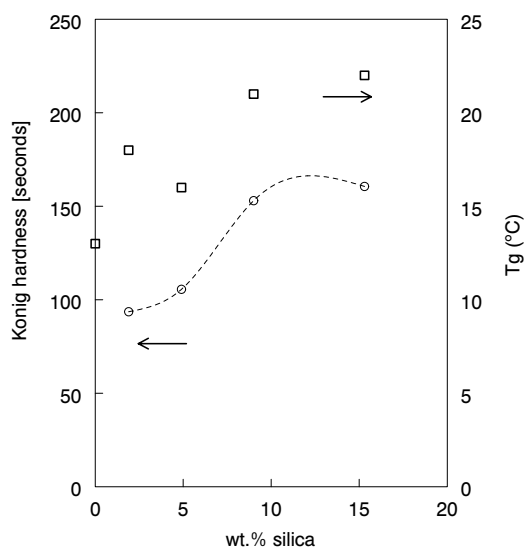
Figure 4.6: *König hardness at a layer thickness of 20 μm (○) and Tg (□) as function of the silica content (determined by TGA) of the PE9(1)-TEOS coatings. They drawn line is only a guide for the eyes.*

Figure 4.6. There is a clear increase in König hardness and Tg with increasing silica content observed, which seems to reach a maximum around 10-12 wt.% silica.

4.3.3   Conclusions

As discussed above interactions between polyester and TEOS take place via reaction of the hydroxyl endgroups of the polyesters and the silanol groups of the inorganic components, which are formed by hydrolysis of TEOS in the presence of water. Furthermore condensation of the latter takes place, thus forming a silica network structure. In this way hydrolyzed and condensed TEOS forms the crosslinker of the polyester, thus forming a true hybrid network.

In the coatings no microstructure could be detected. An increased hardness and Tg with increasing silica content were observed. The scale of the microstructure is supposed to be too small to be determined. Also in a purely organic crosslinked system no microstructure was retrieved, as shown for example in Chapter 5 (Figure 5.6(a) and 5.7(a)). The increased hardness and Tg with increasing silica content can
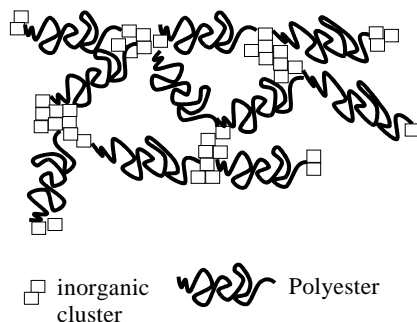
inorganic cluster   Polyester

Figure 4.7: *Schematic representation of the model proposed for the polyester-TEOS system.*

be explained by an increased crosslink density. When all polyester endgroups are crosslinked no further increase in König hardness and Tg is expected. This maximum is reached when the molar ratio polyester:TEOS is about four (10 wt.% SiO_2,), for the bifunctional polyester PE9(1). Therefore it could be concluded that around each endgroup of the polyester on average two TEOS molecules must be clustered to have a complete network formed. The proposed morphological model is schematically pictured in Figure 4.7.

4.4   Degradation

In time degradation of the coatings was observed. This degradation was monitored in time with differential scanning calorimetry (DSC) and König hardness measurements. DSC results of hybrid PE9(1)-TEOS coatings measured after one month were compared with measurements two years later. The results are summarized in Table 4.2. Besides a Tg also a melting peak (Tm) was detected (at around 80 °C), the same Tm was also measured in pure PE9(1), crystallized in MPA. These melting peaks measured in the coating samples show that the polyester crystallizes within the coating, in time. This can only occur when the polyester can move freely in the coating, which means that the network structure is lost. Furthermore, while the relatively fresh coatings showed an increase in Tg with increasing silica content, the old coatings all showed a Tg dropped down to around 13 °C, which is the Tg of PE9(1). This is also a strong indication that the network is lost. The silica content in the freshly made coatings and the old ones were similar, so there was no loss of one of the components in time. Also the extraction experiments, as described in Section

Table 4.2: *DSC results of PE9(1) and coatings made of PE9(1) and various amounts of TEOS, in time. Both the step in Tg and the size of the melting peak, with as maximum Tm (crystallization temperature) were in the range of 10 °C.*

wt.% SiO_2	0	1.9	4.9	9.0	15.3
Tg [°C] after one month	13	18	16	21	22
Tm [°C] after one month					
Tg [°C] after two years			13	13	14
Tm [°C] after two years	76		78	86	80

4.2, showed degradation of the network, as the residue contents of the fresh and old sample with a silica content of around 10 wt.% SiO_2 were compared. By measuring the König hardness as function of the silica content in time, degradation was followed. The results are shown in Figure 4.8. The drop of König hardness in time was seen as a direct result of degradation of the network. When the same type of coatings were kept under dry conditions in an desiccator the decrease in time is strongly reduced, as shown in Figure 4.9.

It is assumed that degradation of the network is caused by hydrolysis of the Si-O-C bond, but since it was not possible to prove the Si-O-C bond directly, it is also impossible to prove the loss of this bond directly. The effect of a dry atmosphere on the coatings, as determined by the König hardness measurements in time, strongly suggests that Si-O-C bonds are broken due to presence of water in the atmosphere. The influence of water on Si-O-C bonds is well known [9]. The so-called hydrolysis is used in the sol-gel process to form SiO_2 [6].

4.5   Conclusions

The interaction between polyester and TEOS is based on covalent Si-O-C bonds. Hydroxyl endgroups of polyester react with silanol groups of hydrolyzed and condensed TEOS. In this way it is possible to form true hybrid networks in which the morphology is under a nanometer scale, thus invisible with electron microscopy. The hardness and Tg increase with increasing silica content, due to an increasing crosslink density. The bonds, though, are not stable. Under influence of water the Si-O-C bonds hydrolysis again and the bondings are broken, resulting in degradation of the coating. The true hybrids, formed via Si-O-C bondings from hydroxyl-terminated polyester and hydrolyzed TEOS, do not have possibilities as either a coating system or a model system, since the behavior of the system in time depends on the relative humidity.

Figure 4.8: *König hardness as function of the silica content, in time of PE9-TEOS coatings with various amounts of silica, prepared in 2-butoxyethanol.*
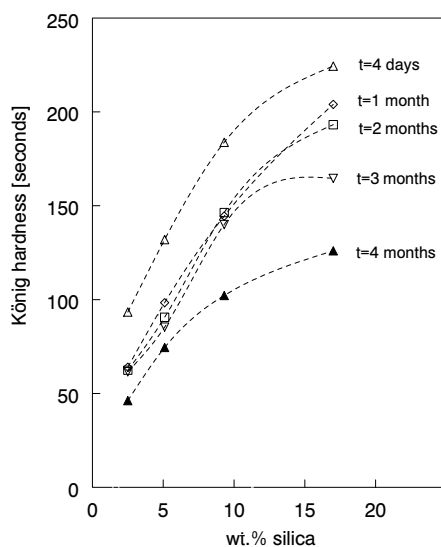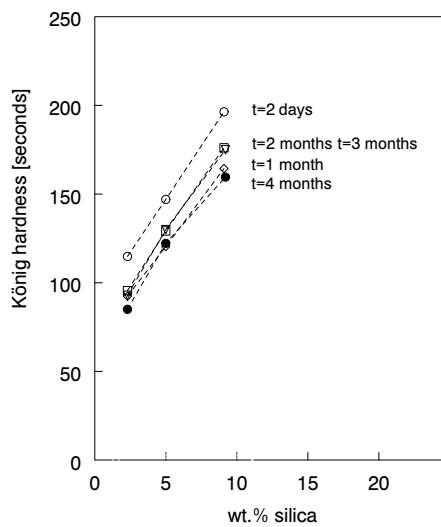

Figure 4.9: *König hardness as function of the silica content, in time of PE9-TEOS coatings with various amounts of silica, prepared in 2-butoxyethanol. The coatings were stored in an desiccator.*

4.6   Experimental details

Fourier transform infrared spectroscopy (FTIR, Matson Polaris) was performed by applying thin films, diluted with THF, on KBr tablets.

NMR spectra were recorded on a Varian Gemini 300, using $CDCl_3$ as solvent with tetramethylsilane as internal standard.

Silica contents were measured by thermal gravimetric analysis (TGA, Perkin Elmer TGA7). The heating rate was 20 °C/min from 30 to 800 °C.

A profilometer (TENCOR-P10 Surface Profiler) was used to measure the thickness of coatings on glass substrates, in the middle of the coated panel. The scan length was 10 mm, the scan speed was 1 mm/s and the stylus force was 5.0 mg.

Scanning electron microscopy (SEM, Cambridge, Stereoscan 200) was performed on cross-sections of coatings on glass substrates. The samples were sputtered with Pd/Au for 3 minutes (BioRad SEM Coating System).

Transmission electron microscopy (TEM, Jeol 2000 FX) with elemental analysis (Noran Instruments Series II) was performed on coatings applied by a wirebar on polycarbonate, which was pretreated with 3-aminopropyltrimethoxysilane, necessary to obtain adhesion between the substrate and the coating.

The glass transition temperature (Tg) and melting temperature (Tm) were determined by differential scanning calorimetry (DSC, Perkin Elmer DSC7), with a heating rate of 20 °C/min.

König hardness was measured with a König pendulum apparatus (Pendelhärteprüfer Model 299/300, Erichsen), according to ASTM D4366, on coatings on glass substrates. The differences in layer thickness of the various coatings were corrected by applying a powerlaw relation on the König hardness versus layer thickness as determined on a coating series of PE9(1) and 9 wt.% silica applied with various layer thicknesses (see also Section 3.3.1).

Chapter 5

Interpenetrating Networks

5.1   Introduction

The term interpenetrating network is mainly used in the context of polymers. According to the polymer technology dictionary [154] IPN or interpenetrating polymer network refers to 'a blend or alloy, formed between two crosslinked polymers'. When only one of the two polymers is crosslinked it is called a semi-IPN [155, 156]. IPNs are generally classified in two classes: sequential and simultaneous IPNs. In the sequential IPNs the networks are synthesized after each other, whereas in the simultaneous IPNs they are formed at the same time. In IPNs phase separation occurs, but to a lesser extend than when the polymers are mechanically blended. The degree of phase separation is controlled by the chemical compatibility, the interfacial tension, the crosslinking density and the kinetics of the polymerizations. The compatibility can be enhanced when the polymers are interlocked in a three dimensional structure during polymerization, before phase separation can occur.

The concept of IPNs can be extended towards organic-inorganic hybrid materials, in which the sol-gel reaction is an inorganic polymerization. Sequential hybrid IPNs can be formed by the synthesis of an porous inorganic sol-gel matrix, which is impregnated by polymerizable monomers. In the second step the monomer can be polymerized, thus forming an organic network within the inorganic network. An example of such a sequential IPN is the polymerization of methyl methacrylate in a silica gel [157]. Since the polymeric phase is not crosslinked, actually a semi-IPN is formed. The resulting properties were found to be intermediate between the properties of the single components. Alternatively, the polymethylmethacrylate phase can be formed first and be
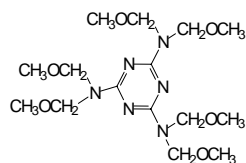
Figure 5.1: *The structural formula of HMMM.*

dissolved in a solution containing inorganic sol-gel precursors afterwards. Then the sol-gel reactions can take place, forming an inorganic network [158]. This method is applied in literature with a number of other polymers, such as for example polyvinylacetates [44, 43], polyorganophosphazenes [150] and polyethylene oxides [142, 159], but since no organic network is formed these hybrids are semi-IPNs as well. By using an organic membrane as a template for acid catalyzed sol-gel reactions, true sequential hybrid IPNs have been formed [160, 161]. In this way various functionalities can be built into the membranes, resulting in new application areas. Novak and co-workers created simultaneous hybrid interpenetrating networks by performing sol-gel reactions with tetraalkoxysilanes containing polymerizable alkoxy groups in polymerizable co-solvents. In this way shrinkage, that normally occurs during drying of sol-gel reaction products could be prevented [24, 25]. Simultaneous IPNs can also be formed when crosslinkable organic compounds are mixed with sol-gel precursors. Examples for this type of hybrids are tetraethoxysilane (TEOS) combined with acrylic acid, methyl methacrylate and the crosslinker ethylene glycol dimethacrylate [162], TEOS combined with phenolic resins, which crosslinks by condensation of hydroxyl groups [163], TEOS combined with polyamic acid, which crosslinks by condensation forming a polyimide-silica IPN [38, 164] and TEOS combined with epoxides which are crosslinked with amines [165, 166]. Soucek and coworkers [81–84] reported on the synthesis of hybrid coatings based on alkyds and titanium or zirconium alkoxides. They suggested the formation of an inorganic network within the alkyd network, thus forming a simultaneous IPN. Furthermore, they suggested reaction between the metal hydroxyl species and the hydroxyl or carbonyl groups in the alkyd, but none of these suggestions were supported by evidence. Moreover, they observed influence on various general coating properties, but these could also be caused by acceleration of the oxidative organic crosslinking by the metal alkoxides.

The polyester-HMMM (hexakismethoxymethylmelamine)-TEOS hybrid system studied in this research is also expected to consist of an organic-inorganic hybrid network. Since the organic crosslinking reaction (polyester-HMMM) is acid catalyzed, the inorganic sol-gel reactions is expected to form an inorganic network [6, 9], as explained in Section 1.1. The polyester in reaction with HMMM, which structural formula is displayed in Figure 5.1, will also form a network. The crosslinking reaction between polyester and HMMM is displayed in Figure 5.2.
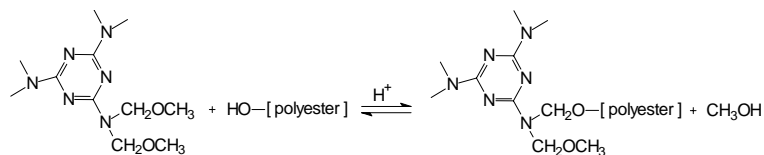
Figure 5.2: *Crosslinking reaction of hydroxyl-terminated polyester with HMMM.*

The crosslinker used in this study is an HMMM resin, which means that the major compound in the resin is monomeric fully methoxylated melamine (HMMM), but also compounds with not fully methoxylated groups are present. This is caused by the two-step synthesis procedure of HMMM [2, 167]. The synthesis reactions are pictured in Figure 5.3. In the first step: methylolation, melamine is reacted with formaldehyde under basic conditions. The second step: etherification, involves the acid catalyzed reaction of methylolmelamine with methanol. Already in the first step a statistical mixture is obtained, containing both unformylated NH groups and over formylated NCH_2OCH_2OH groups. Also the second step will not go to completion. In addition, bridging can occur via the reactive hydroxyl groups. Finally, a HMMM resin is obtained which contains beside pure HMMM also dimers and trimers, and other end-groups than CH_2OCH_3. The various functional groups [3, 168] influence the reaction mechanism and rate. Furthermore, during the crosslinking reaction selfcondensation of HMMM can occur, between the various functional groups. The aim of the research was not to study the reaction mechanism of polyester with HMMM resins, but to obtain a fully cured organic network with polyester under acidic conditions. It was chosen to use a fully methoxylated melamine resin, assuming an overall functionality of 3. Due to the various reactive groups and the steric hindrance an overall functionality of 3 is generally accepted for this type of HMMM.

The curing reaction (Figure 5.2) is catalyzed by a strong acid, like para-toluenesulfonic acid. The catalyzing mechanism, proposed by Blank [168], is described in Figure 5.4. Besides protonation of the methylated methoxy group, also protonation of already formed crosslinks can occur, followed by reactions with the alcohol just formed. In this way crosslinks will be broken again. By the evaporation of the alcohol the equilibrium is shifted to the right and the final crosslinks are made. In the hybrid systems studied, besides polyester and HMMM also water, ethanol and TEOS are present. These compounds can react in a similar way as the alcohol (R_1OH in Figure 5.4), influencing the crosslinking reactions. When TEOS or hydrolyzed TEOS reacts in this way Si-O-C bondings between the organic and inorganic compounds can occur. Another possible reaction is the reaction of hydrolyzed TEOS with the hydroxyl groups of the polyester, as studied and described in Chapter 4, also resulting in the formation of Si-O-C bonds. Si-O-C bonds are known to be sensitive to hydrolysis. Hydrolytically stable connections between the organic and inorganic compounds can be made by applying a silane coupling agent, as a linkage between the organic polyester-HMMM

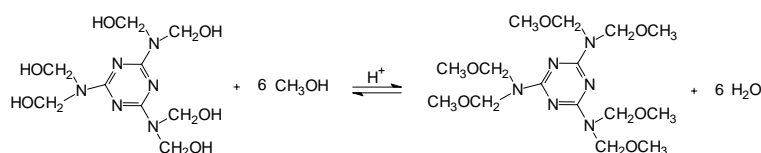Methylolation reaction:
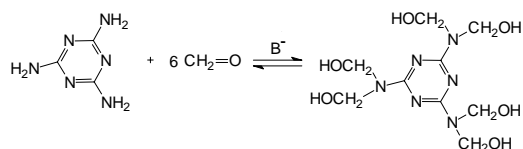
Etherification reaction:

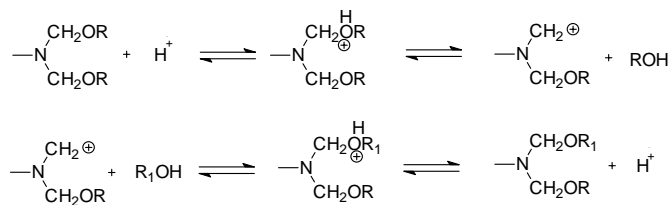Figure 5.3: *Synthesis reactions of HMMM resin.*

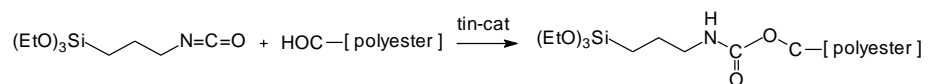Figure 5.4: *Catalyzing mechanism of the reaction of HMMM with polyols.*

Figure 5.5: *Silane-modification of hydroxyl-terminated polyester with isocyanato-propyltriethoxysilane.*

network and the inorganic silica matrix. By reaction of the hydroxyl endgroups of the polyester with isocyanatopropyltriethoxysilane (NCO-silane) a covalent Si-C bond between the organic and inorganic components can be formed. This reaction is shown in Figure 5.5. Strictly speaking, when such linkage is made between the organic and inorganic phase, the term interpenetrating network is no longer valid [155, 156]. It is better to speak of an interlinked polymer-silica network, since there is a polymer network and a silica network which are linked to each other via the coupling agent.

Polyester, HMMM and prehydrolyzed TEOS (pT2, see Section 2.3) were combined under acidic conditions and the morphology and properties have been studied, as described in Section 5.2. In Section 5.3 hybrid coatings based on polyester functionalized with NCO-silane, HMMM and pT2 are described. The final conclusions are drawn in Section 5.4.

5.2 Polyester-HMMM network with in situ formed silica

The influence of the chemical composition on the morphology and mechanical properties of the interpenetrating polyester-HMMM-TEOS systems was studied. For this purpose hydroxyl-terminated polyester and HMMM were combined with prehydrolyzed TEOS (pT2). Starting point, as basis for the parameter variation, was the PE10-HMMM system with a molar ratio HMMM:PE10 of 1.5 (23 wt.% HMMM and 77 wt.% PE10) with various amounts of pT2 as silica source. The influence of the crosslink density of the organic network was studied, as function of the silica content, by applying a HMMM:PE10 molar ratio of 0.75. Also the influence of the type of polyester was investigated by applying PE6 instead of PE10. The influence of the extent of prehydrolyzation was studied by applying pT1 and pT0.5 (prehydrolyzed TEOS with 1 and 0.5 mole water respectively).

When pT2 was used the silica content in the final coatings was in good agreement with the calculated amount, but when pT1 or pT0.5 were used less silica was retrieved. The amounts of silica, determined by thermal gravimetric analysis (TGA), in the various coatings are summarized in Table 5.1. Thorough hydrolysis (pT2) is necessary to prevent evaporation of unreacted TEOS, as described in Section 2.3.

Table 5.1: *The calculated silica content of polyester-HMMM hybrid coatings with various amounts of prehydrolyzed TEOS, cured for 10 minutes at 200 °C, compared to the amount determined by TGA.*

calc. wt.% SiO$_2$		3	4	5	6	8	10	11	12	14
HMMM:PE10	silica source				measured wt.% SiO$_2$					
1.5	pT2		4.2		6.1	7.5		11.4		15.4
0.75	pT2	2.9		5.5			10.5		12.4	14.6
1.5	pT1								7.4	
1.5	pT0.5								3.9	

calc. wt.% SiO$_2$		2	5	7	9	12	15	16	21
HMMM:PE6	silica source		measured wt.% SiO$_2$						
1.5	pT2	1.9	4.0	5.8	8.8	11.4	14.6	16.4	21.0

5.2.1 Morphology

Scanning electron microscopy (SEM) was used to investigate the morphology of the hybrid coatings. The results are described first and discussed afterwards. In Figure 5.6 photographs of the cross-sections of the coatings with a HMMM:PE10 molar ratio of 1.5 and various amounts of silica are shown. The SEM photograph of the pure organic coating (Figure 5.6(a)) shows small pits on the surface, due to the 30 minutes of oxygen etching (Section 3.2). In coatings with an increasing amount of silica up to 6 wt.% (Figure 5.6(c)) silica cannot be distinguished from the organic matrix. At a silica content of 7.5 wt.% (Figure 5.6(d)) silica particles begin to appear. In a transparent coating containing 11.4 wt.% silica (Figure 5.6(e)) smooth spherical particles with a diameter of around 300 nm are clearly present. A coating with 15.4 wt.% silica (Figure 5.6(f)) shows a large number of spherical silica particles, diameter of around 500 nm, in the organic matrix, causing scattering of light, resulting in the observed haziness. Overall, the particle size increases with increasing silica content, ultimately leading to hazy coatings. The small cracks, which are visible in all SEM photographs, are caused by the oxygen etching. This was determined by comparison with unetched samples, where the cracks were absent. The trend of increasing silica particle formation with increasing silica content is characteristic for the polyester-HMMM-silica hybrid system. The same effect was seen, even more pronounced, when a less dense organic network was formed by applying a HMMM:PE10 molar ratio of 0.75. The SEM photographs of the coatings with various amounts of silica are shown in Figure 5.7. Also in the systems with PE6 some particle formation was seen, although only

at very high silica contents. A SEM photograph of a PE6-HMMM coating with 21.0 wt.% SiO_2 is shown in Figure 5.8(a) together with a transmission electron microscopy (TEM) photograph, which shows the particles more clearly (Figure 5.8(b)). The particles in the SEM photograph of PE6 based hybrid coatings appears smaller than for the P10 based coatings (notice the difference in magnification), but from the TEM photograph it is clear that the particle size is of a similar size (few 100 nm). In all cases studied silica particles are formed, only the amount of silica that can be put in before haziness occurs, differs under the various conditions. Haziness occurs when the size of the silica particles becomes larger, causing scattering of light. In a denser network more silica could be built in than in a less dense network. More silica could be built in when PE6 was used instead of PE10. When TEOS was prehydrolyzed with 1 or 0.5 molar water also less silica could be built in before haziness occurred, than when pT2 was used.

To study the morphology in more detail a hybrid coating with 6.1 wt.% silica and a HMMM:PE10 molar ratio of 1.5, which did not reveal the presence of silica particles in SEM (Figure 5.6(d)), was also examined in TEM. The results are shown in Figure 5.9. There are two remarkable features. Firstly, in the bulk of the coating few smooth round particles with a size of around 100 nm was observed, showing that already at lower silica content particles have been formed. Secondly, it was clearly shown that on the surface of the coating small silica particles (around 30 nm) were present at substantially higher concentrations than in the bulk of the coating. Also in hybrid coatings with higher silica contents an increase of silica concentration was noticed at the surface of the coating but single particles could not be distinguished. An example of the substrate, bulk and surface side of a hybrid coating with 11.4 wt.% SiO_2 is shown in Figure 5.10. The dark band on the surface side is identified as silica. But also the small dark line at the substrate side was identified as silica. There was even Si present on the aluminum substrate where this part of the coating had been, indicating strong interaction of the silicon compounds with the substrate.

Discussion on the morphology

From the chemical composition of the hybrid polyester-HMMM-TEOS systems it was expected that both the organic and inorganic phase would form a network, the organic phase by crosslinking of polyester and HMMM and the inorganic phase by polymerization of the silanol groups, forming a silica network. In combination an interpenetrating network was expected. The morphology obtained, though, showed the formation of particles increasing in size and number with increasing silica content. It is concluded that an increased phase separation with increasing silica content is caused by a low compatibility and consequently a lack of interaction between the organic and inorganic phase, resulting in smooth round silica particles. Interaction
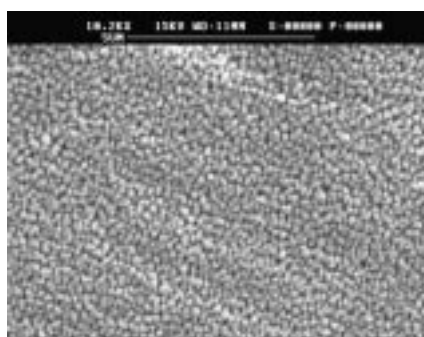
(a) 0 wt.% SiO$_2$
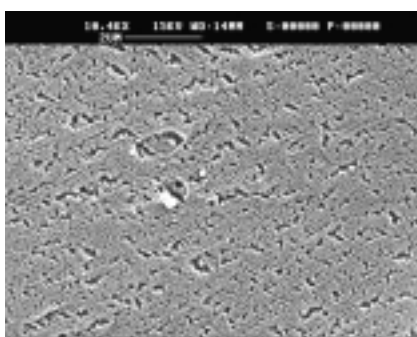
(b) 4.2 wt.% SiO$_2$
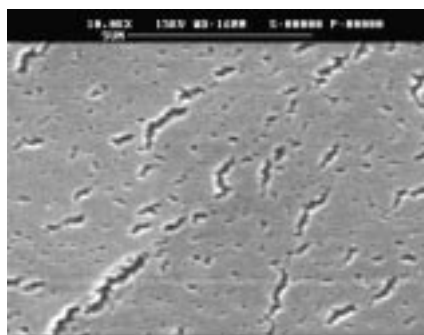
(c) 6.1 wt.% SiO$_2$
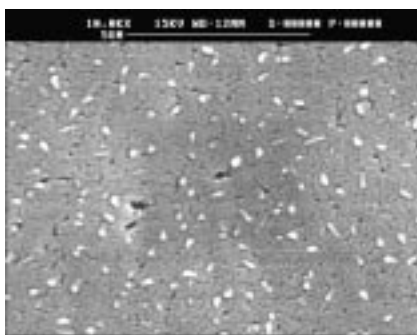
(d) 7.5 wt.% SiO$_2$
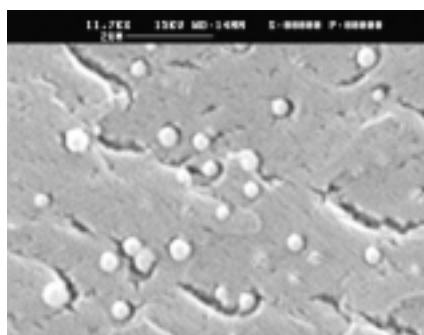
(e) 11.4 wt.% SiO$_2$
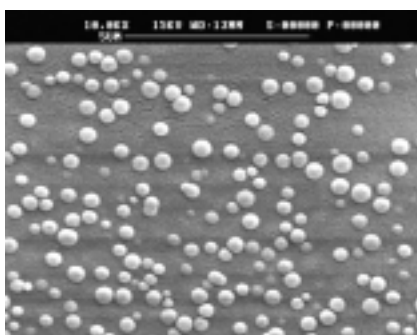
(f) 15.4 wt.% SiO$_2$*

Figure 5.6: *SEM photographs of crosscuts of PE10-HMMM hybrid coatings with a molar ratio HMMM:PE10 of 1.5 and various amounts of pT2. *hazy coatings.*
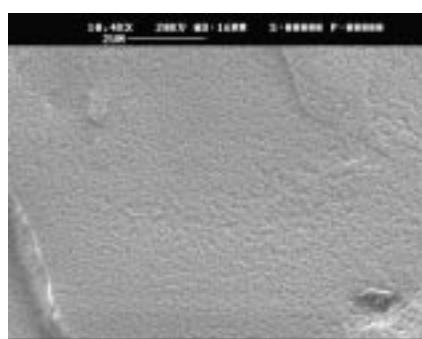
(a) 0 wt.% SiO$_2$
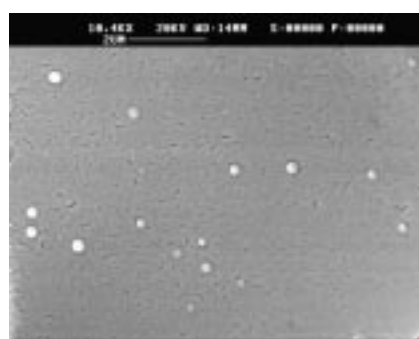
(b) 2.9 wt.% SiO$_2$
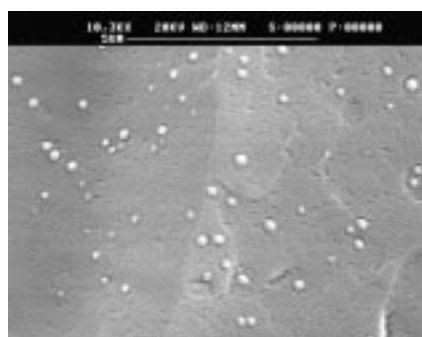
(c) 5.5 wt.% SiO$_2$
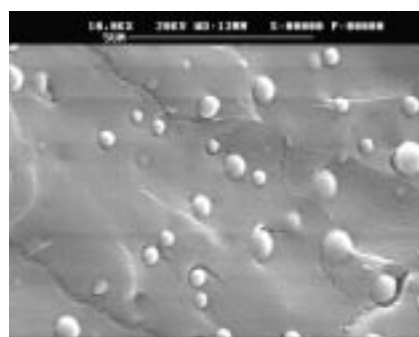
(d) 10.5 wt.% SiO$_2$*
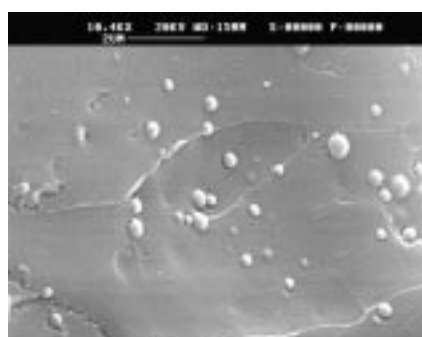
(e) 12.4 wt.% SiO$_2$*
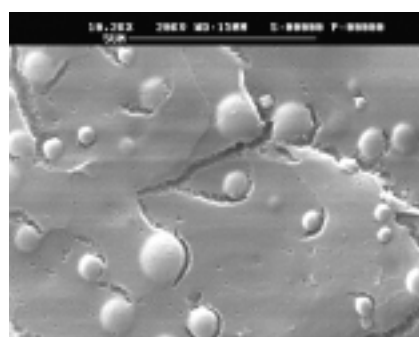
(f) 14.6 wt.% SiO$_2$*

Figure 5.7: *SEM photographs of crosscuts of PE10-HMMM hybrid coatings with a molar ratio HMMM:PE10 of 0.75 and various amounts of pT2. *hazy coatings.*

(a) SEM photograph   (b) TEM photograph
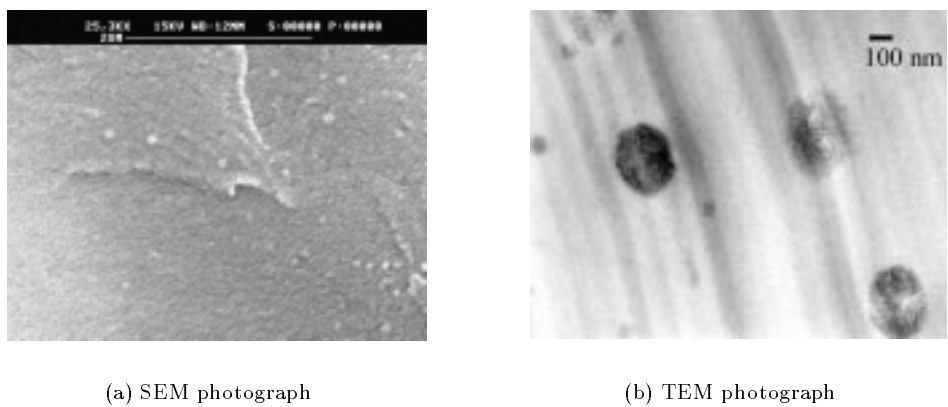
Figure 5.8: *photographs of a PE6-HMMM hybrid coating with 21.0 wt.% silica.*

(a) substrate   (b) bulk   (c) surface
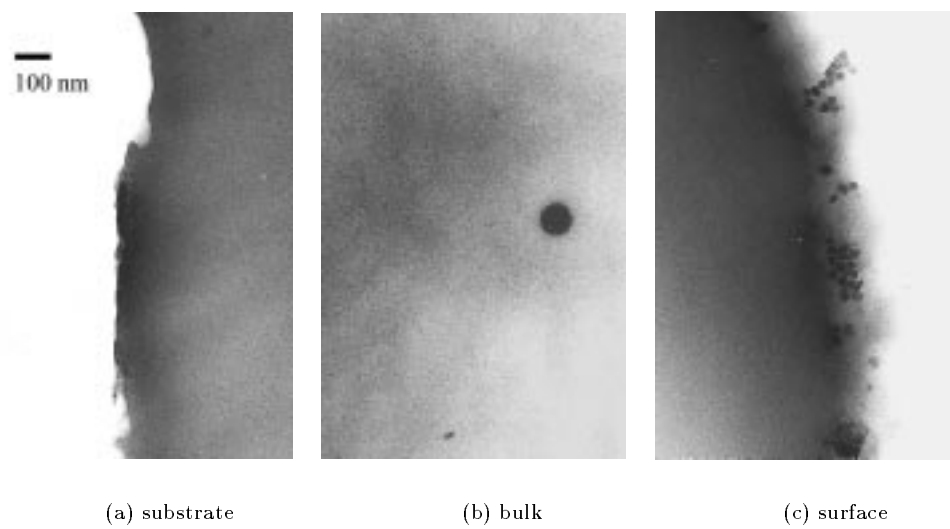
Figure 5.9: *TEM pictures of a hybrid PE10-HMMM coating with 6.1 wt.% SiO_2.*

(a) substrate   (b) bulk   (c) surface
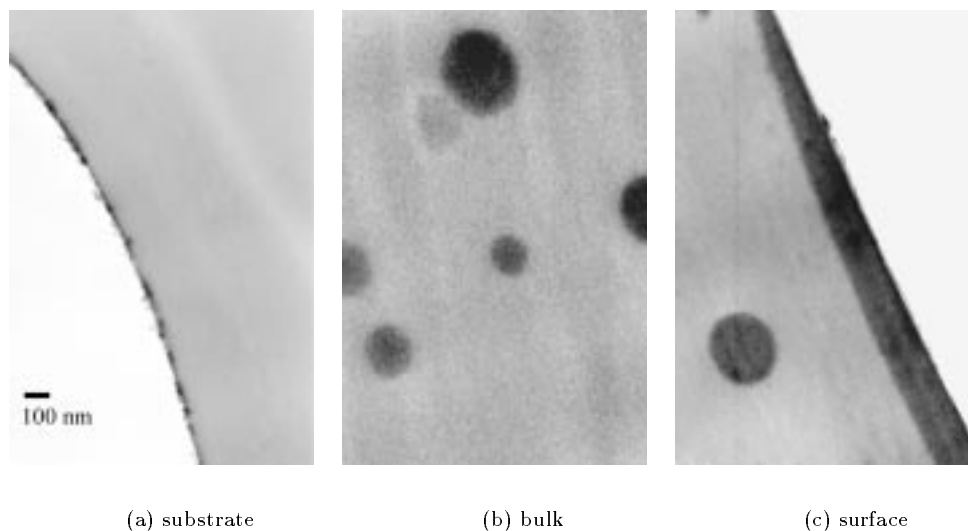
Figure 5.10: *TEM pictures of a hybrid PE10-HMMM coating with 11.4 wt.% SiO$_2$.*

between the organic and inorganic phase in this system can occur through Si-O-C bond formation of silanols with polyester or HMMM, but apparently this reaction cannot compete with the organic and Si-O-Si crosslinking reactions. The lack of interaction can also be the cause that small silica particles are preferentially present at the surface. Possibly differences in surface tension between the organic compounds and the siloxane compounds drive the siloxane compounds to the surface, where they can form small silica particles. It is also possible that silica particles are formed first and are driven to the surface. At higher concentrations of silica, particles could not be distinguished in the top layer, but the dark band at the surface side indicates an increased silica concentration.

With elemental analysis in SEM no discrete Si parts could be distinguished from the matrix: everywhere in the coating Si was measured. With elemental analysis in TEM the silica clusters could be identified as SiO$_2$. Furthermore, Si was detected through the whole coating. These results prove that beside the silica particles an Si-O network is formed through the whole coating so that everywhere in the coating Si is present. This was confirmed by the observation that etching of the hybrid coating containing more silica (PE6: 21.0 wt.%) was less effective than for coatings containing less silica (PE10: 11.4 wt.%). Namely, in the first case the silica particles appeared smaller in SEM, while with TEM it was demonstrated that the size of the particles were of similar. Also in Figure 5.6 the effect of increasing silica content showed a decreasing damaging effect of the oxygen plasma on the matrix. Furthermore, the lines shown

in the TEM photograph of the sample with 21.0 wt.% SiO_2 (Figure 5.8(b)), known as cutting lines from the diamond knife for the sample preparation, indicate a more rigid sample than the sample with 11.4 wt.% SiO_2 (Figure 5.10(b)), in which no cutting lines were observed. It is therefore highly probable that besides particle formation a silica network on the PE6 based system is formed.

Particle formation was less pronounced for the hybrid coatings with a denser organic network, comparing a HMMM:PE10 ratio of 1.5 (Figure 5.6) and 0.75 (Figure 5.7). Particle formation, as a result of phase separation, apparently stopped at an earlier stage in the denser crosslinked system because of a higher decrease of mobility within the system, compared to the less dense crosslinked system. Besides, the crosslink density also the type of polyester has influence on the amount of silica that can be built in. When PE6 instead of PE10 was used more silica could be added. This was unexpected since PE10 was synthesized with a more polar structure to improve compatibility. The changes in polarity in the polyesters appeared to have minor effects on the final compatibility. With almost the same OH value and the same functionality, the only differences in the polyester beside the polarity were the Tg and the number of carbonyl groups per molecule polyester (15 carbonyl groups per PE10 molecule and 18 carbonyl groups per PE6 molecule). The prehydrolyzed TEOS, ethanol and water may have interaction with the carbonyl groups on the backbone of the polyester. Fact is that the compatibility of PE6 with pT2 was better than that of PE10. More silica could be built in and less particles were formed. It was also unexpected that less silica could be added when partly prehydrolyzed TEOS (pT1 or pT0.5) was used as silica source, instead of pT2. Namely, ethanol, water and TEOS are all badly compatible with polyester and for the same amount of silica in the final coating less TEOS, ethanol and water had to be added when TEOS was prehydrolyzed only partly (pT1 and pT0,5). The number of hydroxyl groups in pT2 is larger than in pT1 that is larger than in pT0.5. These hydroxyl groups appeared important for the compatibility. The more hydroxyl groups present the better the interaction or reaction with the polyester and HMMM is possible during mixing, the more silica can be added.

5.2.2   Properties

König hardness and pencil hardness

The König hardness and pencil hardness (the methods are described in Chapter 3) of PE10-HMMM and PE6-HMMM hybrid coatings with various amounts of silica were determined on coatings with a dry layer thickness of 21 ± 4 μm applied on glass substrates. The results of the König hardness are plotted in Figure 5.11. The König

hardness of the PE10-HMMM coatings was close to 250 seconds, which is the value
of the reference glass. According to ASTM standards a layer thickness of at least
25 μmis required to minimize the influence of the substrate, nevertheless it is known
from former measurements on these type of coatings (see Section 3.3.1) that also with
a layer thickness of 21 μm the substrate effect is not dominating. A gradual decrease
in hardness of ultimately less than 3% was found with increasing silica contents up to
11.4 wt.%. Also in the PE6-HMMM system no large influence of the silica content on
the König hardness was observed. The König hardness of the coatings based on PE6
is lower than that of the coatings based on PE10. This is caused by the lower Tg of
PE6, resulting in a more flexible network. From these results it can be concluded that
the König hardness test only reflects the strength of the organic network. Also the
pencil hardness of these coatings was not markedly influenced by the silica content.
The pencil hardness appeared more dependent on time than on the silica content.
Directly after scratching the scratches were seen at very low pencil hardnesses (5B-B
for PE10 based systems, B-F for PE6 based systems), but in time these scratches
recovered resulting in higher pencil hardnesses (HB for PE10 based coatings, 3H for
the PE10 based coating with 11.4 wt.% SiO_2 and 3H for the PE6 based system) These
results qualitatively tell more about the recover behavior of the coatings than about
the hardness. The higher pencil hardness of PE6 based systems, compared to PE10
based systems is subscribed to the higher flexibility of the organic network. Because
of the higher flexibility of the organic network the scratches recover better and as a
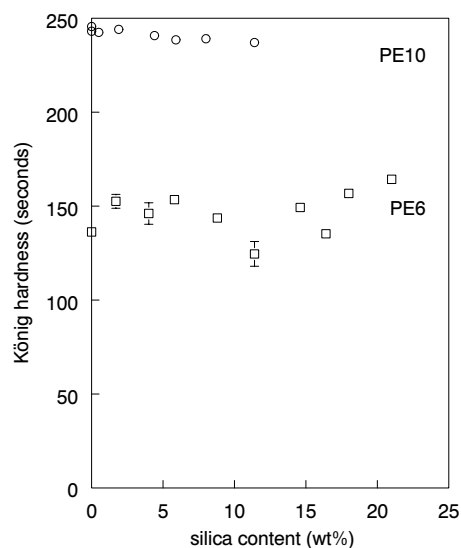consequence a higher pencil hardness was observed.

Figure 5.11: *König hardness as function of the silica content of PE10-HMMM ($\circ$)
and PE6-HMMM ($\square$) hybrid coatings, HMMM:polyester molar ratio of 1.5.*

Table 5.2: *Micro-indentation: Coating thickness of polyester-HMMM hybrid coatings on aluminum substrates, average calculated values of the indentation hardness and reduced elastic modulus and forces of the measurements applied for the calculations.*

Coating sample	Thickness	Used forces for calc.	Hardness	Elastic Modulus
	[μm]	[mN]	[GPa]	[GPa]
PE10-HMMM, 0 wt.% SiO$_2$	22	2-20	0.27	4.9
PE10-HMMM, 11.4 wt.% SiO$_2$	19	5-13	0.23	5.5
PE6-HMMM, 0 wt.% SiO$_2$	26	2-3	0.02	1.1
PE6-HMMM, 21.0 wt.% SiO$_2$	16	2-7	0.15	3.8

Micro-indentation

Micro-indentation measurements have been performed on coatings based on PE10 and PE6 with a molar ratio HMMM:polyester of 1.5 applied on aluminum. Pure organic polyester-HMMM coatings were compared with hybrid polyester-HMMM coatings containing the maximum amount of silica and still being transparent. For the PE10-HMMM system that coating contained 11.4 wt.% silica. In the PE6-HMMM system the hybrid coating contained 21.0 wt.% silica. The layer thicknesses of the coatings are summarized in Table 5.2. Forces from 2 to 20 mN have been applied and force-displacement curves have been determined (see Section 3.3.2). From these curves the maximum indentation depth at the maximum applied forces were determined and the results are plotted in Figure 5.12. This plot shows a large difference between the organic and hybrid coating based on PE6 and almost no difference between the organic and hybrid coatings based on PE10. The maximum indentation should not exceed ten percent of the film thickness, to rule out the substrate influence [108]. For the organic PE6-HMMM coating, with a layer thickness of 26 μm, this means indentation should not be deeper than 2.6 μm. In Table 5.2 the range of applied forces that resulted in an indentation below 10% of the film thickness are summarized.

For the calculations of the indentation hardness the final indented area must be determined, which was done by calculation of the contact depth (see Section 3.3.2). For various applied forces the indentation hardness and the reduced elastic modulus were calculated (further explained in Section 3.3.2) and the results are plotted in Figure 5.13 and 5.14. In Table 5.2 the average values, calculated over the measurements in which the indentation does not exceed 10 % of the layer thickness, are summarized. The calculated hardness and elastic modulus show the same trend as already seen from the indentation depths (Figure 5.12). Namely, in the PE6 based system an
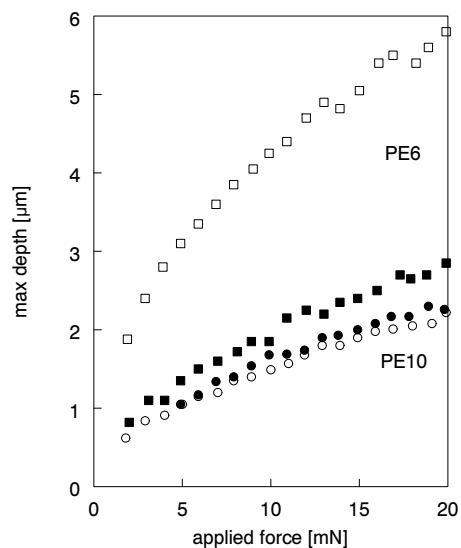
Figure 5.12: *Maximum indentation depth versus the applied forces for PE10-HMMM (○) and PE6-HMMM (□) organic (open marker) and hybrid (filled marker) coatings.*

increased hardness and elastic modulus is clearly observed for the hybrid system compared to the organic system, while for the PE10 based system the effects are minor. Furthermore it can be concluded that the influence of the substrate on the hardness calculations is not large, since no increased values are noticed with increasing applied forces. It is remarkable that the influence on indentation depth is also that small on the organic PE6-HMMM system, which showed the largest indentation depths (up to 6 μm). Instead of an increase with increasing indentation depths (higher forces) an small increase in hardness is noticed at lower forces. This increased hardness is more pronounced for the hybrid coatings than for the organic coatings, suggesting that the silica at the surface causes this increased surface hardness. The effect of the substrate on the elastic modulus is more severe. This is expected since the differences between the value of the elastic moduli of the aluminum and organic coating are much larger than the differences in hardness (see Section 3.3.2). The effect of the silica in the coatings is larger for the PE6-based coatings than for the PE10-based coatings. Also the influence of the substrate is larger on the PE6-based coatings. Both results can directly be related to the larger indentation depths of coatings based on PE6 compared to coatings based on PE10.

Figure 5.13: *Indentation hardness versus the applied forces for PE10-HMMM (○) and PE6-HMMM (□) organic (open marker) and hybrid (filled marker) coatings.*

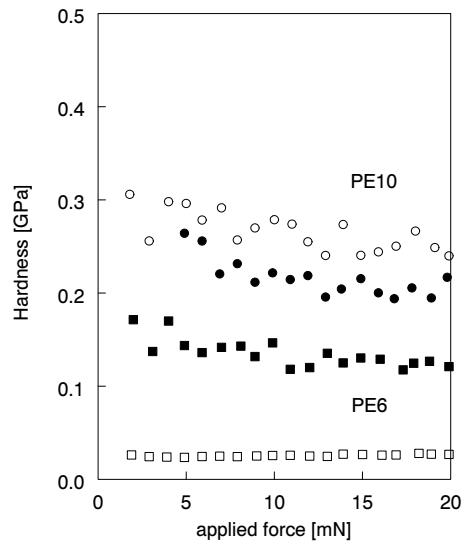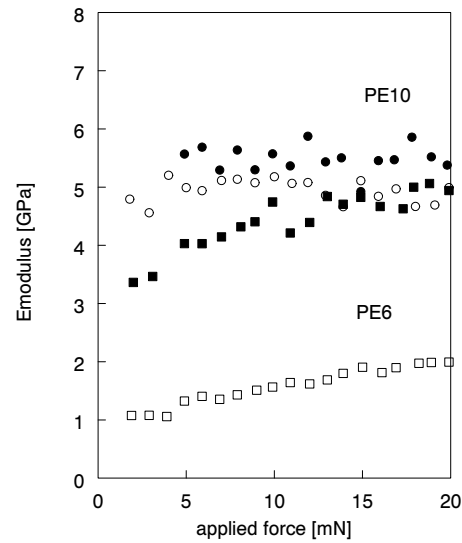Figure 5.14: *Reduced elastic modulus versus the applied forces for PE10-HMMM (○) and PE6-HMMM (□) organic (open marker) and hybrid (filled marker) coatings.*

Micro-scratching

Micro-scratching tests have been performed on PE10-HMMM coatings applied on aluminum. Organic coatings without silica and hybrid coatings with 6.1. 7.5 and 11.4 wt.% silica were compared. Several scratches have been made with normal forces increasing from 0.23 to 7.35 mN. The frictional force as function of the applied normal force is plotted in Figure 5.15. The scratch hardness is calculated applying equation (3.8), of Section 3.3.3, assuming pure horizontal sliding. The averaged values determined for the various scratches on the various coatings are shown in Table 5.3. The atomic force microscopy (AFM) images of a series scratches applied on an organic (PE10-HMMM) and on a hybrid (PE10-HMMM with 11.4 wt.% SiO_2) coating are shown in Figure 5.16, together with their average height profile perpendicular to the scratch direction. There is a remarkable difference in behavior between the organic and the hybrid coatings. The frictional force measured on the hybrid coatings is less than for the organic coating. Also the AFM images clearly show that the scratches made with the same force are deeper in the organic coating than in the hybrid coatings. The calculated scratch hardnesses are higher than the hardness measured by indentation (compare Table 5.2 and 5.3), showing that the surface is indeed harder than the rest of the coating. The results demonstrate an improved scratch resistance of the hybrid coatings compared to the organic coatings. It is remarkable that the influence of the amount of silica is not noticeable: whenever silica is in the coating, the micro-scratch resistance is improved to the same extent.

Discussion on the properties

The influence of silica on the properties of polyester-HMMM-TEOS hybrid coatings could not be retrieved from the hardness measurements on a macroscopic scale (König hardness and pencil hardness). The properties studied on a microscopic scale did show influence of silica. The micro-indentation hardness in the flexible PE6 based system was increased by addition of silica, while on the PE10 based system no increase was noticed, but even a small decrease. The same trend was found for the elastic modulus. These results suggest that the rigidity of the PE10 based system could not further be increased by an inorganic compound, while in the more flexible PE6 based system the flexibility was reduced by the inorganic phase. This effect was not seen in the König hardness measurements. It should be noticed that the comparison between the micro-indentation and König hardness cannot be made directly, as explained in Section 3.3. In this case the time scale of the measurement may have played a role. The measurement of the rolling ball of the König is in terms of seconds. The coating does not have time for relaxation before another swing is made. In the indentation measurements five indentations are made after each other, to rule out the relaxation effect and the final cycle is used in calculations. It was demonstrated in Section 3.3,
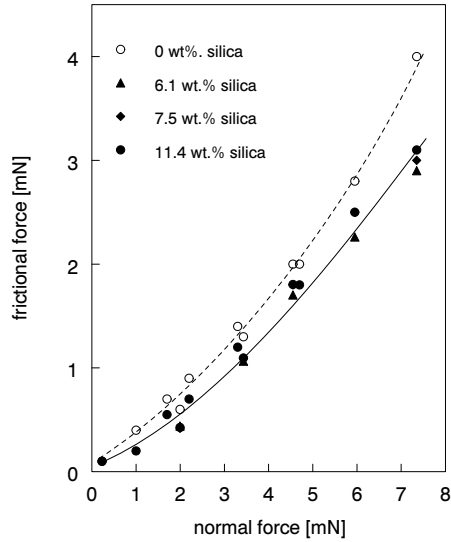
Figure 5.15: *The frictional force as a function of the normal force for the PE10-HMMM coating with 0, 6.1, 7.5 and 11.4 wt.% silica. The drawn lines are only a guide for the eye.*

Table 5.3: *Micro-scratching: the scratch hardness of polyester-HMMM hybrid coatings on aluminum, averaged values over the various scratches.*

Coating sample	Scratch hardness [GPa]
PE10-HMMM, 0 wt.% SiO_2	0.35
PE10-HMMM, 6.1 wt.% SiO_2	0.44
PE10-HMMM, 7.5 wt.% SiO_2	0.42
PE10-HMMM, 11.4 wt.% SiO_2	0.42
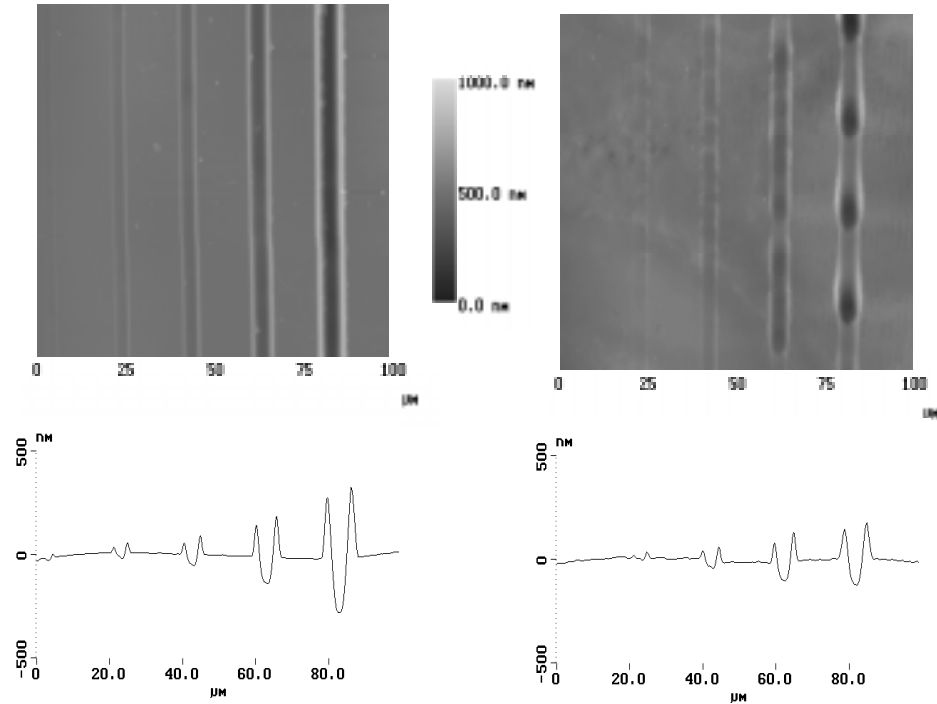
Figure 5.16: *Micro-scratching: AFM images of scratches and average height profile. Left: Organic PE10-HMMM coating without silica, Right: Hybrid PE10-HMMM coating with 11.4 wt.% silica, The scratches from left to right were made with 1, 1.7, 2.2, 3.3 and 4.7 mN normal force.*

by applying different indentation rates, that the PE6 based coatings show more time dependent behavior than PE10 based systems. Also the pencil hardness results shows that relaxation of the coating occurs after days. This may explain why the observed effects in the micro-indentation measurements are not reflected in the König hardness measurements.

In terms of micro-scratch resistance the influence of silica is noticed as well. The hybrid coating shows a better scratch resistance than the organic coating, because of an increased hardness of the surface. The amount of silica added, though, does not influence the results. Already at low silica contents in the hybrid coatings a thin layer of silica at the surface was noticed. This thin layer is held responsible for the increased scratch resistance.

5.2.3   Conclusions

Although an interpenetrating network was expected to be formed in the polyester-HMMM hybrid system, examination of the morphology of the coatings showed with increasing silica content an increase of silica particles in size and number in the organic matrix. It could not be proven, but it is highly probable that beside these silica particles also an Si-O- network throughout the film is formed. The formation of silica particles was more pronounced in hybrid coatings with a less dense network and in coatings based on PE10 instead of PE6. Furthermore it was shown that small silica particles were preferentially present at the surface. Both effects may be ascribed to the lack of interaction between the organic and inorganic phase, causing phase separation and movement of siloxane compounds or silica particles. The influence of the silica on the properties of the coatings is not large. On a macroscopic scale (König hardness and pencil hardness) no influence was seen at all. On measurements on microscopic scale only the flexible PE6 based system showed increased hardness when silica was added. The organic network rigidity was of larger importance for the final properties. Furthermore an improved micro-scratch resistance of the hybrid coatings compared to the organic coating was observed. The amount of silica seemed to have no large influence. The silica domains observed preferentially at the surface of the coating are held responsible for this improved hardness at the surface, which was also observed from the indentation measurements.

5.3   Silane-modified polyester-HMMM network with silica

To improve the interaction between the organic and inorganic compounds a silane coupling agent was used. The trifunctional hydroxyl-terminated polyester (PE6) was modified with NCO-silane in such a way that in average one of the three hydroxyl endgroups had reacted with the silane. In this way the polyester could still form a organic network in combination with HMMM. The synthesis of the silane-functional polyester is described in Section 5.3.1. The reaction is described in Section 5.1, Figure 5.5.

The modified polyester was combined with HMMM and with various amounts of pT2. The ratio HMMM:polyester was chosen in such a way that the OCH_3:OH ratio was 1.5 (15 wt.% HMMM and 85 wt.% Si-PE6) as it was in the unmodified system, assuming the effective functionality of HMMM to be 3. The final silica content in the coating was determined by TGA. Because silane is present in the polyester, the calculations for the expected silica content needed more assumptions, resulting in

Table 5.4: *The silica content of silane-modified polyester-HMMM hybrids coatings with various amounts of pT2, cured for 10 minutes at 200 °C, determined by TGA.*

calc. wt.% SiO_2	2	4	5	7	9	13	18	24
measured wt.% SiO_2 (batch 1)	3.3			6.7	9.4	12.9	17.6	
measured wt.% SiO_2 (batch 2)	2.2	3.9	6.6				19.5	24.9

less accurate numbers, but overall the amount of silica was in good agreement with these calculations. The results are summarized in Table 5.4. The amount of silica was in good agreement with the calculated values. Using silane-modified polyester more silica could be added in the system than in the unmodified system, before phase separation occurred. The limitation of the amount of silica that could be added was not based on phase separation of the coating mixture, as it was in the unmodified system, but on the possibility of applying a layer of more than 10 μm, since pT2 diluted the system and thus lowered the viscosity too much, when added in large quantities. In this system it would be possible to apply the pre-reaction method, as suggested in Chapter 2, allowing an increase of viscosity by pre-reaction of polyester and HMMM before curing.

5.3.1 Synthesis

One mole of NCO-silane was added to one mole PE6, so that on average one hydroxyl group per polyester molecule could react with the isocyanate function. The reaction was performed in 1-methoxy-2-propylacetate (MPA) at 60 °C. As a catalyst 0.5 wt.% dibutyltin dilaurate was used. After one hour the reaction was stopped and the hydroxyl value (OHV) of the reaction product was determined. The reaction product was further characterized by ^{1}H and ^{13}C NMR. The characteristics of the modified polyester are summarized in Table 5.5. The OHV was in agreement with the calculated value, indicating that reaction had taken place. Because of the overruling signals of polyester and MPA no prove for the reaction could be deduced from the NMR data.

5.3.2 Morphology

The morphology of the hybrid coatings based on silane-modified PE6, HMMM and various amounts of silica was studied by SEM and TEM. Even up to the highest amounts of silica no morphological structure could be determined. Both a SEM and

Table 5.5: *The characteristics of silane-modified PE6.*

Si-PE6	fn°	OHV [mg KOH/g]		Conversion[†]	Mn*
		before reaction	after reaction	OH groups	[g/mole]
batch 1	3	79.7	50.7	36%	2383
batch 2	3	79.7	50.8	36%	2383

° Calculated from composition. [†] Based on the total number of hydroxyl groups present

* Calculated by endgroup titration.

a TEM photograph of a silane-modified PE6 based hybrid coating with 32.4 wt.% SiO$_2$ are shown in Figure 5.17. This indicates that by applying a silane coupling agent the interaction between the organic and inorganic phase is thus improved that no phase separation occurs during curing. Both the organic and inorganic phase form a network that is connected to such an extent that phase separation is prevented. An interlinked polymer-silica network with covalent bonding between the organic and inorganic network seems to be obtained. A schematic plot of the proposed structure is pictured in Figure 5.18.
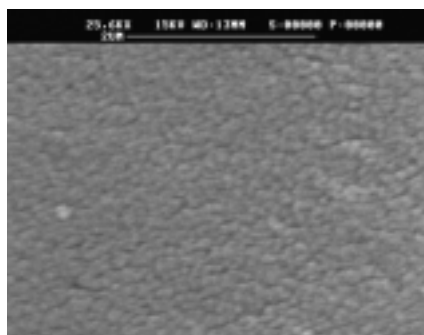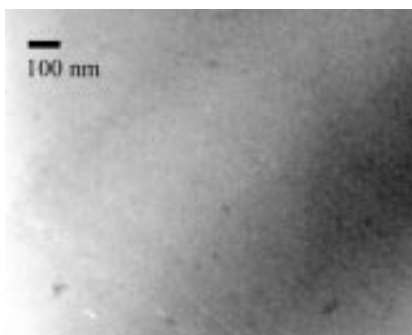
(a) SEM photograph   (b) TEM photograph

Figure 5.17: *SEM and TEM photograph of a silane-modified polyester-HMMM hybrid coating with 32.8 wt.% silica.*
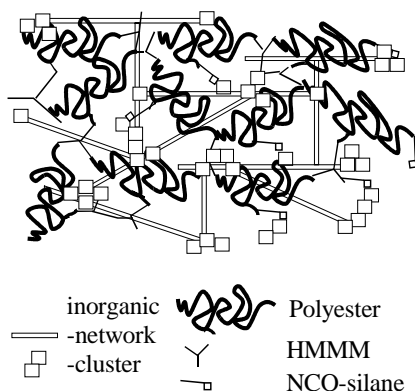
Figure 5.18: *Schematic representation of the model proposed for the silane-modified polyester-HMMM-pT2 system.*

5.3.3   Properties

The influence of the amount of silica on the silane-modified hybrid coatings was studied by König hardness and micro-indentation. In Figure 5.19 the results of the König hardness as function of the silica content of the hybrid coatings based on silane-modified PE6 are compared with the hybrid coatings based on unmodified PE6, both measured on coatings of 21 ± 4 μm applied on glass substrates. There is not much difference noticeable.

In the micro-indentation measurements the results of the silane-modified coatings without extra prehydrolyzed TEOS (total silica content of 2.2 wt.%) are compared with coatings with extra prehydrolyzed TEOS added (24.9 wt.% SiO_2), in relation with the system based on unmodified polyester (already discussed in Section 5.2). The results are summarized in the Figure 5.20, 5.21 and 5.22. The thickness of the coatings, the range of applied forces used for the calculations and the calculated average values are summarized in Table 5.6. The influence of silica on the coatings based on silane-modified polyesters were similar to the results obtained with the coatings based on the unmodified polyesters. Since the addition of the silane functional group caused an increase in molecular weight of the polyester the flexibility of the chain increased slightly, resulting in a deeper indentation in the coating without extra silica under various applied forces, compared to the unmodified coatings (Figure 5.20). Without extra prehydrolyzed TEOS added (the open markers) there is not much difference in the final hardness and reduced modulus, for the modified and unmodified polyester based coatings. But when extra silica is added and the modified and unmodified
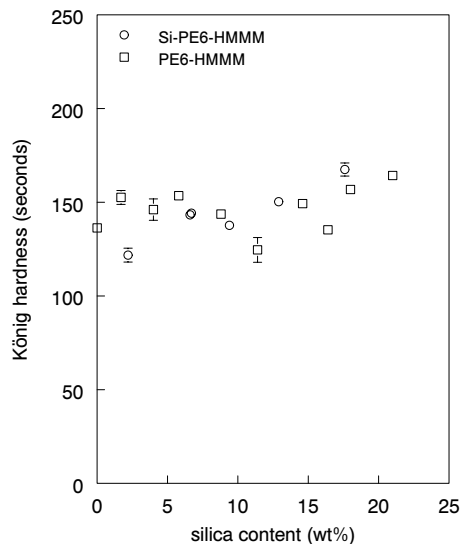
Figure 5.19: *König hardness as function of the silica content of silane-modified PE6-HMMM (○) and PE6-HMMM (□) hybrid coatings, OCH_3:OH molar ratio of 1.5.*

based coatings are compared, the indentation hardness is slightly increased further for the silane-modified based system, while the elastic modulus remains at the same level.

Silica in the form of a network does apparently not contribute to an improved König hardness. Addition of pT2 though, increases the indentation hardness, in the same way as was seen by the addition of extra pT2 in the unmodified polyester system. The increased hardness is expected to be caused by the silica network that is formed in the coating. The fact that no difference is noticed between the silane-modified (interlinked network) and the unmodified system (particles) is an extra indication that also in the unmodified system a silica network is present. The slightly improved hardness of the silane-modified system, compared to the unmodified system can be explained by the better distribution of the silica network in the silane-modified system. This results in a better distribution of the impact of the forces applied, resulting in a better resistance to indentation.
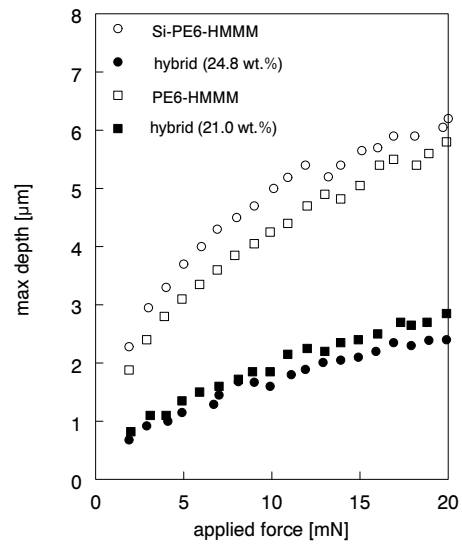
Figure 5.20: *Maximum indentation depth versus the applied forces for Si-PE6-HMMM (○) and PE6-HMMM (□) organic (open marker) and hybrid (filled marker) coatings.*
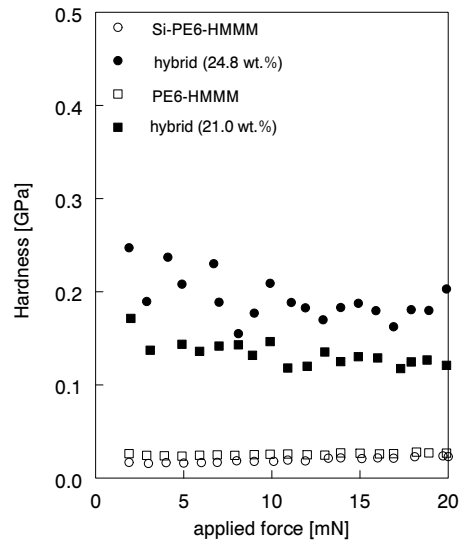
Figure 5.21: *Indentation hardness versus the applied forces for Si-PE6-HMMM (○) and PE6-HMMM (□) organic (open marker) and hybrid (filled marker) coatings.*
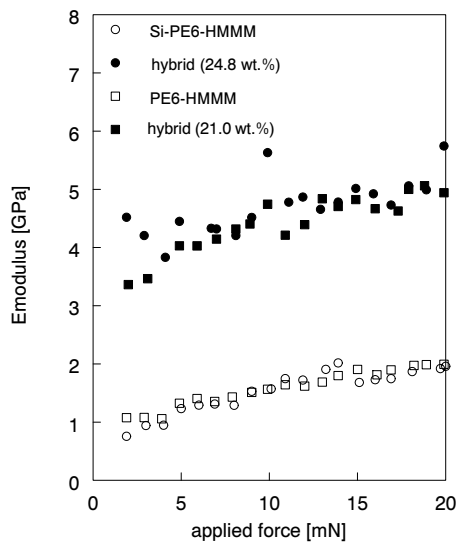
Figure 5.22: *Reduced elastic modulus versus the applied forces for Si-PE6-HMMM (∘) and PE6-HMMM (□) organic (open marker) and hybrid (filled marker) coatings.*

Table 5.6: *Micro-indentation: Coating thickness of silane modified PE6-HMMM hybrid coatings on aluminum substrates, average calculated values of the indentation hardness and reduced elastic modulus and forces of the measurements applied for the calculations.*

Coating sample	Thickness	Used forces	Hardness	Elastic Modulus
	$[\mu m]$	for calc.	[GPa]	[GPa]
2.2 wt.% SiO_2	28	2-3 mN	0.02	0.8
24.9 wt.% SiO_2	17	2-7 mN	0.22	4.3

5.4 Conclusions

Although an interpenetrating polymer-silica network was expected when polyester was crosslinked with HMMM in the presence of sol-gel silane precursors (prehydrolyzed TEOS) under acidic conditions, a morphology of silica particles in an organic matrix was obtained. Severe phase separation occurred due to the lack of interaction between the organic and inorganic phase. When the polyester was modified with a silane coupling agent as expected the interaction between the organic and inorganic phase was improved and an interlinked polymer-silica network was obtained. There are strong indications that also in the unmodified polyester-HMMM system and Si-O network is present. Firstly, this was seen in the effect of etching on the surface, for SEM preparation (Section 5.2.1). With a high silica content less contrast was obtained than with lower silica contents. Furthermore, the fact that the indentation hardnesses do not differ much, comparing silane-modified polyester based system with unmodified polyester based system (Section 5.3.3) is an indication of silica network formation. Finally, it was demonstrated in TEM that Si was present throughout the whole coating.

The silica particle formation in the unmodified system can be influenced by the organic crosslink density and the type of polyester. A denser organic network or a polyester with better compatibility can increase the amount of silica that can be incorporated in the coating before haziness occurs, but particle formation cannot be prevented this way. Furthermore, due to the lack of interaction small silica particles are preferentially present at the surface. The influence of silica on the hardness of the coatings is not large. The micro-indentation hardness is not influenced by the addition of silica in the PE10 based system, in which large silica particles were found to be present, but there is an increased hardness measured in the PE6 based systems in which the particle formation is less. A further increase of hardness is obtained when silane-modified PE6 is used, in which no particles are formed. The silica particles present in the coatings have a negative influence on the micro-indentation hardness. It is assumed that the silica particles are part of an inorganic network. In this way they are less effective in overcoming stress than when the silica is more uniformly distributed. The more uniform the structure, the better the overall stress relaxation, the better the indentation can be absorbed. It appears thus that for a high indentation hardness an uniform inorganic network is preferable. For improved scratch resistance it is preferable that silica is present at the surface of the coating. Furthermore it is observed that the flexibility of the organic network has a large influence on the final properties. When a flexible polyester is chosen in combination with an inorganic network that causes improved microscopic rigidity, the macroscopic flexibility can be kept while on the microscopic scale properties are improved. This can be interesting for improved mar resistance in coatings (see Chapter 3), since those damages are on the microscopic scale [116].

5.5   Experimental details

Silica contents were measured by thermal gravimetric analysis (TGA, Perkin Elmer TGA7). The heating rate was 20 °C/min from 50 to 800 °C.

NMR spectra were recorded on a Varian Gemini 300, using $CDCl_3$ as solvent with tetramethylsilane as internal standard.

Layer thicknesses of the coatings on glass substrates were determined by a micrometer (Coatchecker VC-2, Evano Instruments). On aluminum substrates they were measured with the eddy current principle (Twincheck, List Magnetik).

Scanning electron microscopy (SEM, Cambridge, Stereoscan 200) was performed on cross-sections of coatings on glass substrates. The samples were etched for 30 minutes with an oxygen plasma (Nanotech Plasmaprep 100) and sputtered with Pd/Au for 3 minutes (BioRad SEM Coating System).

Transmission electron microscopy (TEM, Philips CM200 TEM) and (Jeol 2000 FX) with elemental analysis (Noran Instruments Series II) was performed on samples with a thickness of 100 nm were studied. The samples were microtomed (Reichert Ultracut E/FC-4D) at -50 °C and subsequently floated on a dimethyl sulfoxide/water mixture.

König hardness was measured with a König pendulum apparatus (Pendelhärteprüfer Model 299/300, Erichsen), according to ASTM D4366, on coatings on glass substrates. Pencil hardness measurements were performed with a pencil hardness tester (Ritzhärteprüfer nach Wolff-Wilborn Model 291, Erichsen), according to ASTM D3363. The noted hardness is the highest pencil hardness that did not show damage after scratching.

Micro-indentation was performed on a homebuilt nano-indenter, with a Berkovich pyramid indenter. The used indentation speed was 10 nm/s.

Micro-scratching was performed on a homebuilt micro-scratcher, using a diamond tip, with a radius of 8 μm. A normal force, perpendicular to the coating surface was applied and scratches were made with a speed of 10 μm/s. The scratches were studied afterwards with AFM (Nanoscope 3100, Digital Instruments).

Chapter 6

Nano-structured Coatings

6.1 Introduction

A material in which two or more materials are combined in such a way that they cannot be distinguished as individual materials is called hybrid material. In such a material compounds have intermolecular interactions so that the final material is one material, a so-called nanocomposite. On the other hand, 'a composite material is a combination of two or more materials each of which retains its identity in the finished component' [154]. The term composite material [169–171] is mostly used for binder materials that are reinforced with fibers or particles of which the latter two are called reinforcements. While the reinforcements enhance the strength and stiffness, the matrix transfers the load to the reinforcements and distributes the stress among them. By choosing the right compounds and concentrations the composites can be tailored to given requirements.

The synthesis of both composites and nanocomposites is aiming at improved properties by combining different materials together. It appears though that mixing on a molecular scale results in a further improvement of the properties. An example is provided by a composite of phenolic resin with glass fibers compared with a hybrid material consisting of phenolic resin and silica, in situ formed from tetramethoxysilane [163]. The morphology of the hybrid material shows a more homogeneous distribution of the silica through the organic matrix, which improves the mechanical properties to a further extent than in the composite. The fracture strain, as well as the strength and modulus are improved in the hybrid material, while it is normally observed in corresponding conventional composites that the modulus and strength in-

crease but the fracture strain decreases. Another example is provided by an epoxide rubber, conventionally vulcanized and filled with silica (composite) compared with a vulcanized rubber in which silica is formed in situ by the sol-gel process and crosslinks are made with γ-aminopropyltriethoxysilane (hybrid) [172]. The sol-gel vulcanizates were more rigid and stronger than the typical sulfur-cured vulcanizates with comparable amounts of silica, probably due to a better distribution of the silica in the matrix. It is known that in coatings inorganic pigments also can improve strength and stiffness, although this is not the aim of their application [1,3]. It is expected that such mechanical properties can further be improved by decreasing the size of the inorganic compound, thus creating hybrid materials. Due to the small sizes of such inorganic compounds, they do not scatter light and can be applied also in transparent coating systems.

In literature various studies on the incorporation of nanoparticles are reported to improve the scratch resistance of coatings. Beside fumed silica (200-300 nm) [80] and boehmite particles (γ-Al_2O_3, < 50 nm) [69,90] pre-synthesized TiO_2 nanoparticles (4 nm), synthesized from tetraisopropyltitanate, and SiO_2 nanoparticles (10 nm), synthesized from tetraethoxysilane (TEOS), have been applied [91]. Silica nanoparticles can also be synthesized in situ using a base catalyzed sol-gel procedure [6,173]. An example is the in situ synthesis of silica particles from tetramethoxysilane with diethylamine as base catalyst in polybenzoxazoles and polybenzobisthiazoles [39,51,174]. It was found that a covalent bonding of the organic and inorganic compounds via a silane coupling agent is required to improve the compatibility. With scanning electron microscopy (SEM) it was shown that silica domains of less than 1 μm were uniformly distributed in the organic matrix.

In the research presented in this chapter polyester-epoxide-TEOS hybrid system have been studied, aiming at the in situ formation of nanosized particles within the organic polyester-epoxide matrix, by basic conditions. To improve the compatibility of the components of this system, the acid-terminated polyester has been silane-functionalized with γ-glycidoxypropyltrimethoxysilane (glymo) as described in Section 6.2. The reaction aimed for is the ring opening addition reaction of the epoxide group of glymo with the carboxylic group of the polyester, as described in Figure 6.1. Possible side reactions between acid-terminated polyester and the epoxy groups are discussed below. Hydrolysis of the methoxy groups and reaction of the oxirane ring with the silanol groups may also take place [148,175–177]. In literature the relative rates of the reactions of glymo with a mixture of n-butyric acid and water under basic conditions have been studied [175]. It was found that both hydrolysis of the Si-O-CH_3 functions (formation of silanol groups) and ring opening of the epoxy function takes place simultaneously and independently. No reaction of epoxy with silanol was mentioned. The rate of epoxy ring opening was reported to be slower than the hydrolysis reaction. When no catalyst was added reaction of silanol groups with the oxirane rings was noticed [148,176,177]. Therefore, it is expected that as
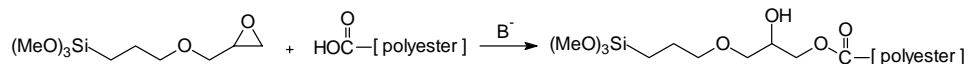
Figure 6.1: *Silane-modification of acid-terminated polyester with glymo.*

long as no water is involved during synthesis and basic conditions are applied mainly the reaction described in Figure 6.1 will take place.

The silane-modified polyester is crosslinked with an expoy resin for the formation of an organic network The epoxide resin used (Epikote 155, Shell) is based on novolac phenolic resins. By reaction of novolac phenol resin and epichlorohydrin phenol novolac glycidyl ether is obtained (Figure 6.2). The epoxy resin has an epoxy molar mass (EMM) of 182 g/mole, which means that in 182 grams of resin one mole of epoxy functions is present. The number of epoxy groups per molecule is about 3.6 [98], therefore the epoxy resin can form an organic network with a bifunctional polyester. The occurring reactions have been described in literature [178]. The main crosslinking reaction is the base catalyzed reaction of the carboxylic acid with the epoxide group (Figure 6.3, which is the same ring opening reaction as between glymo and the acid-terminated polyester (Figure 6.1)). The formed secondary alcohol can also react with both epoxy (etherification, Figure 6.4) and carboxylic acid (esterification, Figure 6.5). By the esterification reaction water is formed that also can react with the epoxide (hydrolysis, Figure 6.6). Furthermore, transesterification can occur by reaction of two hydroxyesters (Figure 6.7). From a study with epoxy and polyester model compounds [179], it was concluded that in a base catalyzed system the reaction between polyester and epoxy (Figure 6.3) proceeds in the initial stage. The other reactions occur only after the acid or epoxide has been consumed, and then etherification occurs fastest. In the hybrid systems studied also water, ethanol and silanol groups (hydrolyzed TEOS) are present. It should be considered that these compounds can also react with the acid and epoxy groups, thereby influencing the crosslink reactions.

In this chapter the synthesis of silane-modified acid terminated polyester is described in Section 6.2. These polyesters are combined with epoxides and prehydrolyzed TEOS under basic conditions. It is expected that an organic network will be formed together with in situ formation of small silica particles, due to the sol-gel reactions in the presence of an base catalyst. This should result in the formation of an organic matrix with a uniform distribution of very small silica particles. The morphology (Section 6.3) and properties (Section 6.4) of the coatings were studied. The final conclusions are summarized in Section 6.5.
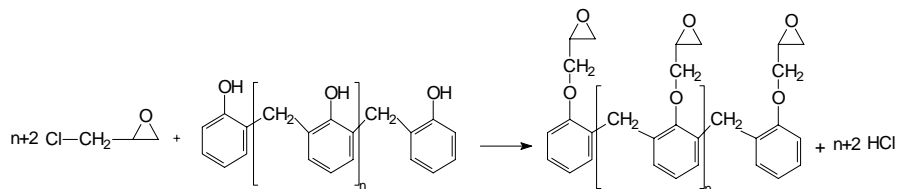
Figure 6.2: *Forming of epoxide resin from epichlorohydrin and novolac phenolic resin.*
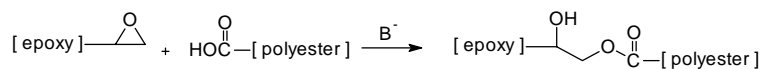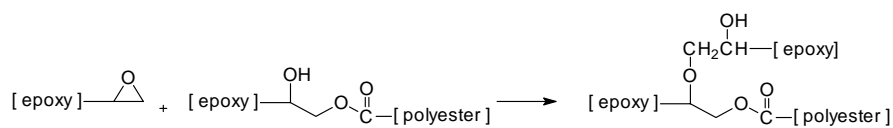

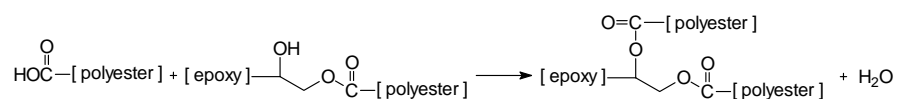Figure 6.3: *Polyester-epoxy reaction.*

Figure 6.4: *Etherification.*

Figure 6.5: *Esterification.*
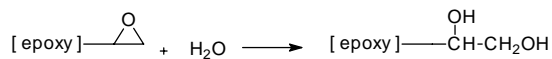
Figure 6.6: *Hydrolysis.*
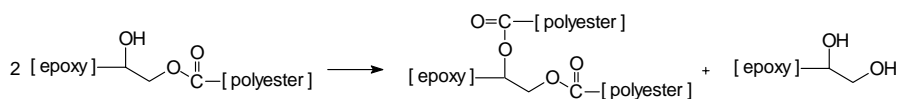
Figure 6.7: *Transesterification.*

6.2   Synthesis

Since the compatibility of both the acid-terminated polyester and the epoxide with
TEOS is low, it was not possible to prepare transparent hybrid coatings based on
acid-terminated polyester, epoxide crosslinker and TEOS with sufficient thickness and
silica content. To improve the compatibility the acid-terminated polyester has been
modified with the silane coupling agent, glymo, to form a silane-modified polyester.
Hereto, the trifunctional acid-terminated polyester was reacted with glymo to such
an extent that on average one third of the acid endgroups were linked to the epoxy
groups of glymo. In this way the polyester can still form an organic network when
the remaining acid groups are crosslinked with a trifunctional epoxide. Two methods
have been applied to synthesize this silane-modified polyester: the so-called excess
method (Section 6.2.1) and the stoichiometric method (Section 6.2.2). In the excess
method an excess of glymo is added and the reaction is short, to prevent gelation.
The excess of glymo is removed by precipitation. In the stoichiometric method one
mole of glymo is added per one mole polyester and the reaction time is longer, since
all glymo must react with the acid groups. The possibility of gelation is larger with
the stoichiometric method, due to the longer reaction time.   The disadvantage of
the excess method, with a short reaction time, is that the excess must be removed,
increasing the number of synthetic steps and the possibility to introduce water in the
system, which can also lead to gelation.

6.2.1   Excess method

An excess of glymo (five times the necessary amount) was added to the acid-ter-
minated trifunctional polyester (PE6a) in 1-methoxy-2-propylacetate (MPA). To the
mixture 1 wt.% 1,4-diazobicyclo[2.2.2]octane (DABCO) was added as catalyst. The
reaction was performed under nitrogen in a flask contained in an oil bath at 90 °C for
45 minutes. The product was precipitated in heptane to remove the excess of glymo
still present and dried in vacuo. The acid value (AV) of the reaction product was
determined and the molecular weight was calculated. The characteristics of the ob-
tained polymers are summarized in Table 6.1. The product was further characterized
by FTIR, ^{1}H and ^{13}C NMR. The complete NMR assignments can be found in Section
6.6. In this section some relevant details are discussed.

In Figure 6.8 the infrared spectra of glymo, PE6a and the silane-modified polyester
(Si-PE6a) are shown. The epoxy signal is assigned at 910 cm^{-1} [180]. Although there
is some overlap with the polyester signals and possibly formed silanol (assigned at
915 cm^{-1} [177]), it appears that there is epoxy left in the silane-modified polyester.
Also in the ^{1}H NMR spectrum (Figure 6.9) the residual epoxy groups are visible at

Table 6.1: *The characteristics of silane-modified PE6a.*

Si-PE6a by method	fn°	AV [mg KOH/g]		Conversion[†] acid groups*	Mn* [g/mole]
		before reaction	after reaction		
excess	3	85.3	44.1	48%	2313
stoich.	3	85.3	49.8	42%	2268

° Calculated from composition. [†] Based on the total number of acid groups present.

* Calculated by endgroup titration.

3.00 (C) and 2.63 ppm (A). In literature [180] silanol groups have also been assigned in the same region. It appears from Figure 6.9 that there is no extra signal in that region, meaning that no silanol groups are present in the silane-modified polyester. According to literature [181], after ring opening all protons of the oxirane shift to around 3.4 ppm. Also in this region there is overlap with other signals and therefore the reacted epoxy groups could not be demonstrated. In the ^{13}C NMR spectrum of silane-modified polyester (Figure 6.10) also the residual epoxy groups are visible at 50.4 and 43.7 ppm. After reaction of the epoxy group with the acid groups of the polyester a shift of the carbons of the former oxirane ring to lower field was expected [69, 181], but not observed. The hydrolysis and possible further reaction of the methoxy groups was noticed (Figure 6.10), since the methoxy signal (50.0 ppm) was relatively decreased. The signal at 49.8 ppm is assigned to methanol (MeOH) that was formed during hydrolysis of the methoxy groups. But it might also be the signal of methylated endgroup of the polyester by reaction with methanol or a methoxy group of glymo. From the carbonyl signals in the ^{13}C NMR (Figure 6.11) it could be retrieved that the acid groups had reacted. The signal at 176 ppm of the succinic acid endgroup (SA) had disappeared. The other carbonyl group of SA at 171 ppm and the CH_2 signals of SA at 28.7 and 28.5 ppm (Figure 6.12) were shifted and broadened.

From these analyses it has become clear that part of the acid endgroups of the polyester had reacted but the reaction of the epoxy groups could not be proven, due to the large amount of unreacted glymo that was still present and the overlapping signals. It also appears that part of the glymo is hydrolyzed, since there was a decrease in the methoxy signal noticed in ^{13}C NMR, but no silanol was found in the ^{1}H NMR spectrum. The silanol groups can react with each other forming Si-O-Si bonds. Another possibility is the reaction with the carboxylic acid end groups of the polyester.
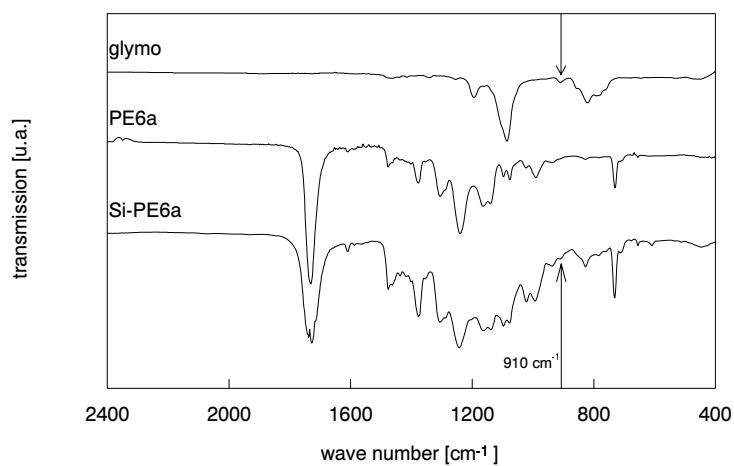
Figure 6.8: *The FTIR spectra of glymo, PE6a and Si-PE6a, synthesized by the excess method.*
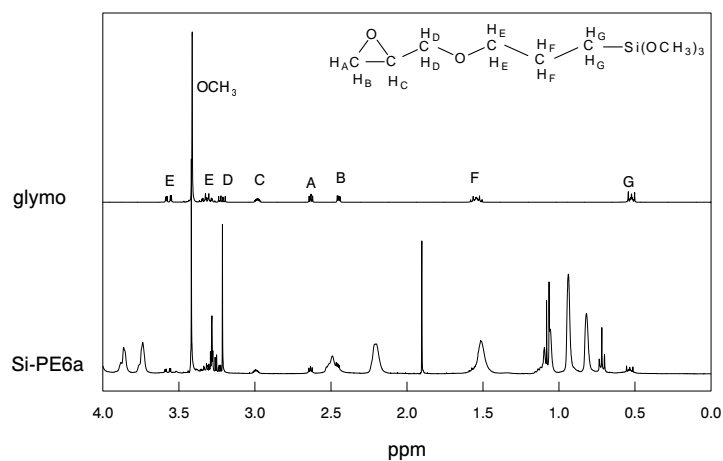
Figure 6.9: *The ^1H NMR spectra of glymo and Si-PE6a, synthesized by the excess method.*
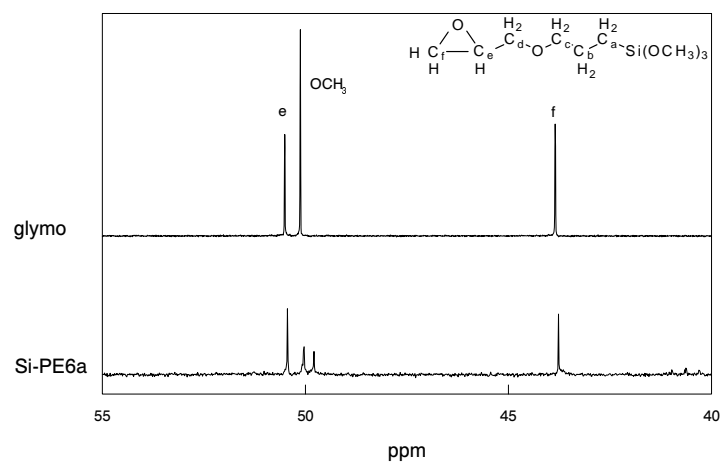
Figure 6.10: *The epoxy and methoxy group region of* ^{13}C *NMR spectra of glymo and Si-PE6a, synthesized by the excess method.*
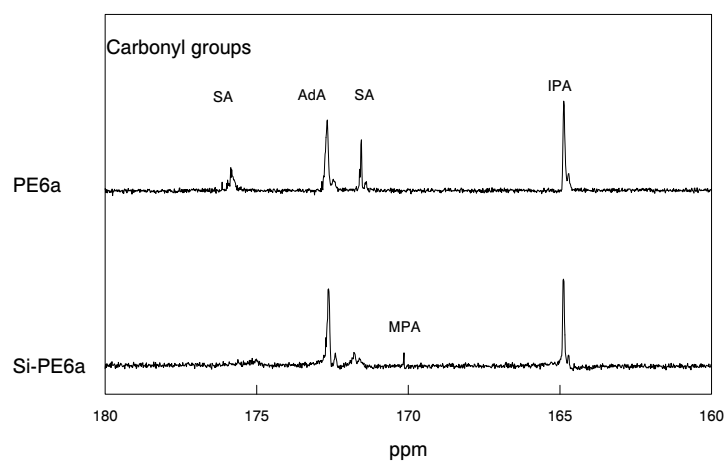
Figure 6.11: *The carbonyl region of* ^{13}C *NMR spectra of PE6a and Si-PE6a, synthesized by the excess method.*
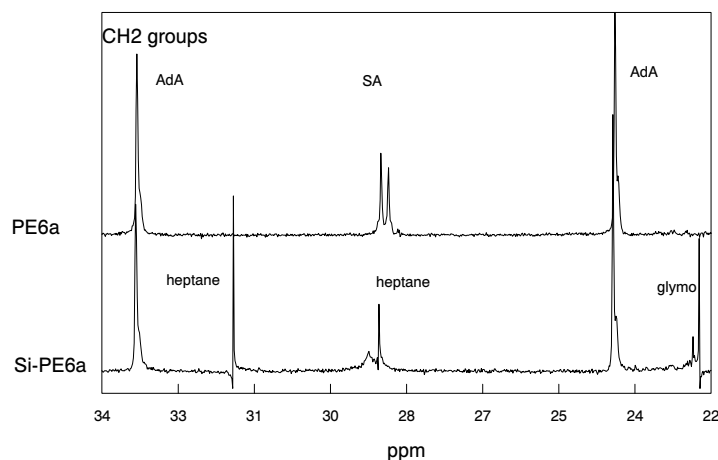
Figure 6.12: *The CH_2 region of ^{13}C NMR spectra of PE6a and Si-PE6a, synthesized by the excess method.*

6.2.2   Stoichiometric method

Glymo was added to acid-terminated trifunctional polyester (PE6a), in a 1:1 molar ratio, so that on average one acid group per polyester molecule could react with glymo. (Although strictly taken this is not stoichiometric this term was used to facilitate the comparison with the excess method.) To the mixture 1 wt.% DABCO was added as catalyst. The reaction was performed under nitrogen in a flask contained in an oil bath at 90 °C for 6 hours. The reaction was followed by titration of the acid groups and epoxide groups in the system. The conversion of the acid and epoxy groups are plotted in Figure 6.13. The starting and final acid value and calculated molecular weight are summarized in Table 6.1. While the acid groups reached over the calculated 30% conversion not all epoxy groups had reacted to completion. This means that beside the epoxide-acid reaction also other reactions occur. During the synthesis also etherification, esterification and transesterification, as explained in Section 6.1, can occur. Furthermore, water originating from the esterification reactions or present in the polyester or solvent, could cause hydrolysis of the methoxy groups and the methanol thus formed can react with the acid endgroups. In the reaction product, though, there are enough acid groups left, as determined by titration, for the organic crosslinking reaction with the trifunctional epoxide.
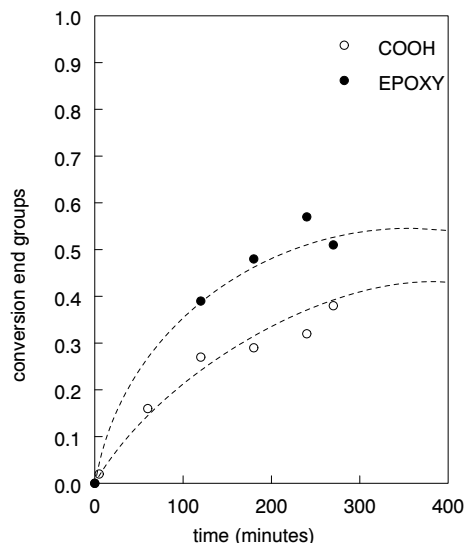
Figure 6.13: *The conversion of acid (○) and epoxy (●) groups in reaction of PE6a with glymo, using the stoichiometric method.*

6.2.3   Comparison of the synthetic methods

The excess method and the stoichiometric method both show drawbacks. In the excess method the excess of glymo must be removed, resulting in various synthetic steps that can introduce water in the system, resulting in gelation. Furthermore, it is difficult to control the reaction and to prove the occurrence of the reaction, because of unreacted glymo still present in the reaction mixture. In the stoichiometric method the long reaction time is the cause of gelation, due to a number of possible side reactions. It was found that the epoxy had only partly reacted with the acid groups, while the acid groups had reacted also with other functions. The silanization could not be proven. An other synthetic procedure should be developed for a better controlled reaction. Possibilities are addition of glymo dropwise, using other reaction conditions and working completely water free. Anyhow, even if unreacted glymo is present in the polyester it is not expected to have a negative influence on the system, since glymo enhances the compatibility and the silica content in the system.

6.2.4   Hybrid coatings

By combining the silane-modified polyesters, synthesized as described above, with a trifunctional epoxy resin (Epikote 155, Shell) with an acid:epoxy molar ratio of 1:1, an organic network is formed. Various amounts of prehydrolyzed TEOS (pT2, described in Section 2.3) were added to study the effect of the silica content on the morphology (Section 6.3) and the properties (Section 6.4) of the coatings. In Table 6.2 the silica content in the coatings, determined by thermal gravimetric analysis (TGA), is compared with the calculated amount. The final amount of silica in the coatings using the silane-modified polyester synthesized with the excess method is higher than the calculated amount, due to the excess of glymo present in the resin (see Section 6.2.1). Taking this into account the experimentally determined amount of silica is in good agreement with the calculated amounts.

Table 6.2: *The silica content of Si-PE6a-Epikote hybrid coatings with various amounts of pT2, cured for 10 minutes at 200 ° C, determined by TGA. Si-PE6a synthesized by the excess and the stoichiometric method.*

calc. wt.% SiO_2	2	3	5	6	8	9	13	18	24	32
Si-PE6a					measured wt.% Si					
Excess method		3.7		7.3	9.2		15.6	21.8		34.8
Stoich. method	1.8		4.2	5.2		8.8	13.1	15.4	25.1	33.0
						9.2		19.7		

6.3   Morphology

The morphology of the hybrid coatings was studied with SEM. No silica structure could be retrieved, as shown in Figure 6.14 for three coatings with various amounts of silica. The structures visible in the photographs were caused by oxygen etching. The effect of the oxygen plasma is reduced with increasing silica content, showing increased homogeneity and improved resistance to the oxygen plasma. These coatings were further studied by transmission electron microscopy (TEM). The photographs are pictured in Figure 6.15. With increasing silica content an increase in structure is seen. This shows that the observed structure is not caused by the resolution of the TEM, but by the increased amount of silica particles, which are smaller than 10 nm. Another remarkable feature was seen at the borders of the samples. In Figure 6.16 both edges of the coating with 21.8 wt.% SiO_2 are shown. There is clearly an increased silica content near the surface. This effect was also seen for other concentrations. The morphological structure of these hybrid coatings can be described as an organic matrix with inorganic nanosized particles. A schematic plot of the proposed structure is pictured in Figure 6.17.

(a) 3.7 wt.% SiO_2 (b) 9.2 wt.% SiO_2 (c) 21.8 wt.% SiO_2
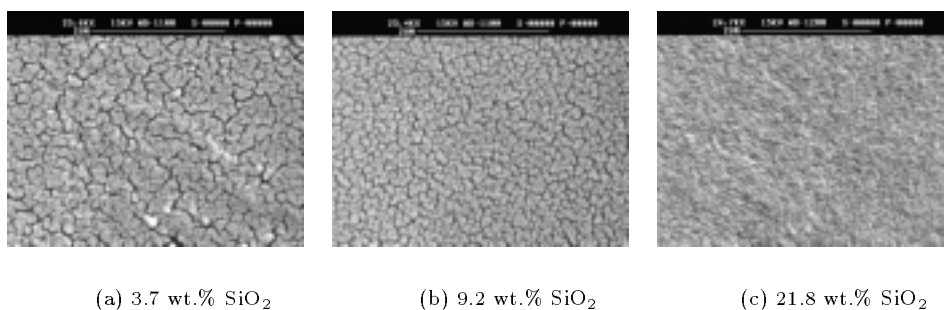
Figure 6.14: *SEM pictures of hybrid Si-PE6a-Epikote coatings with various amounts of silica. Si-PE6a was synthesized by the excess method.*

(a) 3.7 wt.% SiO$_2$ (b) 9.2 wt.% SiO$_2$ (c) 21.8 wt.% SiO$_2$
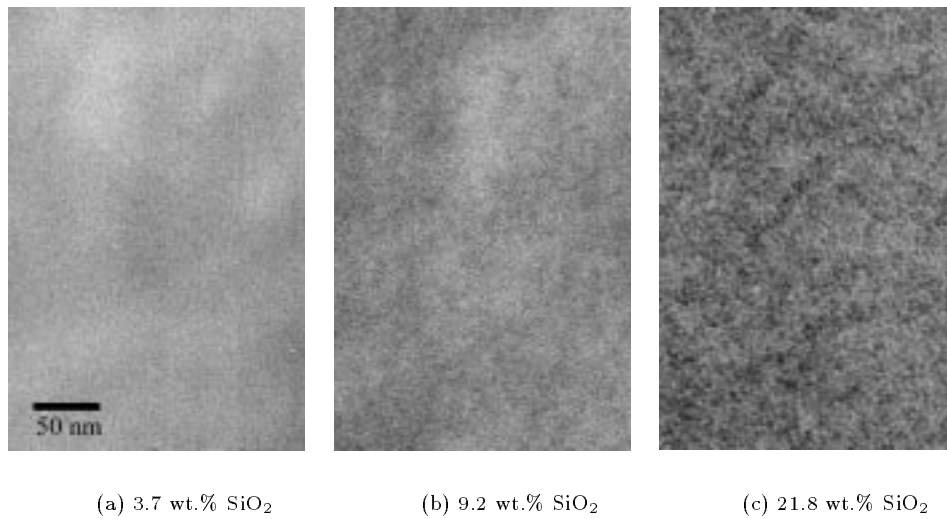
Figure 6.15: *TEM pictures of hybrid Si-PE6a-Epikote coatings with various amounts of silica. Si-PE6a was synthesized by the excess method.*

(a) Substrate side   (b) Surface side
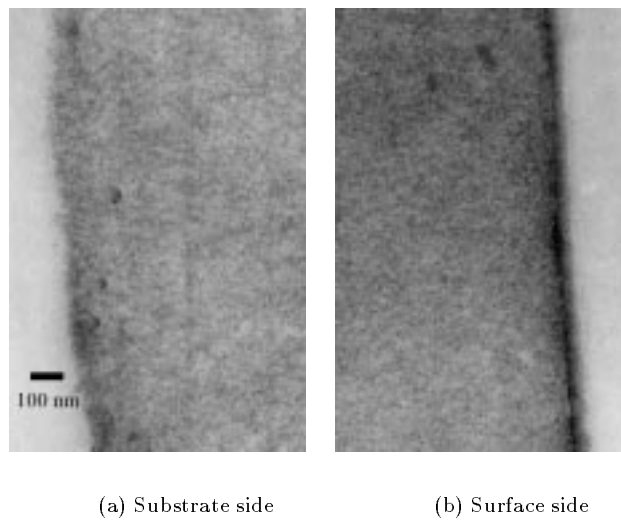
Figure 6.16: *TEM pictures of the borders of the hybrid Si-PE6a-Epikote coating with 21.8 wt.% SiO$_2$. Si-PE6a was synthesized by the excess method.*
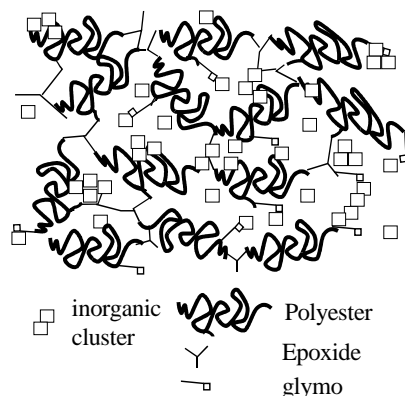
Figure 6.17: *Schematic representation of the model proposed for the silane-modified polyester-epoxide-pT2 system.*

6.4 Properties

6.4.1 König hardness and pencil hardness

The König hardness and pencil hardness of hybrid coatings based on silane-modified acid-terminated polyester and Epikote were determined as a function of the silica content on the coatings applied on glass substrates. The König hardness as function of the silica content is shown in Figure 6.18, comparing coatings based on silane-modified polyester synthesized by the two synthetic methods. Because the film thickness varied from 5 to 22 μm, as indicated in Table 6.3, power law relations were used to determine the calculated König hardness at a layer thickness of 15 μm. The power law relation describes the König hardness as function of the layer thickness. This is explained in further detail in Section 3.3.1. The used equations are shown in Figure 6.19. The pencil hardnesses of the coatings directly after scratching and 6 days later are summarized in Table 6.3. There is a recovery of the scratches noticed, resulting in a set of apparently increased pencil hardness data after 6 days. Both the König hardness and pencil hardness (directly after scratching) show an increase in hardness with increasing silica content. The coatings based on the silane-modified polyesters synthesized by the excess method shows a slightly lower König hardness, probably due to the weakening effect of unreacted glymo. The trend in pencil hardness is for all coatings synthesized the same, independent of the used synthetic method for the silane-modified polyester.
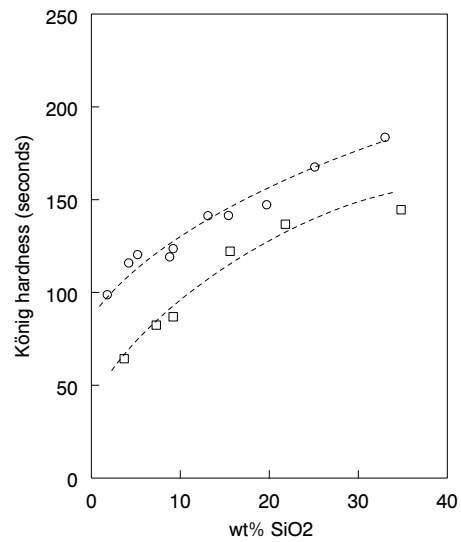
Figure 6.18: *König hardness as function of the silica content of coatings based on Si-PE6a-Epikote and pT2, for the polyester synthesized with the excess method (□) and with the stoichiometric methods (○), calculated at a layer thickness of 15 μm, using the power law relation. The drawn lines are only a guide for the eyes.*
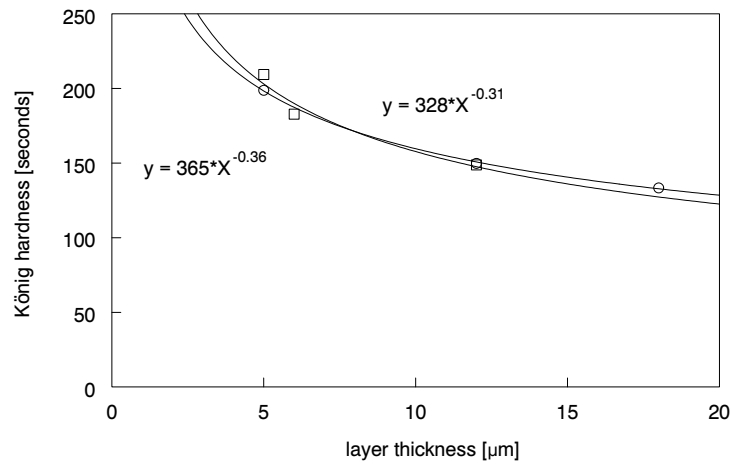
Figure 6.19: *The power law relations of the König hardness as function of the layer thickness for hybrid coatings based on Si-PE6a-Epikote and pT2, for the polyester synthesized with the excess method (□) and with the stoichiometric method (○).*

Table 6.3: *The film thickness and pencil hardness of coatings based on Si-PE6a-Epikote and pT2. Si-PE6a synthesized by the excess and stoichiometric method.*

The excess method

					wt.% SiO$_2$					
wt.% SiO$_2$					3.7	7.3	9.2	15.6	21.8	32.8
Film thickness [μm]					10	14	12	12	8	5
Pencil hardness										
direct					F	F	B	2H	4H	4H
after 6 days					3H	H	F	2H	4H	4H

The stoichiometric method

wt.% SiO$_2$	1.8	4.2	5.2	8.8	9.2	13.1	15.4	19.7	25.1	33.0
Film thickness [μm]	17	22	21	17	16	15	11	10	10	10
Pencil hardness										
direct	F	F	F	F	F	F	4H	2H	2H	2H
after 6 days	7H	F	5H	2H	F	F	4H	2H	2H	4H

6.4.2 Micro-indentation

Micro-indentation measurements have been performed on coatings based on silane-modified PE6a, synthesized with the stoichiometric method without (1.8 wt.% SiO$_2$) and with (25.1 wt.% SiO$_2$) pT2 added, on aluminum substrates. The layer thicknesses of the coatings are summarized in Table 6.4. Forces from 2 to 20 mN have been applied and the force-displacement curves have been determined (see also Section 3.3.2). From these curves the maximum indentation depth at the maximum applied forces were determined and the results are plotted in Figure 6.20. The difference in indentation depths between the coating without and with pT2 is enormous. An indentation depth of at the most 10 % of the total film thickness is allowed to rule out the substrate effect [108]. For the hybrid coatings with pT2 this is valid for a range of applied forces, but for the system without pT2 added none of the measurements meet this demand. The measurements with the maximum indentation below this 10 % of the total film thickness were used for the calculation of the average hardness and reduced elastic modulus, as summarized in Table 6.4, but this could not be done for the system without pT2 added. In that case the calculations at the lowest force (2 mN) are summarized. The influence of the substrate on the measurements on the system without pT2 added, is seen in Figure 6.21 as an increased hardness at higher maximum applied forces. For the elastic modulus (Figure 6.22) in both cases

Table 6.4: *Micro-indentation: coating thickness of Si-PE6a-Epikote coatings on aluminum, applied forces, which were used in calculations and the average calculated values of the indentation hardness and reduced elastic modulus.*

Coating sample	Thickness	Used forces for calc.	Hardness	Elastic Modulus
	$[\mu m]$	[mN]	[GPa]	[GPa]
1.8 wt.% SiO_2	27	2	0.003	0.2
25.1 wt.% SiO_2	17	2-9	0.17	4.1

an increased value is seen with increasing normal force. This effect was also seen in the other systems studied (Chapter 5) and is caused by the large difference between the modulus of aluminum and the coating (see also Section 3.3.2). From the results of the micro-indentation measurements on the silane-modified polyester-Epikote system it can be concluded, qualitatively, that pT2 increases both the indentation hardness and the elastic modulus.
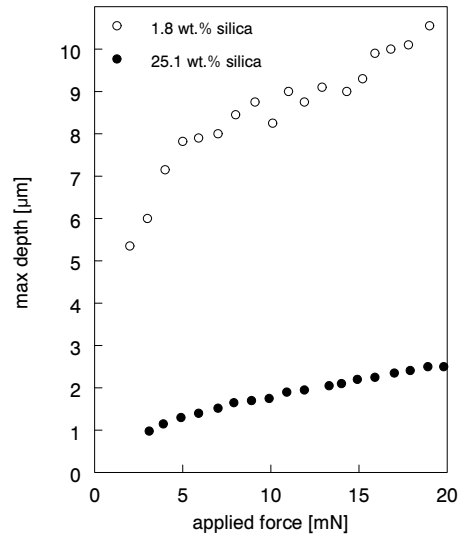
Figure 6.20: *Maximum indentation depth versus applied forces for Si-PE6a-Epikote coatings, without (○) and with (●) pT2 added.*
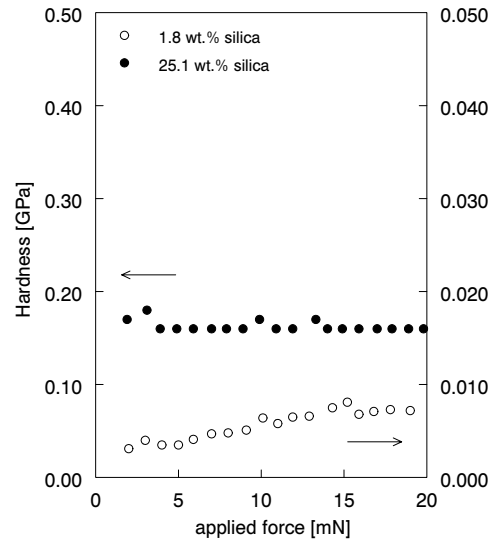
Figure 6.21: *Indentation hardness versus applied forces for Si-PE6a-Epikote coatings, without (○) and with (●) pT2 added. Note that the scale of the right axis is hundred times smaller than the scale of the left axis.*

6.4.3   Micro-scratching

Micro-scratching tests have been performed on coatings based on silane-modified PE6a, synthesized with the stoichiometric method without (1.8 wt.% SiO_2) and with (25.1 wt.% SiO_2) pT2 added, on aluminum substrates. Several scratches have been made with normal forces increasing from 2.6 to 10.2 mN. The frictional force as function of the applied normal force is plotted in Figure 6.23. The coatings with pT2 showed a very high frictional force already at low applied normal forces. Higher forces could not be applied because at that stage other effects started to play a role, so that no pure frictional force could be determined anymore. It is remarkable that, although the frictional forces on the coatings were much higher than on the coatings based on polyester, HMMM and pT2 (Chapter 5), none of the scratches in both systems could be retrieved with AFM. This shows that the coating is fully recovered and no damage remains. The only conclusion that could be drawn form these experiments was that the frictional force increased with the increase in silica content in these coatings.
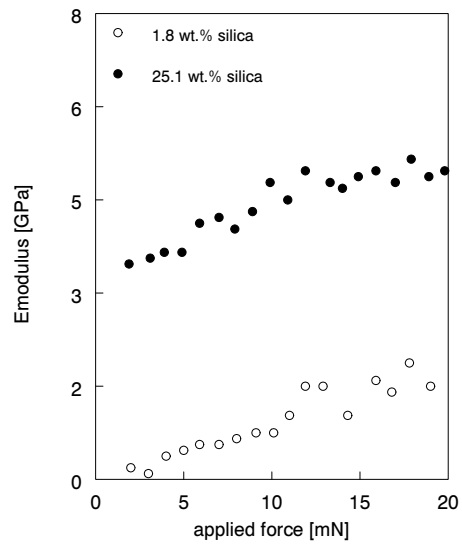
Figure 6.22: *Reduced elastic modulus versus applied forces for Si-PE6a-Epikote coatings, without (○) and with (●) pT2 added.*
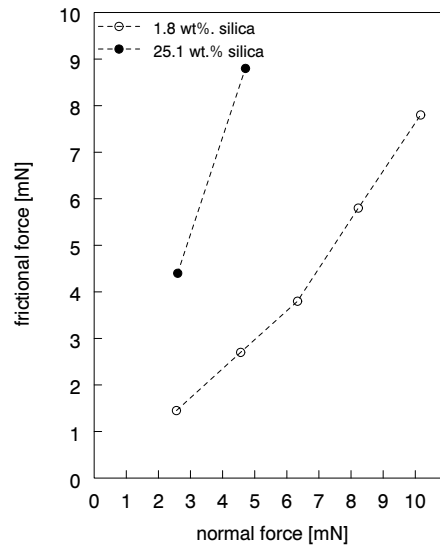
Figure 6.23: *The frictional force as a function of the normal force for Si-PE6a-Epikote coatings, without (○) and with (●) pT2. The drawn lines are only a guide for the eye.*

6.5   Conclusions

Partly silane-modified polyesters were synthesized by reacting acid-terminated poly-ester with γ-glycidoxypropyltrimethoxysilane, although it was not possible to prove the reaction due to overlapping signals and the occurrence of side reactions such as etherification, esterification and partly hydrolysis of the methoxy groups. Both by using an excess or an 'stoichiometric' amount of glymo these side reactions occurred. The silane-modified polyester is therefore susceptible to gelation and must be used in the coating preparation immediately after synthesis. With the silane-modified polyester, trifunctional epoxide and additional pT2 transparent hybrid coatings can be formed.

The morphology of the hybrid coatings consists of very small (less than 10 nm) silica particles within an organic matrix. There is an excess of silica at the surface of the coatings. These so-called nano-structured coatings show an increased König hardness with increasing silica content. Also the micro-indentation hardness is largely increased and the reduced elastic modulus is increased as well. These effects are attributed to the small silica particles in the flexible organic matrix. The organic matrix distributes the load uniformly over the nanosized hard silica particles and the stress can be released through the matrix.

Also the pencil hardness showed an increase with increasing silica content. But in time the pencil hardness changed to higher values, because of the recovery behavior of the coatings. The scratches noticed direct after applying the pencil scratch re-covered in time. Not all coatings showed the same recovery behavior. The coatings containing few silica recovered more than coatings containing more silica. The recov-ery behavior was also noticed with the micro-scratch test. The scratches itself could not be retrieved, because of the time dependent recovery behavior. Furthermore, an increased frictional force was measured with a higher silica content, compared to a lower silica content. An improved scratch resistance was expected, since very fine silica particles were found at the top of the surface, but increased scratch resistance was only measured by the pencil hardness and not confirmed by the micro-scratch test. The increased frictional force at higher silica content is not understood. It ap-pears that the scale of the deformation has influence on the behavior of the coatings. Maybe the size of the silica at the surface disturbs the gliding of a small tip on the surface, resulting in a larger friction. Also the complex visco-elastic behavior of the nanocomposites, which is not studied here, will play a role. Anyhow, no quantitative information could be retrieved from the experiments done so far.

It remains valid that with increasing silica content not the size but the number of very small silica particles increases, resulting in a behavior similar to that in conventional composites. The effects in the hybrid coatings have not been compared to composites,

like pigmented or filled coatings. Hybrid materials, though, can give transparent systems, whereas conventional composites can only be transparent when the refractive indices are comparable. Although only an indication is given, by the results of Chapter 5, it is expected that the increased silica content at the surface of the coatings improves the scratch resistance of the coatings.

6.6   Experimental details

Fourier transform infrared spectroscopy (FTIR, Matson Polaris) was performed by applying thin films, diluted with THF, on KBr tablets.

NMR spectra were recorded on a Bruker AM400, using $CDCl_3$ as solvent with tetramethylsilane as internal standard.

The acid value, the number of acid groups in the polyester in mg KOH/g, was determined by titration with standardized 0.1 M KOH in ethanol, according to DSM Resins test method TM-2401 (based on ISO 3682).

The epoxy groups were titrated with in situ formed HBr by applying standardized 0.1 N perchloric acid in glacial acetic acid in the presence of tetrabutylammonium bromide [182].

Silica contents were measured by thermal gravimetric analysis (TGA, Perkin Elmer TGA7). The heating rate was 20 or 40 °C/min from 50 to 800 °C.

Layer thicknesses of the coatings on glass substrates were determined by a micrometer (Coatchecker VC-2, Evano Instruments). On aluminum substrates they were measured with the eddy current principle (Twincheck, List Magnetik).

Scanning electron microscopy (SEM, Cambridge, Stereoscan 200) was performed on cross-sections of coatings on glass substrates. The samples were etched for 30 minutes with an oxygen plasma (Nanotech Plasmaprep 100) and sputtered with Pd/Au for 3 minutes (BioRad SEM Coating System).

Transmission electron microscopy (TEM, Jeol 2000 FX) with elemental analysis (Noran Instruments Series II) was performed on samples with a thickness of 100 nm. The samples were microtomed (Reichert Ultracut E/FC-4D) at -50 °C and subsequently floated on a dimethyl sulfoxide/water mixture.

König hardness was measured with a König pendulum apparatus (Pendelhärteprüfer

Model 299/300, Erichsen), according to ASTM D4366, on coatings on glass substrates.

Pencil hardness measurements were performed with a pencil hardness tester (Ritz-härteprüfer nach Wolff-Wilborn Model 291, Erichsen), according to ASTM D3363. The noted hardness is the highest pencil hardness that did not show damage after scratching.

Micro-indentation was performed on a homebuilt nano-indenter, with a Berkovich pyramid indenter. The used indentation speed was 10 nm/s.

Micro-scratching was performed on a homebuilt micro-scratcher, using a diamond tip, with a radius of 8 μm. A normal force, perpendicular to the coating surface was applied and scratches were made with a speed of 10 μm/s.

6.6.1   NMR assignments

The assignments of the ^{1}H and ^{13}C NMR spectra of the Si-PE6a(1), synthesized by the excess method, are summarized in Table 6.5 and 6.6, respectively. The polyester assignments are made by comparing them with assignments from literature [102–105]. The other assignments were compared with the spectra of the internet database 'SDBS' from the National Institute of Materials and Chemical Research, which can be found on www.aist.go.jp/RIODB/ SDBS/menu-e.html. The molar ratio Si-PE6a : glymo : MPA : heptane was found to be 2.4 : 1 : 0.4 : 0.2. The numbering of the assignments of glymo can be found in Figure 6.9 for the hydrogens and in Figure 6.10 for the carbons.

Table 6.5: *Assignments of ^1H NMR signals of Si-PE6a, synthesized by the excess method.*

ppm	Polyester	glymo	MPA	heptane
8.52	IPA ring			
8.07	IPA ring			
7.40	IPA ring			
4.91			HC≡	
4.43-3.74	CH_2 of NPG, TMP			
3.58		-CH$_{\underline{a}}$H$_b$-O- (E)		
3.42		-OCH$_3$		
3.34-3.22		-CH$_a$H$_{\underline{b}}$-O-CH$_2$-epoxy (E), (D)	-O-CH$_2$-	
3.21			CH$_3$-O-	
3.00		-CH(O)C (C)		
2.63		-C(O)CH$_{\underline{a}}$H$_b$ (A)		
2.49-2.44	CH_2 of SA	-C(O)CH$_a$H$_{\underline{b}}$ (B)		
2.20	CH_2 of AdA			
1.90			CH$_3$C=O	
1.51	CH_2 of AdA	-CH$_2$- (F)		
1.06-0.70	CH_3 of NPG, TMP		CH$_3$-C≡	CH$_2$, CH$_3$
0.53		-CH$_2$-Si≡ (G)		

Table 6.6: *Assignments of ^{13}C NMR signals of Si-PE6a, synthezed by the excess method.*

ppm	Polyester	glymo	MPA	heptane, MeOH
173	C=O of AdA			
171	C=O of SA			
170			C=O	
164	C=O of IPA			
133-128	IPA ring			
75			-O-CH$_2$-	
73		-CH$_2$-O- (c)		
70		-O-CH$_2$- (d)		
69.5-68.6	CH$_2$ of NPG			
68.8			HC≡	
64.5	CH$_2$ ofTMP			
59			CH$_3$-O-	
50.4		-CH(O)C (e)		
50.0		-OCH$_3$		
49.8				CH$_3$O of MeOH
43.7		-CH(O)CH$_2$ (f)		
41	C$_{quart}$ of TMP			
35	C$_{quart}$ of NPG			
33	CH$_2$ of AdA			
31				CH$_2$ of heptane
28.6	CH$_2$ of SA			
28.4				CH$_2$ of heptane
24	CH$_2$ of AdA			
22		-CH$_2$- (b)		CH$_2$ of heptane
21.4	CH$_3$ of NPG			
20.8			CH$_3$-C=O	
16			CH$_3$-C≡	
14				CH$_3$ of heptane
7	CH$_3$ of TMP			
4.8		-CH$_2$-Si≡ (a)		

Chapter 7

Conclusions and Recommendations

In this thesis organic-inorganic hybrid coatings based on polyester resins and tetraethoxysilane (TEOS) have been investigated. The aim was to control both hardness and flexibility in this new type of coatings. The studied hybrid coatings exhibited various morphologies, namely the so-called *'true hybrids'*, *interpenetrating networks* and *organic matrices with inorganic nanosized particles*. The *'true hybrid'* morphology consisted of polyester resin crosslinked with hydrolyzed and condensed TEOS clusters. The *interpenetrating network* consisted of an organic polyester-hexakis(methoxymethyl)melamine network together with a silica network formed by the acid catalyzed sol-gel reaction of TEOS. The *organic matrix with nanosized particles* consisted of a polyester-epoxide network in which silica nanoparticles are formed by the base catalyzed sol-gel reaction of TEOS. Additionally, silane coupling agents were added for improved compatibility. The influences of the morphology and the amount of silica on various properties were investigated.

The best combination of hardness and flexibility in the hybrid coatings is achieved when an *organic matrix with inorganic nanoparticles* is formed. It is expected that the organic matrix provides the flexibility, while the inorganic nanoparticles cause an increased hardness by distributing applied stresses throughout the film. It was found that the hardness can be adjusted by the amount of silica in the coating. By studying the effect of the polyester backbone on the flexibility the insight in these systems will be further extended. The flexibility should be studied quantitatively by, for example, tensile testing or dynamic mechanical analysis on free films or on coatings on substrates.

Hybrid coatings with the morphology of *interpenetrating networks* show little influence of the amount of silica on the indentation hardness of the coatings. On the other hand, the scratch and mar resistance of these coatings improves when silica is incorporated. In this case, the amount of silica has is not determining. Silica was found to be preferentially present at the surface of the coating, forming a hard and scratch resistant top layer. By optimizing and controlling this phase separation process further it will, therefore, possible to form self-stratifying coatings with a scratch resistant silica top layer and a bulk that adhere well to the substrate.

'True hybrid' systems have been used to investigate the type of interactions between the organic and inorganic phase. The interaction between the polyester resin and TEOS mainly takes place by reaction of the hydroxyl endgroups of the polyester and the hydroxyl groups of hydrolyzed TEOS. In this way Si-O-C bonds are formed. The formation of hydrogen bond interaction between silanol and carbonyl groups of the polyester was not observed. The *'true hybrid'* coatings, only formed with hydroxyl-terminated polyesters under acidic conditions in the presence of water, show an increase in hardness and glass transition temperature with increasing silica content, due to the increase in crosslink density. The Si-O-C bonds, though, are sensitive to water. In time degradation of the coatings occurs by hydrolysis of these bonds.

In the organic crosslinked hybrid systems it appeared necessary to prehydrolyse TEOS to prevent evaporation during curing. By prehydrolysis silica clusters with hydroxyl groups are formed, resulting in a better interaction with the organic components. By applying prehydrolysis before the addition to the coating systems a better homogeneity in the systems is obtained than in the case when hydrolysis takes place in the coating system.

The characterization of the morphology of the hybrid coatings has successfully been done by scanning and transmission electron microscopy. Further characterization with small angle X-ray scattering (SAXS) is recommended. Especially in the low nanometer range SAXS can give additional information about the morphology of the hybrid coatings. Also following the structure growth in the coatings in time, which can be done with SAXS, will be useful.

In this thesis it has been shown that micro-indentation and micro-scratching are methods that can be applied to organic coatings to obtain quantitative information about hardnesses, elastic moduli and friction coefficients. The use of these techniques for organic coatings is relatively new. The visco-elastic behavior of polymeric materials results in a more complex interpretation than for inorganic materials, for which these methods were designed in the first place. Furthermore, the use of small forces gives the possibility to do measurements on substrate supported coatings with only limited and measurable influence of the substrate. Further investigations in this field will give a impetus to a more quantitative characterization of organic coatings.

References

[1] R. Lambourne. *Paint and Surface Coatings: theory and practice*. Ellis Horwood Limited, 1987.

[2] Z.W. Wicks, F.N. Jones, and S.P. Pappas. *Organic Coatings: Science and Technology*. Wiley-Interscience, 1992.

[3] S. Paul. *Surface Coatings Science and Technology*. John Wiley and Sons, 1996.

[4] M Schmitthenner. Basisharze für Coil-Coating-Lacke. *Farbe Lack*, 5(104):50–65, 1998.

[5] W.D. Kingery. *Introduction to Ceramics*. John Wiley and Sons, Inc., 1960.

[6] J. Brinker and G.W. Scherer. *Sol-Gel Science: the physics and chemistry of sol-gel processing*. Academic Press, 1990.

[7] A.C. Pierre. *Introduction to Sol-Gel Processing*. Kluwer Academic Publishers, 1998.

[8] C. Sanchez, J. Livage, M. Henry, and F. Babonneau. Chemical modification of alkoxide precursors. *J. Non-Cryst. Solids*, 100:65–76, 1988.

[9] R.K. Iler. *The Chemistry of Silica, solubility, polymerization, colloid and surface properties, and biochemistry*. John Wiley & Sons Inc., 1979.

[10] C.J. Brinker, K.D. Keefer, D.W. Schaefer, R.A. Assink, B.D. Kay, and C.S. Ashley. Sol-gel transition in simple silicates II. *Mater. Res. Soc. Symp. Proc.*, 327:157–164, 1986.

[11] A.H. Boonstra and T.N.M. Bernards. The dependence of the gelation time on the hydrolysis time in a two-step SiO_2 sol-gel process. *J. Non-Cryst. Solids*, 105:207–213, 1988.

[12] T.N.M. Bernards, M.J.C.H. Janssen, and M.J. van Bommel. Influence of butanol on the hydrolysis-condensation behaviour of TEOS. *J. Non-Cryst. Solids*, 168:201–212, 1994.

[13] T.N.M. Bernards. *Silicate Sol-Gel Chemistry as Studied by Hydrolysis-Gelation Time Curves*. PhD thesis, Philips Research Laboratories, 1997.

[14] H. Schmidt. Chemistry of material preparation by the sol-gel process. *J. Non-Cryst. Solids*, 100:51–64, 1988.

[15] C. Sanchez and J. Livage. Sol-gel chemistry from metal alkoxide precursors. *New J. Chem.*, 14:513–521, 1990.

[16] H. Schmidt. Organically modified silicates by the sol-gel process. *Mater. Res. Soc. Symp. Proc.*, 32:327–335, 1984.

[17] F.D. Osterholtz and E.R. Pohl. Kinetics of the hydrolysis and condensation of organofunctional alkoxysilanes: a review. *J. Adh. Sci. Technol.*, 6(1):127–149, 1992.

[18] E.P. Plueddemann. *Silane Coupling Agents*. Plenum Press, 1982.

[19] H.K. Schmidt. Organically modified silicates as inorganic-organic polymers. In M. Zeldin, K.J. Wynne, and H.R. Allcock, editors, *ACS Symp. Ser. 360*, pages 333–344, 1988.

[20] G. Phillip and H. Schmidt. New materials for contactlenses prepared from Si- and Ti-alkoxide by the sol-gel process. *J. Non-Cryst. Solids*, 63:283–292, 1984.

[21] G. Phillip and H. Schmidt. The reactivity of TiO_2 and ZrO_2 in organically modified silicates. *J. Non-Cryst. Solids*, 82:31–36, 1986.

[22] H. Schmidt. Organic modification of glass structure. *J. Non-Cryst. Solids*, 112:419–423, 1989.

[23] H.K. Schmidt. Organically modified silicates as inorganic-organic polymers. In R.M. Laine, editor, *Inorganic and organometallic polymers with special properties*, pages 297–317. Kluwer Academic Publishers, 1992.

[24] B.M. Novak and C. Davies. 'Inverse' organic-inorganic composite materials. 2. Free radical routes into nonshrinking sol-gel composites. *Macromolecules*, 24:5481–5483, 1991.

[25] M.W. Ellsworth and B.M. Novak. Mutually interpenetrating inorganic-organic network. New routes into nonshrinking sol-gel composite materials. *J. Am. Chem. Soc.*, 113:2756–2758, 1991.

[26] B.M. Novak, M.W. Ellsworth, and C. Verrier. Nanostructured organic-inorganic hybrid materials synthesized through simultaneous processes. *ACS Symp. Series*, 585:86–96, 1995.

[27] C. Barglik-Chory and U. Schubert. Organically substituted titanium alkoxides with unsaturated organic groups. *J. Sol-Gel Sci. Technol.*, 5:135–142, 1995.

[28] J.E. Mark and S.J. Pan. Reinforcement of polydimethylsiloxane networks by in-situ precipitation of silica: A new method for preparation of filled elastomers. *Makromol. Chem. Rapid. Commun.*, 3:681–685, 1982.

[29] J.E. Mark, C.-Y. Jiang, and M.-Y. Tang. Simultaneous curing and filling of elastomers. *Macromolecules*, 17:2613–2616, 1984.

[30] J.E. Mark and J. Wen. Inorganic-organic composites containing mixed-oxide phases. *Macromol. Symp.*, 93:89–96, 1995.

[31] Y. Hu, Y.J. Chung, and J.D. Mackenzie. Gelation of an organically modified silicate. *J. Mater. Sci.*, 28:6549–6554, 1993.

[32] H.-H. Huang, B. Orler, and G.L. Wilkes. Ceramers hybrid materials incorporation polymeric/oligomeric species with inorganic glasses by a sol-gel process. 2. Effect of acid content on the final properties. *Polym. Bull.*, 14:557–564, 1985.

[33] S. Kohjiya, K. Ochiai, and S. Yamashita. Preparation of inorganic/organic hybrid gels by the sol-gel process. *J. Non-Cryst. Solids*, 119:132–135, 1990.

[34] G.L. Wilkes, A.B. Brennan, H.-H. Huang, D. Rodrigues, and B. Wang. The synthesis, structure and property behavior of inorganic-organic hybrid network materials prepared by the sol-gel process. *Mater. Res. Soc. Symp. Proc.*, 171:15–29, 1990.

[35] G.L. Wilkes, H.-H. Huang, and R.H. Glaser. New inorganic-organic hybrid materials through the sol-gel approach. *Adv. Chem. Ser.*, 221:207–226, 1990.

[36] J. Wen and G.L. Wilkes. Organic/inorganic hybrid network materials by the sol-gel process. *Chem. Mater.*, 8:1667–1681, 1996.

[37] A Kioul and L Mascia. Compatibility of polyimide-silicate ceramers induced by alkoxysilane coupling agents. *J. Non-Cryst. Solids*, 175:169–186, 1994.

[38] L.L. Beecroft, N.A. Johnen, and C.K. Ober. Covalently linked transparent silica-poly(imide) hybrids. *Polym. Adv. Technol.*, 8:289–296, 1997.

[39] J. Premachandra, C. Kumudinie, W. Zhao, and J.E. Mark. Polymer-silica hybrid materials prepared from functionalized polybenzoxazoles and polybenzo-bisthiazoles. *J. Sol-Gel Sci. Technol.*, 7:163–175, 1996.

[40] Y. Wei, D. Yang, and R. Bakthavalchalam. Thermal stability and hardness of new polyacrylate-SiO$_2$ hybrid sol-gel materials. *Mater. Lett.*, 13:261–266, 1992.

[41] S Cuney, J.F. Gerard, J.P. Pascault, G. Vigier, and K. Dušek. Hydroxyl-terminated oligomers crosslinked by alkoxysilane sol-gel or polyurethane chemistries: a comparison. *J. Appl. Polym. Sci.*, 65(12):2373–2386, 1997.

[42] D. Tian, Ph. Dubois, C. Grandfils, and R. Jérome. A novel biodegradable and biocompatible ceramer prepared by the sol-gel process. *Chem. Mater*, 9(4):871–874, 1997.

[43] E. Girard-Reydet, T.M. Lam, and J.P. Pascault. In situ polymerization of tetraethoxysilane in poly(vinylacetate). *Macromol. Chem. Phys.*, 195:149–158, 1994.

[44] C.L. Beaudry and L.C. Klein. Sol-gel processing of silica-poly(vinyl acetate) (PVAc) nanocomposites. In G.M. Chow and K.E. Gonsalves, editors, *ACS Symp. Ser. 622*, pages 382–394, 1996.

[45] T. Saegusa. Organic polymer-silica gel hybrids: A precursor of highly porous silica gel. *J. Macromol. Sci. Chem.*, A28(9):817–829, 1991.

[46] S. Kohjiya, K. Ochiai, and S. Yamashita. Synthesis and properties of inorganic/organic hybrid gels. In *Polym. Gels: Fundam. Biomed. Appl. Proc. Int. Symp.*, pages 77–91. Plenum, 1991.

[47] M. Guglielmi, P. Colombo, G. Brusatin, G. Facchin, and M. Gleria. New materials based on the reaction of cyclo- and poly-(organophosphazenes) with SiO_2, TiO_2 and ZrO_2 precursors. *J. Sol-Gel Sci. Technol.*, 2:109–114, 1994.

[48] Ch. B. Amara, N. Gharbi, and H. Zarrouk. A new route to hybrid organic-inorganic gels: synthesis and characterization. *J. Mater. Synth. Process.*, 3(5):287–301, 1995.

[49] D. Ravaine, A. Seminel, Y. Charbouillot, and M. Vincens. A new family of organically modified silicates prepared from gels. *J. Non-Cryst. Solids*, 82:210–219, 1986.

[50] C. Sanchez and F. Ribot. Design of hybrid organic-inorganic materials synthesized via sol-gel chemistry. *New. J. Chem.*, 18:1007–1047, 1994.

[51] J.E. Mark. Ceramic reinforced polymers and polymer modified ceramics. *Polym. Eng. Sci.*, 36(24):2905–2920, 1996.

[52] H. Schmidt. Survey over the state of the art in the field of processing of inorganic-organic composite materials. In S. Vilminot, R. Nass, and H. Schmidt, editors, *Eurogel '91*, pages 65–74, 1992.

[53] B.M. Novak. Hybrid nanocomposite materials: Between inorganic glasses and organic polymers. *Adv. Mater.*, 5(6):422–433, 1993.

[54] P. Judeinstein and C. Sanchez. Hybrid organic inorganic materials: A land of multidisciplinarity. *J. Mater. Chem.*, 6(4):511–525, 1996.

[55] C.J. Brinker, D.E. Clark, and D.R. Ulrich, editors. *Better Ceramics through Chemistry*. Mater. Res. Soc. Symp. Proc. 32, 73, 121, 180 and 271, 1984, 1986, 1988, 1990 and 1992.

[56] S. Komarneni, J.C. Parker, and G.J. Thomas, editors. *ACS Symp. Ser. 286: Nanophase and Nanocomposite Materials*. American Chemical Society, 1993.

[57] J.E. Mark, C.Y.-C. Lee, and P.A. Bianconi, editors. *ACS Symp. Ser. 585: Hybrid Organic-Inorganic Composites*. American Chemical Society, 1995.

[58] B.K. Coltrain, C. Sanchez, and D.W. Schaefer, editors. *ACS Symp. Ser. 435: Organic/Inorganic Hybrid Materials*. American Chemical Society, 1996.

[59] G. Tünker, H. Patzelt, H. Schmidt, and H. Scholze. Neue Wege zur Erhaltung historischer Glasfenster. *Glastech. Ber.*, 59:272–278, 1986.

[60] H. Schmidt, G. Phillip, H. Patzelt, and H. Scholze. Glass sealings by sol-gel derived organically modified silicates. In *Collect. Pap. Int. Congr. Glass, 14th (1986)*, pages 429–436, 1986.

[61] S.R. Holmes-Farley and L.C. Yano. Adhesion promotion and corrosion prevention using thin anisotropic coating. *J. Adh. Sci. Technol.*, 5(2):131–151, 1991.

[62] K. Izumi, H. Tanaka, and Y. Uchida. Hydrolysis of trifunctional alkoxysilanes and corrosion resistance of steel sheets with alkoxysilane-derived films. *J. Mater. Sci. Lett*, 12:724–727, 1993.

[63] B. Lebeau, J. Maquet, C. Sanchez, E. Toussaere, R. Hierle, and J. Zys. Relaxation behaviour of NLO chromophores grafted in hybrids sol-gel matrices. *J. Mater. Chem*, 4(2):1855–1860, 1994.

[64] S. Diré, F. Babonneau, C. Sanchez, and J. Livage. Sol-gel synthesis of siloxane-oxide hybrid coatings with luminescent properties. *J. Mater. Chem.*, 2(2):239–244, 1992.

[65] A. Hinsch. Organic fluorescent dyes in organically modified Al_2O_3 - SiO_2 or TiO_2 - SiO_2 coatings with varying polymethylmethacrylate content. *J. Non-Cryst. Solids*, 147-148:478–482, 1992.

[66] L. Hou, B. Hoffmann., M. Mennig, and H. Schmidt. Preparation and photochromic properties of dye doped aluminosilicate and ormocer gel and coatings. *J. Sol-Gel Sci. Technol.*, 2:635–639, 1994.

[67] H. Krug and H. Schmidt. Organic-inorganic nanocomposites for micro optical applications. *New. J. Chem.*, 18:1125–1134, 1994.

[68] C.J. Wung, Y. Pang, P.N. Prasad, and F.E. Karasz. Poly(p-phenylene vinylene) silica composite a novel sol-gel processed non linear optical material for optical waveguides. *Polymer*, 32(4):605–608, 1991.

[69] H Schmidt. Multifunctional inorganic-organic composite sol-gel coatings for glass surfaces. *J. Non-Cryst. Solids*, 178:302–312, 1994.

[70] J. Kron, S. Amberg-Schwab, and G. Schottner. Functional coatings on glass using ormocer-systems. *J. Sol-Gel Sci. Technol.*, 2:189–192, 1994.

[71] F.H. Wang, X.M. Chen, R.J. Hand, B. Ellis, and A.B. Seddon. The strengthening of glass with epoxy resin and ormosil coatings. *Br. Ceram. Proc.*, 54:119–132, 1995.

[72] Y. Wei, J.M. Yeh, D. Jin, X. Jia, and J. Wang. Composites of electronically conductive polyaniline with polyacrylate-silica hybrid sol-gel materials. *Chem. Mater.*, 7:969–974, 1995.

[73] B.A. Waldman. Silane coupling agents improve performance. *Mod. Paint Coat.*, pages 34–39, 1996.

[74] V. Subramanian and W.J. van Ooij. Effect of the amine functional group on corrosion rate of iron coated with films of organofunctional silanes. *Corrosion*, 54(3):204–215, 1998.

[75] K. Li, T.W. Wu, and J.C.M Li. Contact area evolution during an indentation process. *J. Mater. Res.*, 12(8):2064–2071, 1997.

[76] N. Harui and T. Agawa. Novel ambient temperature curable two-component waterborne silicone-acrylic coatings. *J. Coat. Technol.*, 70(880):73–77, 1998.

[77] S. Ito, T. Matoba, and A. Tominaga. Novel crosslinking system with hydroxyl-containing polymer, alicyclic polyepoxide and polyalkoxysilane. *Prog. Org. Coat.*, 32:97–107, 1997.

[78] H. Furukawa, Y. Kato, N. Ando, and M. Inoue. Cure mechanism and properties of acrylosilane coatings. *Prog. Org. Coat.*, 24(1-4):81–100, 1994.

[79] M.J Chen, F.D. Osterholtz, E.R. Pohl, P.E. Ramdatt, A. Chaces, and V. Bennett. Silanes in high-solids and waterborne coatings. *J. Coat. Technol.*, 69(870):43–51, 1997.

[80] N. Gupta, T.J.M. Sinha, and I.K. Varma. Development of an abrasion resistant coating from organic-inorganic polymeric network by sol-gel process. *Indian J. Chem. Technol.*, 4:130–134, 1997.

[81] S.J. Tuman and M.D. Soucek. Novel inorganic/organic coatings based on linseed oil and sunflower oil with sol-gel precursors. *J. Coat. Technol.*, 68(854):73–81, 1996.

[82] C.R. Wold and M.D. Soucek. Mixed metal oxide inorganic/organic coatings. *J. Coat. Technol.*, 70(882):43–51, 1998.

[83] R.A. Sailer and M.D. Soucek. Oxidizing alkyd ceramers. *Prog. Org. Coat.*, 33:36–43, 1998.

[84] R.A. Sailer, J.R. Wegner, G.J. Hurtt, J.E. Janson, and M.D. Soucek. Linseed and sunflower oil alkyd ceramers. *Prog. Org. Coat.*, 33:117–125, 1998.

[85] H. Schmidt, B. Seiferling, G. Phillip, and K. Deichmann. Development of organic-inorganic hard coatings by the sol-gel process. In D.R. Ulrich J.D. Mackenzie, editor, *Ultrastructure processing of advanced ceramics*, pages 651–660, 1988.

[86] R. Kasemann and H. Schmidt. Coatings for mechanical and chemical protection based on organic-inorganic sol-gel nanocomposites. *New J. Chem.*, pages 1117–1123, 1994.

[87] T. Iwamoto and J.D. Mackenzie. Ormosil coatings of high hardness. *J. Mater. Sci.*, 30:2566–2570, 1995.

[88] H. Schmidt and H. Wolter. Organically modified ceramics and their applications. *J. Non-Cryst. Solids*, 121:428–435, 1990.

[89] R. Nass, E. Arpac, W. Glaubitt, and H. Schmidt. Modeling of ormocers coating by processing. *J. Non-Cryst. Solids*, 121:370–374, 1990.

[90] R. Kasemann, H.K. Schmidt, and E. Wintrich. A new type of sol-gel-derived inorganic-organic nanocomposite. *Mater. Res. Soc. Symp. Proc.*, 346:915–921, 1994.

[91] P.W. Oliveira, H. Krug, A. Frantzen, M. Mennig, and H. Schmidt. Generation of wet chemical AR-coatings on plastic substrates by use of polymerizable nanoparticles. *Proc. SPIE-Int. Soc. Opt. Eng.*, 3136:452–461, 1997.

[92] J. Wen, V.J. Vasudevan, and G.L. Wilkes. Abrasion resistant inorganic/organic coating materials prepared by the sol-gel method. *J. Sol-Gel Sci. Technol.*, 5:115–126, 1995.

[93] J. Wen and G.L. Wilkes. Synthesis and characterization of abrasion resistant coating materials prepared by the sol-gel approach: I. Coatings based on functionalized aliphatic diols and diethylenetriamines. *J. Inorg. Organomet. Polym.*, 5:343–375, 1995.

[94] B. Wang and G.L. Wilkes. Novel hybrid inorganic-organic abrasion-resistant coatings prepared by a sol-gel process. *J. Macromol. Sci. Pure Appl. Chem.*, A31(2):249–260, 1994.

[95] B. Tamami, C. Betrabet, and G.L. Wilkes. New ceramer high optical abrasion resistant transparent coating materials based on functionalized melamine and a tris(m-aminophenyl)phosphine oxide compound. *Polym. Bull.*, 30:39–45, 1993.

[96] C.S. Betrabet and G.L. Wilkes. Determining the extent of reaction by ^{29}Si NMR of abrasion-resistant hybrid sol-gel coatings based on triethoxysilane function-alized organics. *J. Inorg. Organomet. Polym.*, 4(4):343–366, 1994.

[97] G.A. Sigel, R.C. Domszy, and W.C. Welch. Cycloaliphatic epoxide based sol-gel derived materials. *Mater. Res. Soc. Symp. Proc.*, 346:135–141, 1994.

[98] D. Stoye and W. Freitag. *Resins for Coatings*. Hanser/Gardner, 1996.

[99] H.-H. Huang, B. Orler, and G.L. Wilkes. Structure property behavior of new hybrid materials incorporating oligomeric species into sol-gel glasses. 3. Effect of acid content, tetraethoxysilane content and molecular weight of poly(dimethylsiloxane). *Macromolecules*, 20:1322–1330, 1987.

[100] C.J.T. Landry, , B.K. Coltrain, J.A. Wesson, N. Zumbulyadis, and J.L. Lippert. Insitu polymerization of tetraethoxysilane in polymers. Chemical nature of the interaction. *Polymer*, 33(7):1496–1506, 1992.

[101] M. Arens and W. Schoenfelder. Hydroxylzahl - Gemeinschaftsarbeiten der DGF, 116. Mitteilung: Deutsche Einheitsmethoden zur Untersuchung von Fetten, Fettprodukten, Tensiden und verwandten Stoffen, 88. Mit.: Analyse von Fetten XXVIII. *Fat Sci. Technol.*, 9:371–373, 1990.

[102] M. Marshall. NMR analysis of paint media. *J. Oil Colour Chem. Assoc.*, 66(10):285–293, 1983.

[103] H.R Kricheldorf. ^{13}C NMR sequence analysis. 17: Investigation on polyesters from diacids and diols. *Makromol. Chem.*, 179:2133–2143, 1978.

[104] S. Hvilsted and N.U. Jorgensen. Polyol structural elucidation in binder polyesters 1. ^{13}C NMR study of fundamental polyols in aliphatic and aromatic polyesters. *Polym. Bull.*, 10:236–243, 1983.

[105] S. Hvilsted. A route to quantitative ^{13}C NMR analysis of multicomponent polyesters. *Makromol. Chem., Macromol. Symp.*, 52:199–208, 1991.

[106] K. Sato. The hardness of coatings films. *Prog. Org. Coat.*, 8:1–18, 1980.

[107] P. Fink-Jensen. Hardness and theory of its measurement. In *FATIPEC*, pages 26–34, 1968.

[108] P. Fink-Jensen. Hardness testing of organic coatings. *Pure Appl. Chem.*, 10(3):241–292, 1965.

[109] E.M. Corcoran. Hardness and related properties. In G.G. Sward, editor, *Paint Testing Manual*, chapter 5.1, pages 281–300. American Chemical Society, 1972.

[110] L.W. Hill. *Mechanical Properties of Coatings*. Federation of Societies for Coatings Technology, 1987.

[111] P.E. Pierce. Mechanical properties of coatings. In R.R. Myers and J.S. Long, editors, *Treatise on Coatings, Volume 2, Part I: Characterization of coatings: physical techniques*, chapter 4, pages 99–130. Marcel Dekker, 1966.

[112] P.R. Guevin. State-of-the-art instruments to measure coating hardness. *J. Coat. Technol.*, 67(840):61–65, 1995.

[113] H. Berlin and K. Hartmann. Mikroeindringhärte - Pendeldämpfung Wichtige Meßmethoden zur Beurteiling der Schutzfunktion von Lackfilmen. In *FATIPEC*, pages 271–281, 1992.

[114] B.V. Gregorovich and P.J. McGonigal. Mechanical properties of coatings needed for good scratch and mar. In *Adv. Coat. Technol. Conf.*, pages 121–125. ASM International Materials Park, 1992.

[115] W. Shen, C. Ji, F.N. Jones, M.P. Everson, and R.A. Ryntz. Measurements by scanning force microscopy of the scratch and mar resistance of surface coatings. *Surf. Coat. Int.*, 6:253–256, 1996.

[116] J.L. Courter and E.A. Kamenetzky. Micro- and nano-indentation and scratching for evaluation the mar resistance of automotive clearcoats. In R. Curt, editor, *Creat. Adv. Coat. Technol. Congress Papers*, volume 1, pages 351–369. Vincentz Verlag, 1999.

[117] A.B. Perduijn and S.M. Hoogenboom. The pure bending of sheet. *J. Mater Proces. Technol.*, 51:274–295, 1995.

[118] F.A. McClintock and A.S. Argon. *Mechanical Behavior of Materials*, page 8. Addison-Wesley Publishing Company, 1966.

[119] E. Amitay-Sadovsky and H.D. Wagner. Evaluation of Young's modulus of polymers from Knoop microindentation tests. *Polymer*, 39(11):2387–2390, 1998.

[120] W.W. Weiler. Dynamic loading: a new microhardness test method. *J. Test. Evol.*, 18(4):229–239, 1990.

[121] G. Kourtesis, G.M. Renwick, and A.C. Fischer-Cripps. Mechanical property characterization of a number of polymers using uniaxial compression and spherical tipped indentation tests. *J. Mater. Sci.*, 32:4493–4500, 1997.

[122] W.C. Oliver and G.M. Pharr. An improved technique for determining hardness and elastic modulus using load and displacement sensing indentation experiments. *J. Mater. Res.*, 7(6):1564–1583, 1992.

[123] S.S. Duttagupta, X.L. Chen, S.A. Jenekhe, and P.M. Fauchet. Microhardness of porous silicon films and composites. *Solid State Comm.*, 101(1):33–37, 1997.

[124] M.F. Doerner and W.D. Nix. A method for interpreting the data from depth-sensing indentation instruments. *J. Mater. Res.*, 1(4):601–609, 1986.

[125] S.P. Baker. The analysis of depth-sensing indentation data. *Mater. Res. Soc. Symp. Proc.*, 308:209–216, 1993.

[126] J.L. Courter. Mar resistance of automotive clearcoats I. Relationship to coating mechanical properties. *J. Coat. Technol.*, 69(866):57–63, 1997.

[127] W. Shen, S.M. Smith, F.N. Jones, C. Ji, R.A. Ryntz, and M.P. Everson. Use of a scanning probe microscope to measure marring mechanisms and microhardness of crosslinked coatings. *J. Coat. Technol.*, 69(873):123–135, 1997.

[128] K. Holmberg and A. Mattews. *Coatings Tribology, properties, techniques and applications in surface engineering.* Tribology series. Elsevier, 1994.

[129] K. Adamsons, G. Blackman, B. Gregorovich, L. Lin, and R. Matheson. Oligomers in the evolution of automotive clearcoats: mechanical performance testing as a function of exposure. *Prog. Org. Coat.*, 34:64–74, 1998.

[130] B.J. Briscoe, P.D. Evans, E. Pelillo, and S.K. Sinha. Scratching maps for polymers. *Wear*, 200:137–147, 1996.

[131] N.P. Suh. *Tribophysics.* Prentice-Hall, 1986.

[132] D. Tabor. Friction-The present state of our understanding. *J. Lubr. Technol.*, 103:169–179, 1981.

[133] J. Zhang, F.A. Moslehy, and S.L. Rice. A model for friction in quasi-steady-state sliding part I. Derivation. *Wear*, 149:1–12, 1991.

[134] S.M.H. Benabdallah and J.-P. Chalifoux. Ploughing of soft asperities by a hemispherical slider. *Tribol. Int*, 22(6):383–388, 1989.

[135] J.K. Lancaster. Friction and wear. In A.D. Jenkins, editor, *Polymer Science Volume 2*, chapter 14. North Holland Publishing Company, 1972.

[136] A.C.-M. Yang and T.W. Wu. Abrasive wear and craze breakdown in polystyrene. *J. Mater. Sci.*, 28:955–92, 1993.

[137] A.C.-M. Yang and T.W. Wu. Wear and friction in glassy polymers: microscratch on blends of polystyrene and poly(2,6-dimethyl-1,4-phenylene oxide). *J. Polym. Sci. Part B Polym. Phys.*, 35(9):1295–1309, 1997.

[138] R. Consiglio, N.X. Randall, B. Bellaton, and J. von Stebut. The nano-scratch tester (NST) as a new tool for assessing the strength of ultrathin hard coatings and the mar resistance of polymer films. *Thin Solid Films*, 332:151–156, 1998.

[139] F.N. Jones, W. Shen, S.M. Smith, Z. Huang, and R.A. Ryntz. Studies of microhardness and mar resistance using a scanning probe microscope. *Prog. Org. Coat.*, 34:119–129, 1998.

[140] W. Shen, S.M. Smith, H. Ye, F.N. Jones, and P.B. Jacobs. Real time observation of viscoelastic creep of a polymer coating by scanning probe microscope. *Tribol. Lett.*, 5:75–79, 1998.

[141] H. Schmidt. New type of non-crystalline solids between inorganic and organic materials. *J. Non-Cryst. Solids*, 73:681–691, 1985.

[142] L.C. Klein and C.L. Beaudry. Controlling transparency in polyethylene PEO/silica gels. *SPIE*, 3136:20–24, 1997.

[143] T. Saegusa. Organic/inorganic polymer hybrids. *Macromol. Symp.*, 98:719–729, 1995.

[144] D. Tian, Ph. Dubois, and R. Jérome. Biodegrable and biocompatible inorganic-organic hybrid materials. I. Synthesis and characterization. *J. Polym. Sci. Part A: Polym. Chem.*, 35(11):2295–2309, 1997.

[145] B. Coltrain, C.J.T. Landry, J.M. O'Reilly, and A.M. Chambertam. Role of trialkoxysilane functionalization in the preparation of organic-inorganic composites. *Chem. Mater.*, 5:1445–1455, 1993.

[146] J.E. Mark and J.L. Sullivan. Model networks of endlinked polydimethylsiloxane chains. 1. Comparisons between experimental and theoretical values of the elastic modulus and the equilibrium degree of swelling. *J. Chem. Phys.*, 66(3):1006–1011, 1977.

[147] R. Kalfat, N. Gharbi, H. Zarrouk, and F. Babonneau. Préparation et caractérisation des hybrides "organiques-inorganiques" par modification du polyméthyl-hydrosiloxane par les alcools et les alcènes. *J. Soc. Chim. Tunis.*, III(8):533–543, 1994.

[148] G. Xue, J.L. Koenig, D.D. Wheeler, and H. Ishida. Reinforcement mechanism of polyester-fiber-reinforced rubber: A model study. *J. Appl. Polym. Sci.*, 28:2633–2646, 1983.

[149] D. Tian, Ph. Dubois, and R. Jérome. A new poly(ϵ-caprolactone) containing hybrid ceramer prepared by the sol-gel process. *Polymer*, 37(17):3983–3987, 1996.

[150] M. Guglielmi, G. Brusatin, G. Facchin, and M. Gleria. Hybrid materials based on the reaction of polyorganophosphazenes and SiO_2 precursors. *J. Mater. Res.*, 11(8):2029–2034, 1996.

[151] J. Gnado, P. Dhamelincourt, C. Pélégris, M. Traisnel, and A. Le Maguer Mayot. Raman spectra of oligomeric species obtained by tetraethoxysilane hydrolysis-condensation process. *J. Non-Cryst. Solids*, 208:247–258, 1996.

[152] M.C. Matos, L.M. Ilharco, and R.M. Almeida. The evolution of TEOS to silica gel and glass by vibrational spectroscopy. *J. Non-Cryst. Solids*, 147-148:232–237, 1992.

[153] A. Bertoluzza, C. Fagnano, and M.A. Morelli. Raman and infrared spectra on silica gel evolving towards glass. *J. Non-Cryst. Solids*, 48:117–128, 1982.

[154] T. Whelan. *Polymer Technology Dictionary*. Chapmann & Hall, 1994.

[155] D. Klempner and L. Berkowski. Interpenetrating polymer networks. In H.F. Mark, N.M. Bikaler, C.G. Overberger, and G. Mengs, editors, *Encyclopedia of Polymer Science and Engineering Vol. 8*, pages 279–341. Wiley-Interscience, 1987.

[156] L.H. Sperling. Interpenetrating polymer networks (overview). In J.C. Salamone, editor, *Polymeric Materials Encyclopedia Vol. 5*, pages 3292–3302. CRC Press, 1996.

[157] E.J.A. Pope, M. Asami, and J.D. Mackenzie. Transparent silica gel-PMMA composites. *J. Mater. Res.*, 4(4):1018–1026, 1989.

[158] K.F. Silveira, I. Valeria, P. Yoshida, and S.P. Nunes. Phase separation in PMMA/silica sol-gel systems. *Polymer*, 36(7):1425–1434, 1995.

[159] R.A. Zoppi and S.P. Nunes. Hybrids of poly(ethylen oxide-co-epichlorohydrin) and silica: phase separation, morphology and thermal properties. *Polyner*, 39(25):6195–6203, 1998.

[160] Q. Deng, R.B. Moore, and K.A. Mauritz. Novel Nafion/ormosil hybrids via in situ sol-gel reactions. 1. Probe of ormosil phase nanostructures by infrared spectroscopy. *Chem. Mater.*, 7:2259–2268, 1995.

[161] S.K. Young, K. Page, and K.A. Mauritz. Novel Nafion/ormosil and telechelic polymer/ormosil hybrids via in situ sol-gel chemistry. *Polym. Mater. Sci. Eng.*, 76:391–292, 1997.

[162] Mukkamala. R. and H.M. Cheung. Acid and base effects on the morphology of composites formed from microemulsion polymerization and sol-gel processing. *J. Mater. Sci.*, 32:4687–4692, 1997.

[163] K. Haraguchi, Y. Usami, K. Yamamura, and S. Matsumoto. Morphological investigation of hybrid materials composed of phenolic resin and silica prepared by in situ polymerization. *Polymer*, 39(25):6243–6250, 1998.

[164] L. Mascia and A. Kioul. Polyimide-silica hybrid materials by sol-gel processing. *J. Mater. Sci. Lett.*, 13:641–643, 1994.

[165] L. Matějka, K. Dušek, and J. Noga. Formation, structure and mechanical properties of organic-silica hybrid networks. In *Polym. Network Group Rev. Ser.*, volume 1, chapter 22, pages 301–311. Wiley, 1998.

[166] L. Matějka, J. Pleštil, and Dušek. K. Structure evolution in epoxy-silica hybrids: sol-gel process. *J. Non-Cryst. Solids*, 226:114–121, 1998.

[167] U. Samaraweera, S. Gan, and F.N. Jones. Enhanced reactivity of melamine-formaldehyde resins by fractionation. Crosslinking at ambient temperature. *J. Appl. Polym. Sci.*, 45:1903–1909, 1992.

[168] W.J. Blank. Reaction mechanism of melamine resins. *J. Coat. Technol.*, 51(656):61–70, 1979.

[169] F.P. Gerstle. Composites. In H.F. Mark, N.M. Bikaler, C.G. Overberger, and G. Mengs, editors, *Encyclopedia of Polymer Science and Engineering Vol. 3*, pages 776–820. Wiley-Interscience, 1985.

[170] T.J. Reinhart and L.L. Clements. Introduction to composites. In *Engineered Materials Handbook, Vol. 1*, pages 27–34. ASM International, 1987.

[171] J. Karger-Kocsis. Composites. In J.C. Salamone, editor, *Polymeric Materials Encyclopedia, Vol. 2*, pages 1378–1383. CRC Press, 1996.

[172] A. Hashim, N. Kawabata, and S. Kohjiya. Silica reinforcement of epoxidized natural rubber by the sol-gel method. *J. Sol-Gel Sci. Technol.*, 5:211–218, 1995.

[173] C.J.T. Landry and B.K. Coltrain. Organic-inorganic composite prepared via the sol-gel method some inside into morphology control and physical properties. *Polym. Prep.*, 32:514–515, 1991.

[174] J.P. Chen, Z. Ahmad, S. Wang, J.E. Mark, and F.E. Arnold. Preparation and mechanical properties of polybenzoxazole-silica hybrid materials. In J.E. Mark, C.Y.-C. Lee, and P.A. Bianconi, editors, *Hybrid Organic-Inorganic Composites*, pages 297–306. ACS Symp. Ser. 585, 1995.

[175] Y.G. Hsu and J.H. Huang. Model reaction of epoxy-containing siloxane. *J. Non-Cryst. Solids*, 208:259–266, 1996.

[176] G. Xue, H. Ishida, and J.L. Koenig. Chemical reactions in the bulk of the epoxy-functional silane hydrolyzate. *Angew. Makromol. Chem.*, 140(2282):127–134, 1986.

[177] G. Xue, J.L. Koenig, and H. Ishida. Chemical reactions of an epoxy-functional silane in aqueous solution. *Rubber Chem. Technol.*, 64(2):162–171, 1991.

[178] L. Shechter and J. Wynstra. Glycidyl ether reactions with alcohols, phenols, carboxylic acids, and acid anhydrides. *Ind. Eng. Chem.*, 48:86–93, 1956.

[179] L. Matějka, S. Pokorný, and Dušek. K. Network formation involving epoxide and carboxyl groups, course of the model reaction monoepoxide-monocarbonic acid. *Polym. Bull.*, 7:123–128, 1982.

[180] Y. Huang, Y. Yu, and J.P. Bell. Studies on a novel polymeric coupling agent: 3-glycidoxypropyltrimethoxysilane-modified polycarbonate. *J. Appl. Polym. Sci.*, 56:1–8, 1995.

[181] T.J. Horr and G.D. Reynolds. The reaction of 3-glycidoxypropyltrimethoxy-silane in acidic solutions on polymerization in the presence of silica. *J. Adhes. Sci. Technol.*, 11(7):995–1009, 1997.

[182] R.R. Jay. Direct titration of epoxy compounds and aziridines. *Anal. Chem.*, 36(3):667–668, 1964.

Summary

The new field of organic-inorganic hybrid materials has been largely expanding over the past fifteen years. The possibility of combining organic and inorganic material properties originates from another relatively new field: the sol-gel science. In the sol-gel process inorganic materials are formed at temperatures which organic compounds can withstand, in contrast to the conventional methods of inorganic material synthesis. The aim of the synthesis of most hybrid materials is to combine specific organic and inorganic material properties in one material. Our aim is to improve the hardness and scratch resistance of organic based coatings, while at the same time maintaining the flexibility.

In this thesis the possibilities of organic-inorganic hybrid solvent-based coatings as hard, scratch resistant and still flexible coatings on steel and aluminum are described. The organic component is a flexible polyester resin crosslinked with organic crosslinkers, thus forming an organic coating network. The polyester resins synthesized contained a hydroxyl functionality. By addition of succinic anhydride acid-terminated polyesters were formed. In this way only the end function was changed, while hardly changing the composition and structure of the polyesters. The inorganic part is meant to provide hardness and scratch resistance of the hybrid coatings and consists of tetraethoxysilane (TEOS) that forms silica under acidic or basic conditions via hydrolysis and condensation in the presence of water: the so-called sol-gel process. It was found that at the curing temperatures of the organic crosslinking, the silicon compounds evaporated from the coatings. Therefore, the precursor was prehydrolyzed with water under acidic conditions, prior to application in the coating systems. In this way silica clusters with hydroxyl groups were pre-formed, preventing evaporation and improving the interaction with the organic compounds.

For a systematic study on the influence of the morphology of hybrid coatings on the hardness and flexibility several hybrid coatings have been prepared. One acid catalyzed system and one base catalyzed organic crosslinking system were chosen. It is known that the pH of the reaction mixture influences the morphology of the in situ

formed inorganic silica. By applying both and acid and base catalyzed system two different microstructures of compositional comparable hybrid coatings were obtained. Under acidic conditions *interpenetrating organic and inorganic networks* are formed, while under basic conditions *silica nanoparticles are embedded in the organic matrix*. A third morphological structure type was obtained by the reaction of polyester resin and TEOS, without the presence of an organic crosslinker. In this way the silicon compound forms the crosslinks of the polyester resin, thus forming a so-called *'true hybrid'*.

The morphology has been studied with scanning and transmission electron microscopy. The study on properties was focused on the effect of the amount of silica on the hardness and scratch resistance. This was studied by techniques commonly used in the coatings industry (König hardness, pencil hardness), but also with better defined methods like the micro-indentation and micro-scratching method.

Polyester resin crosslinked with hydrolyzed and partially condensed TEOS only results in the formation of *'true hybrids'* when hydroxyl-terminated polyesters are used, under acidic conditions in the presence of water. It is shown that reaction between the organic and inorganic phase takes place via the hydroxyl endgroups of the polyester and the silanol groups of the inorganic component. An increase in König hardness and glass transition temperature with increasing TEOS content is determined, showing the increase in crosslink density. It was determined that the formed Si-O-C crosslinks, though, are easily hydrolyzed leading to degradation of the coatings.

When hydroxyl-terminated polyesters are crosslinked with hexakis(methoxymethyl)-melamine in combination with prehydrolyzed TEOS under acidic conditions phase separation occurs within the organic-silica *interpenetrating network*. Phase separation in the coatings results in the formation of silica particles, which increase in size and number with increasing silica content, finally resulting in hazy coatings. Furthermore, it was found that the silicon compounds migrate to the surface of the coating. The silica on the surface increases the scratch resistance of the coatings. When the polyester was modified with silane coupling agents the compatibility between the organic and inorganic phase improves largely. No phase separation is observed and an interlinked interpenetrating organic-inorganic hybrid networks is formed. The effect of the amount of silica in the coating on the indentation hardness is small.

For coatings of acid-terminated polyester with epoxides and prehydrolyzed TEOS under basic conditions also silane coupling agents are necessary to be able to form an *organic matrix with nanosized inorganic particles* (less than 10 nm). The hardness (König, pencil and micro-indentation) increases with increasing silica content. The scratch tests (pencil and micro-scratchers) show strong recovery of the scratches in time and can therefore not give much information on the influence of the silica on the scratch resistance.

In conclusion, from the three morphologies studied the *organic matrix with nanoparticles* formed by the basic catalyzed process shows the best results in combining and controlling hardness and flexibility. Furthermore, it was shown that migration of silica to the surface, which was seen in both organic crosslinked systems, successfully improves the scratch and mar resistance of the coatings.

Samenvatting

Het gebied van de organische-anorganische hybride materialen is pas vijftien jaar jong. Het combineren van anorganische en organische componenten tot één materiaal komt voort uit een andere recente ontwikkeling: het sol-gel proces. Via het sol-gel proces kunnen, in tegenstelling tot conventionele methoden, anorganische materialen worden gemaakt bij lage temperaturen, zodat de synthese te combineren is met organische materialen. Het doel van hybride materialen is om de eigenschappen van zowel organische als anorganische componenten te combineren. Ons doel is om de hardheid en krasvastheid van organische coatings te verhogen met behoud van de flexibiliteit door middel van hybride materialen.

In dit proefschrift wordt de toepassing van organische-anorganische hybride materialen als coatings op staal en aluminium met dit doel bestudeerd. De organische component is een flexibele polyester hars, die door reactie met organische crosslinkers vernet tot een organisch netwerk. De polyesters zijn gesynthetiseerd met hydroxyl eindgroepen. Door deze te laten reageren met barnsteenzuur worden carbonzuur eindgroepen verkregen. Op deze manier verandert de functionaliteit van de polyester, terwijl de samenstelling en structuur van de polyester vrijwel gelijk blijft. De anorganische component wordt gevormd door reactie van tetraethoxysilaan (TEOS) tot silica onder zure of basische condities in aanwezigheid van water: het sol-gel proces. Er is geconstateerd dat TEOS uit de coatings verdampte tijdens het uitharden in de oven. Daarom wordt TEOS gehydrolyseerd onder zure condities voordat het wordt toegevoegd aan het coatingmengsel. Op deze manier worden silica clusters met hydroxyl groepen gevormd, wat verdamping voorkomt en de interactie met de polyester verbetert.

De invloed van de morfologie op de eigenschappen van de hybride coatings is systematisch bestudeerd aan diverse hybride coatings. Er is gekozen voor een zuur en een basisch gekatalyseerd organisch vernettend systeem, omdat de pH de morfologie van het in situ gevormde silica beïnvloedt. Door het gebruik van zowel zure als basisch katalyse, in verder vergelijkbare systemen, worden verschillende microstructuren verkre-

gen. Onder zure condities wordt een *interpenetrerend organisch-anorganisch netwerk* gevormd, terwijl onder basische omstandigheden de morfologie bestaat uit *silica nano-deeltjes in een organische matrix*. Een derde morfologie werd verkregen door reactie van polyester met TEOS zonder aanwezigheid van een organische crosslinker. Op deze manier werd een zogenaamde *'ware hybride'* gevormd, waarin de anorganische component de crosslinker is voor de polyester.

De morfologie van de systemen is bestudeerd met elektronenmicroscopie. De studie naar de eigenschappen was vooral gericht op de invloed van de hoeveelheid silica op de hardheid en krasvastheid. Dit werd bestudeerd met technieken uit de coatings-industrie (König hardheid en potlood hardheid) maar ook met beter gedefinieerde methoden zoals de micro-indentatie en micro-krasser.

Polyester harsen gecombineerd met gehydrolyseerd en gecondenseerd TEOS resulteert alleen in een *'ware hybride'* als gebruikt gemaakt wordt van polyester met hydroxyl eindgroepen, onder zure condities en in aanwezigheid van water. Het is aangetoond dat de reactie tussen de polyester en TEOS plaatsvindt via the hydroxyl groepen van beide componenten. De toename in König hardheid en glasovergangstemperatuur met toenemende hoeveelheid TEOS toont de toename in vernettingsdichtheid. Het is ook aangetoond dat de gevormde Si-O-C bindingen eenvoudig worden verbroken door hydrolyse, wat degradatie van de coating veroorzaakt.

Wanneer polyester met hydroxyl eindgroepen en hexakis(methoxymethyl)melamine worden gecombineerd met geprehydrolyseerd TEOS onder zure condities treedt fa-sescheiding op. Dit resulteert in een morfologie van silica deeltjes in een organisch-silica *interpenetrerend netwerk*. De grootte en het aantal deeltjes nemen toe met toenemende hoeveelheid TEOS, uiteindelijk leidend tot wazige coatings. Daarnaast migreert silica naar het oppervlak van de coatings. Dit resulteert in verhoogde krasvastheid. Wanneer de polyester gemodificeerd wordt met silaankoppelingsmid-delen verbetert de compatibiliteit tussen de organische en anorganische componenten aanzienlijk. Er treedt geen fasescheiding meer op en een interpenetrerend netwerk met onderlinge verbindingen wordt gevormd. De invloed van de hoeveelheid silica op de indentatie hardheid is klein.

Voor coatings van polyester met zure eindgroepen vernet met epoxides in combinatie met geprehydrolyseerd TEOS onder basische condities zijn silaankoppelingsmiddelen noodzakelijk voor het verkrijgen van een *organische matrix met silica nanodeeltjes* (kleiner dan 10 nm). De hardheid (König, potlood en indentatie) neemt toe met toenemende hoeveelheid silica. De krastesten (potlood en micro-krasser) kenmerken zich door groot herstel van de krassen in de tijd. Daarom is het niet mogelijk de invloed van het silica op de krasvastheid te bepalen.

Van de drie bestudeerde morfologieën levert de *organische matrix met silica nano-deeltjes* de beste resultaten wat betreft de combinatie van hardheid en flexibiliteit. Daarnaast is aangetoond dat de migraties van silica preferent naar het oppervlak, wat voorkomt in beide systemen met organische crosslinkers, de krasvastheid van de coatings aanzienlijk verbetert.

Dankwoord

Hierbij wil ik graag een persoonlijke noot plaatsen voor iedereen die heeft bijgedragen aan het totstandkomen van dit proefschrift.

Allereerst wil ik mij ouders, grootouders en zus bedanken voor hen nimmer aflatende steun en vertrouwen. Dat is zonder meer de basis voor dit proefschrift. Ook wil ik mijn eerste promotor en begeleider professor Rob van der Linde bedanken voor het geven van richting aan het begin van het onderzoek, en de warme belangstelling voor mijn werk. Daarnaast wil ik professor Han Meijer bedanken voor de financiële vrijheid om de wereld in te trekken en mijn werk daar te kunnen presenteren. Verder wil ik Harry, Arend-Jan en Corné van TNO-TPD bedanken voor de samenwerking en maandelijkse discussies en alle leden van de begeleidingscommissie (Leo van Dijk, Rinus Hoeflaak, Michel Klijn, Hub Meuwissen, Cor van Rossum en Anouschka Versleijen) voor de halfjaarlijkse discussies en de bedrijfsbezoeken. Harry, ook reuze bedankt voor je altijd zeer kritische leesvermogen.

Bij eens startende groep is weinig apparatuur en kennis aanwezig en daarom ben ik blij dat ik gebruik heb mogen maken van de kennis en tijd van vele mensen van andere groepen. Paul van der Varst en Bert de With, bedankt voor het gebruik van de nano-indenter, maar ook voor de discussies en het aanvaarden van de taak als tweede promotor, respectievelijk. Kees Hendriks bedankt voor de kras metingen, terwijl je zelf onder zo'n tijdsdruk stond. Ik ben blij dat mijn coatings ook voor jou hun nut hebben bewezen. Voor al het SEM en TEM werk en vooral het zoeken naar de juiste methodes om de coatings te bekijken wil ik Chris van Roost van Agfa-Gevaert bedanken voor de 'doorbraak', Anne Spoelstra voor de snelle vervolgstappen en de mooie plaatjes en verder Hartmut Fischer voor de diverse pogingen, maar ook Hans Heijligers en Dick Klepper voor hun bijdragen in de elementen analyses van alle mogelijke en onmogelijke samples. The group of professor Dušek I would like to thank for their kindness during my stay at their institute. Although the SAXS measurements can not be found back in this thesis, the experience was great and my love for Prague is guaranteed. Helaas haalde ook de AFM metingen, gedaan door

Maarten van der Wielen aan die rare coatings van mij, dit boekje niet. Toch niet minder bedankt Maarten voor je geduld, tijd en nuchtere kijk op de wereld. In dit rijtje hoort ook een bedankje aan Francis thuis, die voor mij te pas en te onpas NMR's heeft gemeten.

Verder wil ik mijn studenten (Joep van Houten, Corné Rentrop, Niels Lutke-Schipholt en Maud Kastelijn) bedanken voor al het werk dat zij hebben gedaan. Al lijkt er maar een klein deel terug te komen in het uiteindelijke boekwerk, jullie werk heeft er wel degelijk aan bijgedragen. Zonder de hulp van mijn persoonlijke LATEX-experts Thomas Arts, Marnix Tas en Piet Tutelaers zou dit boekje er niet zo uit hebben kunnen zien, hiervoor mijn welgemeende dank. En vanzelfsprekend wil ik ook de vaste staf, al mijn kamergenoten, collega's en studenten van het 'oude' TPK en het 'nieuwe' SKT + SPC bedanken voor de sfeer in de groep(en). Tenslotte wil ik hier bedanken mijn paranimfen, Henk en Ruud, voor hun vriendschap en voor het (symbolische) bijstaan tijdens mijn verdediging.

Allerliefst wil ik eindigen met een dank je wel voor jou, Simon. Zonder jou als steun en toeverlaat was het me nooit gelukt.

Curriculum Vitae

Suzanne Frings is geboren op 17 maart 1970 te Wageningen. In 1988 behaalde zij haar diploma Atheneum B aan het R.K. Lyceum Dominicus College te Nijmegen. Vervolgens studeerde zij Scheikundige Technologie aan de Technische Universiteit Eindhoven, waar zij in 1989 haar propaedeuse behaalde en in 1994 afstudeerde bij professor R.A. van Santen op het onderwerp 'Plasma-induced catalytic reactions of methane over transition metals at atmospheric pressure'. Februari 1995 begon zij met haar promotie onderzoek aan dezelfde faculteit binnen de vakgroep Polymeerchemie en Kunststoftechnologie, later Polymeerchemie en Coatingtechnologie, onder leiding van professor R. van der Linde. De resultaten van dit onderzoek staan beschreven in dit proefschrift. Vanaf 1 november 1999 is Suzanne Frings werkzaam bij Akzo Nobel Coatings te Sassenheim.